ResearchGate

See discussions, stats, and author profiles for this publication at:
https://www.researchgate.net/publication/215451086

# Redox Reactions of Heme-Containing Metalloproteins: Dynamic Effects of Self-Assembled Monolayers on Thermodynamics and Kinetics of Cytochrome c Electron-Transfer Reactions

**ARTICLE** *in* COORDINATION CHEMISTRY REVIEWS · NOVEMBER 2000

Impact Factor: 12.24 · DOI: 10.1016/S0010-8545(00)00292-7

CITATIONS
169

READS
85

**1 AUTHOR:**

Milan Fedurco
Michelin Switzerland
**54** PUBLICATIONS **2,864** CITATIONS

SEE PROFILE

Available from: Milan Fedurco
Retrieved on: 25 January 2016

ELSEVIER

Coordination Chemistry Reviews
209 (2000) 263–331

COORDINATION CHEMISTRY REVIEWS

www.elsevier.com/locate/ccr

# Redox reactions of heme-containing metalloproteins: dynamic effects of self-assembled monolayers on thermodynamics and kinetics of cytochrome *c* electron-transfer reactions

Milan Fedurco *

*Department of Chemistry, University of Geneva, CH-1211 Geneva, Switzerland*

Received 19 August 1999; received in revised form 4 January 2000; accepted 18 January 2000

## Contents



* Fax: +41-22-7026830.
*E-mail address:* milan.fedurco@chiam.unige.ch (M. Fedurco)

0010-8545/00/$ - see front matter © 2000 Elsevier Science B.V. All rights reserved.
PII: S0010-8545(00)00292-7

**Abstract**

The ability of metalloproteins to recognize their biological redox partners, as well as kinetics of inter-protein electron-transfer reactions may be affected by chemical modification of amino acid residues located on the protein surface. Similarly, the rate of heterogeneous electron transfer can be tuned either via protein or electrode surface modification. Both of these methods allow one to modulate the extent of protein–protein or protein–electrode association, called also adsorptivity. On the other hand, the use of chemical coupling agents allows for a covalent attachment of metalloproteins to electrode surfaces and results in corresponding monolayers, or robust multilayers, with more or less preserved catalytic function of the redox protein. The latter approach is of prime importance in the construction of biosensors, immunosensors, optoelectronic devices, and other applications. The main goal of the present review is to summarize multidisciplinary efforts in bioelectrochemistry (during the last decade or so), attempting to comprehend kinetics of redox reactions associated with metalloproteins at the electrode/solution interface. Experimentally obtained kinetic data for the reduction of cytochrome *c* on chemically modified electrodes are correlated with its electronic structure, heme solvation and the protein contribution to the total reorganization energy. Two modes of charge transfer between the electrode and cytochrome *c* are discussed, namely, the heme edge and axial ligand-assisted electron tunneling. Rates of electrode reactions associated with corresponding redox process are shown to depend not only on the thickness of a self-assembled thiol monolayer, but also on its polarizability and ability to undergo ionization reactions. Acid–base equilibria existing on ω-mercaptoalkanoic acid-covered gold electrodes exposed to aqueous solutions of varying pH, seem to be directly responsible for strong electrostatic binding of this positively charged metalloprotein to carboxyl-terminated interface. In this respect, the latter type of self-assembled monolayers serves as very interesting model systems for protein binding to biological membranes. Furthermore, the possibility of variation in the reaction driving force at the electrode/long-chain thiol/solution interface offers one the possibility of measuring reorganization energy $\lambda$ for a given metalloprotein. Both dynamics of cytochrome *c* rotational movements in self-assembled thiol monolayer, as well as the amount of electronic coupling between the heme and metal electrode, are shown to affect kinetics of non-adiabatic charge-transfer process. Dramatic differences in kinetics of cytochrome *c* reduction on gold electrodes modified by aliphatic and aromatic thiols are pointed out. This phenomenon is assigned as due to differing facility of establishment of hydrogen-bonding contacts between the protein and corresponding thiolate monolayer. On the other hand, a mixed hydrophilic thiol monolayer (i.e. containing OH/COOH, $NH_3^+/COO^-$ terminal groups), and the hydrophobic–hydrophilic thiol films ($CH_3$/OH, $CH_3$/COOH, $CH_3$/4-mercaptopyridine), show either acceleration effects on the redox reactions of cytochrome *c*, or lead to their diminution, depending on the thiol mole fraction in the solution during the self-assembly process. Future directions in the area of metalloprotein electrochemistry are briefly outlined. © 2000 Elsevier Science B.V. All rights reserved.

*Keywords:* Cytochrome c; Cytochrome $b_5$; Cytochrome c oxidase; Cytochrome c peroxidase; Self-assembled monolayer; Electron tunneling; Bis(4-pyridyl) disulfide; *n*-Mercaptoalkanoic acid

## 1. Introduction

Recently, significant progress has been made in understanding the structure, function and redox properties of heme-containing metalloproteins [1–39]. It is noteworthy that to date as many as 150 cytochromes (containing from one up to 16 hemes) have been isolated from various eukaryotic, bacterial and plant cells, and an increasing number of new species comes from site-directed mutation studies. Among the experimental methods used for the characterization of these electron-transfer (ET) proteins and their model compounds such as, for example, X-ray crystallography [1–5], NMR [6–8,11,12], or EPR [34–36], electrochemistry became one of valuable tools in their classification and testing for their stability under in vitro conditions [17,19,24,30,33]. The most intensive work in the area of bioelectrochemistry during the last two decades or so has certainly been devoted to the iron-containing metalloprotein called cytochrome *c*. Various aspects of its electrochemical behavior on metal, semiconductor and carbon electrodes have been summarized in several articles and book chapters [14,15,17,24–26,30,38,39]. Specific problems associated with the kinetics of its heterogeneous and interprotein electron-transfer (ET) reactions were reviewed by Marcus and Sutin [15] and, almost one decade later, by Bond [25]. Effects of the chemical modification of electrode surfaces on the kinetics of cytochrome *c* redox reactions were briefly mentioned in these reports, but were not subjected to a more detailed analysis. The main goal of the present review is to summarize and critically evaluate previous kinetic work on the reduction of cytochrome *c* on chemically modified electrodes, namely, on gold electrodes covered by self-assembled thiol monolayers (SAMs). Possible electron-transfer pathways between this redox protein and a metal electrode will be discussed in light of the most recent knowledge on the electronic structure of heme, and 3D structural data for cytochrome *c* in solution [6,8].

Among other biological functions, horse-heart cytochrome *c* plays an important role as an electron carrier in the mitochondrial inter-membrane space (cytosol) between two membrane-bound protein complexes, cytochrome *c* reductase and cytochrome *c* oxidase. Its redox center consists of heme iron, complexed by four nitrogen atoms of the porphyrin ring, while two amino acids, histidine (His-18) and methionine (Met-80), serve as axial ligands (see Figs. 1 and 2). The formal redox potential ($E^{\circ\prime}$) for ferri/ferrocytochrome *c* couple is 0.265 V versus NHE (pH 7) [24,40], and is known to vary with temperature [41–43], pressure [44,45], electrolyte composition and ionic strength [46–48]. The standard redox potential of 0.291 V versus NHE, obtained upon potential extrapolation to an ionic strength of zero, has been recently reported [49]. Even though, from the structural point of view, horse-heart cytochrome *c* is a relatively simple metalloprotein (consisting only of 104 amino acids), and is often considered as a model metalloprotein, its electrochemical studies were for a long time hampered due to its strong adsorptivity on Pt, Hg, Au, Ag, and other electrodes [19,50]. The adsorption has been shown to result in serious conformational changes of the cytochrome *c*, protein unfolding and, eventually, its denaturation, even though this has been disputed [26,51,52]. Problems of this kind persisted for several decades in cytochrome *c* electrochemistry

since the pioneering polarographic studies of Brdicka in 1933 (polarographic work on cytochrome *c* reduction published prior to year 1972 has been summarized in an excellent work by Betso et al. [53]). The latter authors have performed electrochemical and spectroelectrochemical studies on cytochrome *c* on Hg, Pt and Au electrodes, and have realized the importance of the adsorbed layer of cytochrome *c* molecules on the thermodynamics and kinetics of interfacial ET reactions. They note: 'The slow step in the diffusional mass transport of cytochrome *c* may be a rotational diffusion of adsorbed cytochrome *c* molecules necessary to transfer electrons from the electrode surface to freely diffusing ferricytochrome *c* molecules'. Following their work, irreproducibility of experimental results coming from different laboratories has frequently been ascribed to strong protein adsorption or, eventually, to the differences in electrode surface preparation and/or protein purification protocols. Hawkridge and co-workers [26,51] have suggested that it is not cytochrome *c* itself which is responsible for surface blocking, but rather its oligomers, deamidated forms, and various surface-active impurities resulting from insufficient sample purification. However, recent surface-enhanced Raman spectroscopy (SERS) experiments [54,55] have shown that even in the case of highly purified cytochrome *c* samples, conformational changes of the protein adsorbed on a metal surface may not be avoided. Changes in the heme–iron ligation, accompanied by low-spin to high-spin transition, were observed in the latter studies at potentials close to the potential of zero charge of silver in contact with neutral aqueous solutions.

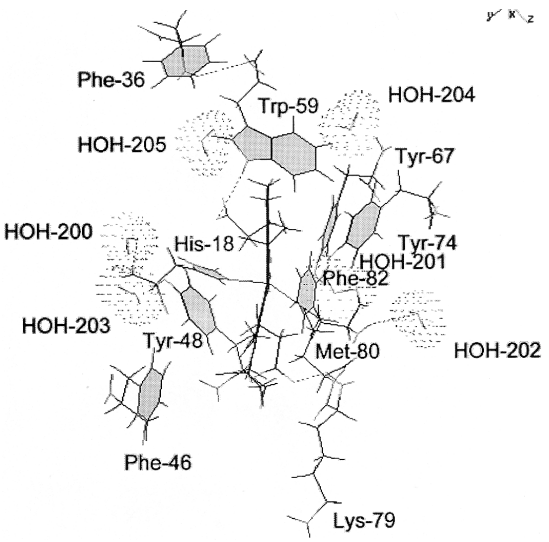


Fig. 1. Spatial arrangement of six water molecules, of some aromatic residues constituting the hydrophobic heme cavity in horse-heart ferricytochrome *c* (created using the Swiss PdbViewer [254] and the solution NMR data (1OCD [6], deposited at RCSB Protein Data Bank). Dotted lines represent hydrogen-bonding contacts within the heme cavity.

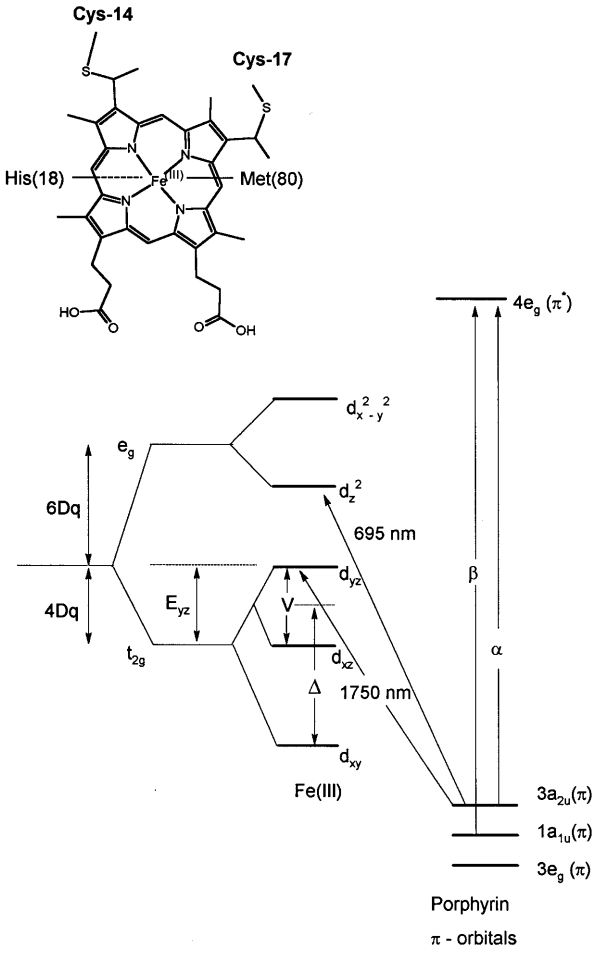


Fig. 2. Schematic representation of the energy levels in cytochrome *c*, of some transitions observed in the UV–vis, NIR range of the electronic spectra.

It is interesting to note that problems associated with the cytochrome *c* adsorption on solid electrode surfaces eventually led to the concept of their chemical modification. The latter process often involves spontaneous self-assembly of a monolayer-thick molecular film on a metal surface. An adsorbed molecule (physisorbed or chemisorbed), being a component of a self-assembled monolayer (SAM), and allowing for a rapid exchange of electrons between the cytochrome *c* and the electrode, is called a 'promoter' of electron transfer. Hill and co-workers [14,16,40,56–58] have reported that 4,4′-bipyridine (PyPy), when adsorbed on a gold electrode surface, allowed for reversible electrochemistry of cytochrome *c* (during several volumetric cycles), while virtually no electrochemical response was perceptible on the unmodified electrode. Their work was shortly followed by that of

Taniguchi et al. [59,60], who reported that bis(4-pyridyl) disulfide (PySSPy), and the corresponding sulfide manifest similar promoting effects of redox reactions of cytochrome *c*. The PySSPy-monolayers revealed themselves as much more stable mechanically, and promoting effects persisted for extended periods of time. In this respect, it is rather surprising that the first promoter of ET which allowed the observation of a reversible electrochemistry of cytochrome *c* on Hg (namely, 6-mercaptopurine) has been described only recently [61]. Despite the still persistent contrasting views regarding the nature of the species responsible for blocking of electrode surfaces in the presence of cytochrome *c* [26,46–48], it is presently well agreed among electrochemists that sulfur-containing promoters work well with purified as well as less pure cytochrome *c* samples. Undoubtedly, the discovery of promoting effects of PyPy [40] and PySSPy [59] on the redox reactions of cytochrome *c* contributed to a large extent to the development of bioelectrochemistry as we know it today. Furthermore, recent progress in the understanding of thiol and disulfide self-assembly on solid electrode surfaces [62–94], and the stability of the resulting films towards reductive and oxidative desorption [95–107], is an important incentive to bioelectrochemists in designing new chemically-modified electrodes (CMEs), where the protein adsorptivity on electrode surfaces can be tuned.

It is interesting to note that while early electrochemical studies were almost exclusively directed towards bioenergetics and electroanalytical chemistry of metalloproteins, more recent research efforts try to elucidate, on a molecular level, which factors are responsible for the redox potential of a given metalloprotein. For example, very good agreement between experimentally measured $E°$ values for several metalloproteins, and those calculated using the protein dipole Langevin dipole method (PDLD), has been recently reported [37]. Elegant electrochemical studies were conducted on cytochrome *c* [41,108–110] and cytochrome *c* peroxidase [22] mutants having amino acid replaced directly in the heme cavity. Semiempirical and molecular dynamics (MD) studies have started to shed some light on how and why such mutations affect kinetics of electron-transfer reactions. MD simulations were performed on ferri- and ferrocytochrome *c* [111–114], as well as on their complexes with other proteins that make use of complete crystallographic, or solution NMR structural data [112,115,116]. Theoretical studies help us to elucidate the relative contributions of the heme, of the internal solvent molecules and of the protein, to the energy barrier for a charge-transfer reaction associated with a given cytochrome. In this respect, electrochemical experiments are particularly helpful, since kinetic and activation data for various metalloproteins can be obtained from a single cyclic voltammetric scan [117,118]. Recent electrochemical studies address such aspects as folding and unfolding of cytochrome *c* in the presence of various denaturating agents [119–122], anion binding to its surface [123,124], or formation of complexes with cytochrome *c* oxidase [125], cytochrome $b_5$ [12,126,127], cytochrome *c* peroxidase [32,128] and plastocyanin [129]. Electrochemical experiments on these rather complex biological phenomena could certainly not be envisaged some 20 years ago before the appearance of CMEs. Also, in situ spectroscopic techniques such as SERS [54,55], SERRS [130,131], FTIR [132,133], electroreflec-

tance [134–138], or ellipsometry [139], when combined with electrochemistry, give precise information on the nature of interactions between the cytochrome *c* and SAMs. Adsorption of cytochrome *c* on solid electrode surfaces has also been monitored using AFM [140], STM [141–144], and electrochemical quartz-crystal microbalance techniques [145].

## 2. Factors affecting thermodynamics and kinetics of cytochrome *c* redox reactions

### 2.1. Solvent and protein

Kinetics of unimolecular electron self-exchange as well as heterogeneous ET reactions, can be modulated by varying the three parameters: the reorganization energy of a given redox couple ($\lambda$), the driving force of the reaction ($-\Delta G°$) and the magnitude of the pre-exponential factor ($A$).

$$k_{et} = A \exp[-(\Delta G° + \lambda)^2/4\lambda RT] \quad (1)$$

Importantly, both $A$ and $\lambda$ might, under some conditions, be affected by the solvent. Before addressing various aspects of the theoretical and experimental determination of these parameters for cytochrome *c*, it is important to understand the relative contributions of solvent (e.g. water), and that of the protein envelope surrounding the heme, to the total reorganization energy. The purpose of the present section is to point at large differences between the kinetics of reduction of model porphyrins in aprotic solvents, and for ferricytochrome *c*, in which the heme iron is buried in the hydrophobic protein interior, thus limiting the accessibility of bulk water molecules to the redox center.

Let us first consider an adiabatic heterogeneous charge-transfer process (e.g. occurring at the electrode/solution interface), where all the diffusing reactant molecules are successfully converted to reaction product upon their arrival at the electrode surface. At the electrode potential where the reaction driving force is effectively zero, so that the exponential part is limited to $\lambda/4RT$ (e.g. $E = E°$, and the double-layer effects can be neglected), the standard heterogeneous rate constant ($k°_{het}$) is simply related to the pre-equilibrium constant ($K_p$), the nuclear frequency at which the activated complex is formed ($\nu_n$), and the sum of the inner-shell ($\Delta G^*_{in}$) and outer-shell ($\Delta G^*_{os}$) Gibbs reorganization energies

$$k°_{het} = K_p \nu_n \exp[-(\Delta G^*_{in} + \Delta G^*_{os})/RT] \quad (2)$$

In cases where the electrode reaction associated with porphyrin reduction is accompanied only by very small bond length and bond angle changes ($\Delta G^*_{in} \ll \Delta G^*_{os}$), the corresponding reaction kinetics are known to be very fast ($k°_{het} > 0.1$ cm $s^{-1}$), and controlled essentially by solvent dynamics [146,147]. In polar aprotic solvents composed of monomer species (no hydrogen bonding) solvent relaxation follows essentially the exponential decay represented by the autocorrelation function $C(t) = \exp(-t/\tau_L)$, from which the solvent longitudinal relaxation time ($\tau_L$) can be extracted

$$\tau_L = \varepsilon_\infty \tau_D / \varepsilon_s \quad (3)$$

where $\varepsilon_\infty$ is the infinite (high-frequency) dielectric constant, $\varepsilon_s$ is the static dielectric constant, and $\tau_D$ is the Debye relaxation time (the time it takes for the polarization of a liquid to decay to zero after the electric field has been turned off) [148–150]. In the adiabatic limit, solvent is expected to affect not only the exponential part of Eq. (1), but also its pre-exponential term, since $\nu_n$ depends inversely on $\tau_L$ [149–151]

$$\nu_n = (1/\tau_L)(\Delta G^*_{os}/4\pi RT)^{1/2} \quad (4)$$

Even though $k^\circ_{het}$ is much more sensitive to variation in the exponential part of the rate law, the solvent effect on $A$ should not be neglected. For example, due to the differences in solvent relaxation properties, $k^\circ_{het}$ for the one-electron reduction of chloro(tetraphenylporphyrinato)–Mn(III) complex, $Mn^{III}$(TPP)Cl, decreases ca. 10-fold when going from acetonitrile ($\tau_L = 0.18$ ps) to nitrobenzene ($\tau_L = 5.4$ ps) [146]. Similarly, in the case of one-electron benzophenone reduction, acetonitrile replacement by hexamethylphosphoramide ($\tau_L = 8.8$ ps) leads to a ca. 25-fold reduction in $k^\circ_{het}$ [152]. In the former work, the plot of $(\log k^\circ_{het} + \Delta G^*_{os}/2.3RT)$ versus $\log \tau_L^{-1}$ has been found to be linear for six different organic solvents with the slope equal unity, which indicates a perfectly adiabatic ET process. Additional spectroelectrochemical studies conducted by Mu and Schultz [153] indicate that the axial $Cl^-$ ligand is bound to the metal in both oxidation states, while ligand-solvent replacement reactions take place in strong donor solvents such as DMSO, DMF or THF.

As mentioned above, a theoretical treatment of fast ET processes involving a relatively simple solute in an aprotic solvent is more or less understood. However, the situation when treating kinetics of ET associated with highly charged reactants is much more complex in polar solvents such as water or alcohols (non-Debye solvents). During the last decade, polar solvent dynamics has been subject of numerous experimental and theoretical studies [148,154–170]. One of the main outcomes of these studies is that the kinetics of ET processes in water are mainly determined by librational solvent movements and electrostatic friction, rather than translational and collective diffusional solvent motions. In fact, photoinduced electron transfer in water (e.g. indole, coumarin dyes, etc) might occur on time scales faster than required for a complete rotation of the solvent dipole around the solute, and is completed within several femtoseconds [161–163,165]. Jimenez and co-workers [161] have concluded that, at least in the case of uncharged reactants undergoing photoinduced ET (accompanied by large dipole moment changes), water is the fastest solvent known. Whether or not this applies also to fast heterogeneous ET processes in water (having a small intrinsic energy barrier) remains to be verified experimentally. It is interesting in this respect, that Miller and co-workers [118,171,172] have reported experimental measurements of $\lambda$ for several transition metal complexes in water on long-chain ω-hydroxyalkanethiol-modified gold electrodes. In order to explain the magnitude of the measured $\lambda$ for their reactants, including several heme proteins, the authors have used a simple Born

continuum model. Unfortunately, quantum Monte Carlo simulations and umbrella sampling calculations [173–177] suggest that solvation effects in such ET reactions cannot be captured by the Born model, mainly due to specificities of metal ion hydration in aqueous solutions. Furthermore, any artificial separation of the corresponding $\lambda$ into inner- and outer-shell components should be highly discouraged. The same message comes from the density functional calculations of Li et al. [178], who suggest that the effective radius of redox species such as $M(H_2O)_x^{n+}$ (M = Fe, Mn, . . . ) in water changes with the oxidation state of the metal. The situation is further complicated by extensive hydrogen bonding between the individual hydration shells, the differing extent of charge transfer between the water molecules and iron during the redox transition, and a slight Jahn–Teller distortion of the complex. It is also likely that the librational water movements within the hydration envelope in these iron complexes could lead to friction effects, which are known to affect the dynamics of energy barrier crossing by electrons. Such friction effects were noticed previously in the case of photoinduced charge transfer occurring within the $(NH_3)_5Ru^{III}CNFe^{II}(CN_5)^-$ complex in water [163]. Certainly, new theoretical approaches and fully flexible ion hydration models (for example, as recently described in Ref. [179]), will be required to clarify this point.

In the previous discussion, we have pointed at some differences between kinetics of fast ET processes in aprotic solvents and water, the solvent in which significant hydrogen-bonding interactions may be expected. Solvation effects in the case of cytochrome *c* redox reactions that take place at its heme iron center constitute yet another problem, however, for quite different reasons. In fact, heme hydration contained in the cytochrome *c* interior may be very different from that normally experienced in bulk water.

One of the sensitive indicators of heme exposure to an aqueous solvent is the magnitude of the reorganization energy, $\lambda$, for a given metalloprotein. Importantly, Miller and co-workers c [117,118] have recently determined $\lambda$ for several heme-containing metalloproteins, including cytochrome *c*. The authors have concluded that $\lambda$ values for Fe, Ru and Os complexes in water are quite close to those found for horse-heart cytochrome *c* and cytochrome $b_5$, and state:... 'The measured reorganization energy of the cytochromes is therefore consistent with the size of the axially coordinated heme, suggesting only a minimal role of the protein in controlling the activation energy of the cytochromes' [117]. The latter conclusion is not likely to be correct and is contrasted by the results of recent solution NMR experiments on oxidized and reduced cytochrome *c* in aqueous solutions [6,8,10,13]. Accordingly, several amino acids located in the interior of cytochrome *c*, including aromatic residues of tyrosine, tryptophan and phenylalanine (being part of the hydrophobic heme pocket), effectively separate water molecules from the heme iron (Fig. 1). In fact, $\lambda_{os}$ for cytochrome *c* is ca. four–fivefold larger than the corresponding $\lambda_{in}$ [211], and the protein contribution to the overall energy barrier for ET is important (and might exceed that of water contained in the protein interior) [180–182]. Also, the protein plays an important role in limiting the solvent contribution to the outer-shell reorganization energy. Nuclear Overhauser enhancement and exchange spectroscopy (NOESY) [6,8] and enhanced protein hydration observed through

gradient spectroscopy (ePHOGSY) [9] measurements have clearly established that there exist six long-lived water molecules in the heme cavity of oxidized (and reduced) horse-heart cytochrome *c*. During the reduction of ferricytochrome *c*, five water molecules remain in roughly the same location, while the so-called 'catalytic' water (in the proximity of His-18), moves towards the protein surface. The distance between this water molecule and the heme iron is 9.3 Å in ferrocytochrome *c* but only 6.5 Å in ferricytochrome *c* [9]. Recent reorganization energy calculations by Sharp [182] using the linear and nonlinear Poisson–Boltzmann solutions indicate that water makes a smaller contribution to the total reorganization energy than the protein despite its greater ability to reorganize (higher dielectric) just because it is located further away from the redox center. Changes associated with Fe(III) reduction also trigger conformational rearrangement of Ile-81 linked to Lys-79, which further limits access of solvent molecules to the heme [181]. MD simulations on cytochrome *c* in aqueous solution by Simonson and Perahia [111] suggest that protein modes in ferricytochrome *c* up to at least 60 $cm^{-1}$ contribute to the average relative permittivity of the protein interior of ca. 4. Here, not only water monomers contained in the heme cavity, but also functional groups of higher polarizability than water itself (e.g. carbonyl, hydroxyl, amide, etc) contribute to the total reorganization energy. The latter then depends not only on structural changes taking place on the porphyrin ring during the redox transition, but on both protein and water monomer vibrational motions (low-frequency vibrations, $\omega < 150$ $cm^{-1}$), which cannot be simply decoupled from each other [111,146–148]. Warshel et al. [37] state in their work: 'The microscopic nature of the protein polar regions involves constrained but not fixed dipoles, so that relevant dielectric constants cannot be obtained from any macroscopic concept. The proper dielectric constant in the protein interior is obtained from the fluctuation of the average dipole moment. What counts is not just solvent accessibility but the electrostatic field of the solvent, which of course, depends on the charges of the cofactor and the effect of the protein dipoles on the given solvent molecule'.

It is interesting to compare theoretical estimates of $\lambda$ for cytochrome *c* with the experimental data. For example, Muegge's MD estimate of $\lambda_{os}$ for ferri/ferrocytochrome *c* couple falls in the range 9–15 kcal $mol^{-1}$ [181], while an older microscopic treatment of Churg et al. [180] (based on X-ray structures of oxidized and reduced forms of cytochrome *c*), gave $\lambda_{os} = 6.4$ and 32 kcal $mol^{-1}$, for heme placed in the protein interior, and in water, respectively. Providing one would take a mean value of the Muegge's estimate ($\lambda_{os} = 12$ kcal $mol^{-1}$) and add to it $\lambda_{in} = 3$ kcal $mol^{-1}$ (taken as 1/4 of $\lambda_{os}$ [211]), the total reorganization energy $\lambda$ would be ca. 0.65 eV, which is close to 0.58 eV obtained experimentally using electrochemical techniques [117,118].

It is interesting that the authors of Ref. [181] suggest that the hypothetical heme (a reference system composed of the heme with its two ligands His-18 and Met-80) transfer from water into the hydrophobic heme cavity would result in reduction of reorganization energy by ca. 75%. However, it is also likely that their estimate of the reorganization energy for Met/His-ligated heme (37 kcal $mol^{-1}$) in water is somewhat overestimated. Providing water would indeed behave as a 'slow' solvent,

it would be difficult to explain why kinetics associated with redox reactions of hexacoordinated iron porphyrins (low-spin) in water [183] and water–ethanol mixtures [184] are so fast that either quasi-reversible or reversible cyclic voltammetric behavior is usually observed (comparable to that observed and dimethylsulfoxide [185] and other polar solvents). Unfortunately, heme octapeptide, which can be prepared by selective proteolysis of cytochrome *c* [186], might not be the best cytochrome *c* model, especially because of its low solubility in water, its oligomerization and low-spin to high-spin transitions during such polymerization reactions [186–188]. Furthermore, providing one would be able to eliminate all those problems named above, p$K_a$ values for the carboxylic groups on the heme octapeptide surface are expected to be quite different for COOH groups buried in the hydrophobic cytochrome *c* exterior (similar applies to protonation/deprotonation equilibria associated with $NH_2$ groups on the heme octapeptide surface and, on the other hand, in cytochrome *c* interior). Importantly, such ionized amino acid residues might stabilize the charge on the heme iron and affect directly the charge distribution on the heme during the redox transition. This is then expected to have significant effect on the magnitude of the overall reorganization energy $\lambda$ associated with the Fe(III)/Fe(II)–heme octapeptide couple as compared to Fe(III)/Fe(II)–cyt *c* where only heme propionates are known to undergo ionization reactions, while the redox center is well shielded from the surface $COO^-$ and $NH_3^+$ groups on the protein surface.

In the previous discussion, it has been mentioned that one should not separate artificially $\lambda$ for the $Fe(H_2O)_6^{3+/2+}$ couple in water into its inner- and outer-shell components due to the unique solvation (hydration) of this, and other complexes, in water. In the following text, we will discuss whether or not such a separation is possible in the case of cytochrome *c*. Some indications along these lines come from normal mode reorganization energy spectrum (NMRES) analysis [113,114]. The latter method has been successfully used for the reorganization energy determination in the case of Ru(His-33)-cytochrome *c*, a molecule with the 3D structure known from solution NMR experiments. The total reorganization energy for the photoinduced ET between Fe(II) and Ru(III)–His-33 has been estimated as 15.6 kcal $mol^{-1}$, while $\lambda_{os}$ accounts for 7.2 kcal $mol^{-1}$. Importantly, the latter authors have shown for the first time that the total reorganization energy can be obtained theoretically by making the integration over all the normal vibrational modes in cytochrome *c*, rather than artificially separating it into the $\lambda_{in}$ and $\lambda_{os}$ components. Thus, the heme vibrations are coupled here to vibrations of amino acid residues in the heme cavity and, furthermore, long-lived water monomers surrounding the heme are being considered as an integral part of the protein. There exist as well experimental ways of assessing solvent contribution to the total reorganization energy in ET associated with a given metalloprotein. For example, $\lambda_{os}$ for azurin can be obtained from the time-dependent line broadening (solvent-induced dephasing in a sub-picosecond regime) along the resonance Raman vibration associated with the redox transition [189]. While such reorganization energy measurements were demonstrated to be possible in the case of sulfur-to-copper charge transfer reactions in the latter metalloprotein, it remains to be seen whether a similar type of experiment could be done for cytochrome *c*.

As discussed above, the internal water molecules in horse-heart cytochrome *c* are kept at a certain distance from the heme and might be hydrogen-bound to polar amino acid residues in the heme cavity (see Fig. 1). Disruption of such hydrogen bonding may occur as a result of the conformational changes in the protein, or in the cases where organic solvent molecules such as tetrahydrofuran (THF) [190], dimethylsulfoxide (DMSO) [191], or glycerol [192], enter the heme cavity. Horse-heart cytochrome *c* is naturally designed to withstand exposure to non-physiological conditions, and thereby minimizes thus the extent of water removal from the heme pocket and subsequent protein conformational changes. However, in spite of the remarkable stability of cytochrome *c* towards unfolding, the above mentioned organic solvents show some effects on the kinetics of its ET reactions. Thus, De Sanctis and co-workers [192] have reported that increase in the glycerol content in water up to 50% v/v (in 50 mM phosphate buffer, pH 7.0) led to a slight change in the heme pocket region of the protein (optical density data in the Soret region), accompanied by ca. 8% increase in the circular dichromism (CD) signal in the 200–250 nm region. This has been assigned as due to an increased number of amino acid residues that become part of protein helical segments. The authors propose that glycerol affects ET kinetics as a consequence of the increased viscosity of a mixed solvent. However, it exerts no effect on its redox properties. Addition of glycerol to a neutral electrolyte solution (50% v/v) then resulted in a decrease in the apparent rate constant from $k^{\circ}_{het}{}' = 8.8 \times 10^{-3}$ to $2.2 \times 10^{-3}$ cm $s^{-1}$. On the other hand, an increase of DMSO content in the aqueous electrolyte up to 40% caused the reduction potential of native cytochrome *c* to shift cathodically by about 150 mV compared to that observed in aqueous solution of the native form of cytochrome *c* at pH 7.0 [191]. Importantly, CD and $^{1}$H-NMR spectral features for cytochrome *c* were indistinguishable when the aqueous solution contained up to 40% v/v DMSO. The authors assign the effect on the heterogeneous rate constant to the decrease in the dielectric constant in the heme cavity. However, the above explanation seems unlikely, as the dielectric constant in the heme cavity of cytochrome *c* is ca. 2–4 [181,193–195]. It is therefore difficult to picture how $\varepsilon$ could be further decreased in the presence of polar DMSO molecules ($\varepsilon_s = 49$). Note that the ability of an amino acid dipole to stabilize a charge on the heme iron depends not only on the polarity of amino acid residues in the heme cavity, but also on their orientation with respect to the redox center [37,180–182]. It is possible that some steric rearrangement of polar amino acid residues in the heme cavity takes place in aqueous DMSO solutions which could not be identified in the above mentioned spectroscopic experiments.

### *2.2. Heme electronic structure*

Cytochromes are involved in important biological processes ranging from plant and bacterial photosynthesis to the cell respiration in eukaryotic organisms. In most of the cytochromes known today, the combinations of histidine and three amino acid residues: methionine, lysine and cysteine are known to serve as axial ligands. For example, His/Met ligation is found in the native form of horse-heart cy-

tochrome *c*, bis(histidine) ligation in cytochrome $b_5$, and in four hemes of cytochrome $c_3$, His/Lys in alkaline form of cytochrome *c*, etc. Such persistence in nature is not accidental, and is dictated directly by the biological functions of a given heme protein. Thermodynamic control in metalloproteins is achieved by an intimate interplay between axial ligation, chemical structure of amino acid residues forming the heme pocket, solvent accessibility to the heme iron as well as solution composition and its ionic strength (affecting also the nature of charge and its distribution on the protein surface). Since cytochrome *c* reduction is a simple one-electron process (no proton transfer to the redox center), a negative shift in its reduction potential might indicate adsorption-induced conformational changes or, ligand-exchange reactions induced by variation in the solution pH (i.e. so-called alkaline transition). This is of special importance on chemically-modified electrodes, where the pH at electrode surfaces might significantly differ from that found in the bulk of the solution (cf. Section 3.2). Serious structural changes in tertiary structure of cytochrome *c* also occur in the presence of organic molecules such as pyridine, imidazole, and their alkylated analogs, which are able to replace one of axial ligands in ferricytochrome *c* (Met-80). In principle, these molecules do not induce a complete protein unfolding as do typical denaturating agents, i.e. guanidine hydrochloride or urea. Therefore, it is interesting to investigate how such perturbations in the protein structure affect the redox behavior of cytochrome *c* as well as kinetics of electrode reactions. Several examples of Met-80 replacement by these strong ligands will be discussed within the framework of crystal-field theory in the following text.

Two heme axial ligands in cytochrome *c* as well as two thioether linkages (Cys-14 and Cys-17) to the heme decrease the original $D_{4h}$ symmetry of the porphyrin to $C_{4v}$, or even to $C_s$ [196], which leads to a complete loss of degeneracy in the Fe $t_{2g}$ subshell (see Fig. 2). In ferricytochrome *c*, a hole is localized in the $d_{yz}$ orbital ($S = 1/2$), while lower energy $d_{xy}$ and $d_{xz}$ orbitals are fully occupied. Important information about the effect of axial ligand replacement on the electronic structure of the heme iron d-shell can be readily obtained from NIR MCD and EPR experiments [197,198,202]. Especially the EPR measurements allow one to identify both axial ligands as well as to determine the energy level splitting within the $t_{2g}$ sub-shell of low-spin heme proteins and some of their model compounds [34,199,200]. Shokhirev and Walker [201], have studied the orientation of the principal axes of the g tensor with respect to the relationship of axial ligand planes to the porphyrin nitrogens. They have shown that in the cases where the axial ligand eclipses two opposite equatorial ligands (and the $d_{xy}$-level is the lowest one in the $t_{2g}$-subset), the *g*-values are expected to be ordered in the following way: $g_z > g_y > g_e > g_x$ ($g_e$ is the free electron value equal to 2.0023). This seems to be the case for various strong field ligands as shown in Table 1. In fact, the sensitivity of $g_z$-values to the nature of the axial ligand has been often used for the purposes of classification of heme metalloproteins and to test whether or not a given cytochrome undergoes serious conformational changes in vitro, following its separation from its natural environment (i.e. the biological membrane) [202].

Contributions of the rhombic ($V$) and axial ($\Delta$) field into the total crystal field (CF), can be readily obtained from the EPR experiment [202,203] since

$$V/\lambda = E_{yz}/\lambda - E_{xz}/\lambda = g_x/(g_z + g_y) + g_y/(g_z - g_x) \quad (5)$$

$$\Delta/\lambda = E_{yz}/\lambda - E_{xy}/\lambda - V/2\lambda = g_x/(g_z + g_y) + g_z/(g_y - g_x) - V/2\lambda \quad (6)$$

where $\lambda$ is the spin–orbit coupling constant for low-spin cytochromes, reported to be either 400 [10], or 741 $cm^{-1}$ [197]. The rhombic field of axial ligands removes equivalence of $d_{yz}$ and $d_{xz}$ orbitals thus making $g_x$ and $g_y$ unequal. This also applies to native horse-heart ferricytochrome *c* and to all the low-spin complexes shown in Table 1. Unusually large $g_z$ value for the alkaline form of cytochrome *c* suggests that lysine is a stronger axial ligand than Met-80 ($g_z = 3.05$), $CN^-$ ($g_z = 3.26$) and pyridine ($g_z = 3.29$). Note that $g_z$ and $g_y$-values were erroneously reversed in Ref. [204], which would lead to negative rhombic field values (original EPR data can be found in Ref. [214]). Analysis of EPR data [202,203] allows one to determine not only the energy splitting for individual iron $t_{2g}$ orbitals, but also energy of $d_{yz}$ orbital since (providing $\Delta/3 = V/2$)

$$-E_{xy} + E_{yz} = \Delta/3 + V/2 \quad (7)$$

Results of simple calculations using Eqs. (5) and (6) are summarized in Table 1. It can be seen that $\Sigma g^2$-values are close to 16 for all the cytochrome *c* complexes. One would expect that Met-80 replacement in cytochrome *c* by another axial ligand (as shown in Table 1), should result in negative $E°$ shifts for such complexes by $V/2\lambda$ compared to His/Met-ligated cytochrome *c* [202]. However, as can be seen from Table 1, $\Delta E_{exp}$ shifts are several hundreds millivolts larger than expected on the basis of CF theory considerations. For example, the pyridine and cyanide-ligated forms lead, respectively, to 294 [205] and 665 mV [206] cathodic shifts in

Table 1
Effect of replacement of the sixth ligand in low-spin metalloproteins as reflected in EPR *g*-values, tetragonal ($V$), rhombic ($\Delta$) field splitting, redox potential shifts, $\Delta E_{exp}$, for resulting complexes (with respect to $E°'$ for ferricytochrome *c* at pH 7)[a]

| Axial ligands | $g_x$ | $g_y$ | $g_z$ | $V$ ($\lambda$) | $\Delta$ ($\lambda$) | $\Sigma g^2$ | $E°'$ (V) | $\Delta E_{exp}$ (V) |
|---|---|---|---|---|---|---|---|---|
| His/Met[b] | 1.25 | 2.25 | 3.06 | 1.47 | 2.67 | 15.99 | 0.265 | 0.000 |
| His/pyridine[d] | 1.48 | 1.99 | 3.29 | 1.38 | 1.41 | 15.51 | −0.029 | −0.294 |
| His/Lys[c] | 1.13 | 2.05 | 3.33 | 1.17 | 3.34 | 16.57 | −0.055 | −0.320 |
| His/$CN^-$[d] | 1.15 | 2.01 | 3.26 | 1.17 | 3.42 | 15.99 | (−0.400) | (−0.665) |
| His/His[c] | 1.50 | 2.25 | 3.02 | 1.83 | 3.56 | 16.43 | −0.150 | −0.415 |
| His/Im[c] | 1.51 | 2.26 | 2.96 | 1.88 | 3.37 | 16.30 | −0.161 | −0.426 |

[a] All the *g*-values apply to complexes of horse-heart ferricytochrome *c*, except for His/His-ligated cytochrome $c_3$ from *Desulfovibrio desulfuricans* (Norway strain). The spin–orbit coupling constant $\lambda = 741$ $cm^{-1}$ [197].

[b] EPR data taken from Ref. [29].

[c] EPR data taken from Ref. [197].

[d] EPR data taken from Ref. [214].

respect to $E°'$ for the His/Met-ligated cytochrome *c* (pH 7). As evident from Table 1, the most negative $E°$ shifts (except for cyanide) occur in the presence of imidazole ($pK_a = 6.65$) and histidine ($pK_a \sim 6.3$), the latter two showing somewhat higher basicity than pyridine ($pK_a = 5.22$). One could consider that a reduction potential is simply a measure of the ratio of ligand binding constants for the Fe(III) and Fe(II) so that $\Delta E_{exp} \sim \log (K^{III}/K^{II})$ [5]. Correspondingly, a potential shift of 294 mV, observed during the Met-80 replacement by pyridine, would mean that the log of the ratio of the Fe(III) to Fe(II) binding constants changes by $0.294 \times (nF/2.303RT) = 5.0$, or the equilibrium constant $K_{eq}$[cytc(III)] has increased over $K_{eq}$[cytc(II)] by a factor of $10^5$ upon binding this ligand in place of Met-80! Even larger potential shifts were noticed in a recent study by Liu et al. [49], who report that replacement of Met-80 in ferricytochrome *c* by Im, 1-MeIm, and 1-EtIm results, respectively, in 0.426, 0.359, and 0.327 V cathodic shifts relative to $E°'$ for the native cytochrome *c*. Again, one could assign such large experimental $\Delta E$ shifts mainly as due to a larger affinity of these exogeneous ligands to ferriheme as compared to ferroheme. However, this is not the only reason for the observed behavior. In fact, $\Delta E_{exp}$ is also expected to be affected by changes in the solvent accessibility to the heme during such complexation reactions and, furthermore, steric changes and rearrangement of amino acid residues in the heme cavity introduced by the exogeneous ligand. It is reasonable to assume that a small ligand such as cyanide will introduce different steric changes in the heme cavity as compared to bulkier ligands such as pyridine or imidazole. Indeed, Met-80 replacement by pyridine seems to affect conformations of eight amino acid residues, all being located on the Met-80 side of the heme. Such conformational changes involve the disappearance of the $3_{10}$ helix (67–70), type II turn (75–78) and the distortion of the 50's helix, as also detected using 2D EXSY spectroscopy [207]. Interestingly, equilibrium constants for the binding of pyridine and its 3-methyl- and 4-methyl derivatives [208] suggest that pyridine causes less severe perturbation in the 3D structure of cytochrome *c* than the latter two ligands. Also, increasing values in the entropic $\Delta S°$ term in the order py < 3MePy < 4MePy (148, 272 and 548 J $K^{-1}$ $mol^{-1}$, respectively) suggest that the last ligand causes the most serious structural perturbation in the heme environment. Thus it can be concluded that relative stabilities of cytochrome *c* complexes of pyridine, imidazole and their alkylated analogs, do not seem to depend exclusively on the affinity of these molecules for the heme iron, but also on the extent of steric changes introduced in the protein during such complexation reactions and, importantly, on the hydrophobicity of the newly restructured heme cavity. Correspondingly, one would expect significant differences in reactivity and ET properties of cytochrome *c* complexes in which Met-80 is replaced by exogeneous ligands (vide infra), as compared to native cytochrome *c*. In the above discussion we have pointed out effects of various axial ligands on $E°$; however, we have not paid any attention to how such axial-ligand replacement reactions affect the kinetics of heterogeneous ET reactions between cytochrome *c* and the electrode.

The total reorganization energy for a given redox couple (i.e. ferri-/ferrocytochrome *c*) depends on the degree of electron delocalization in the system that is,

on the effective reactant and product radii, i.e. as well as on the polarizability of the medium surrounding the redox center (protein residues and solvent molecules). The latter determine the magnitude of $\lambda_{os}$ (Section 2.1), while the relative changes in bond lengths and bond angles during the redox transition, and the stiffness of force constants in both oxidation states are contained in the inner-shell component

$$\lambda_{in} = 1/2\Sigma\, k_j(\Delta x_j)^2 + 1/2\Sigma\, f_b(\Delta\theta)^2 \quad (8)$$

where $k_j$ are normal-mode force constants, $\Delta x_j$ are differences in equilibrium bond lengths between the reduced and oxidized forms of a redox center, $f_b$ are angle-dependent force constants, while $\Delta\theta$ represents differences in bond angles between two oxidation states [31].

As mentioned above, all of the combinations of axial ligands in cytochromes containing hexacoordinated heme, i.e. methionine, histidine, cysteine and lysine, are able to keep the Fe(III) ion in its low-spin state, just as $CN^-$, $N_3^-$, or other strong-field ligands. However, in contrast with small inorganic ligands, the former serve at the same time as protein building blocks, which introduces a certain degree of rigidity in the system. For example, His-18 and Met-80, are locked above and below the porphyrin plane in cytochrome *c*, and there occurs only little change in ligand geometry during the redox process. This is quite different from hexacoordinated low-spin porphyrins in the bulk of the solution, where ligands are more or less free to rotate. Another striking difference between bis-ligated free porphyrin in solution and that contained in the protein interior, is the degree of the porphyrin ring deformation. While iron porphyrins are usually planar in solution, once placed in the protein interior, they are significantly deformed, having differing geometries in oxidized and reduced state. Two-dimensional total correlation spectroscopy and Overhauser enhancement and exchange spectroscopy (NOESY–TOCSY) measurements in solution [6] have shown that heme in horse-heart cytochrome *c* remains non-planar with a distorted saddle-shaped geometry in both oxidized and reduced state. Such differences in porphyrin ring geometry were shown to affect the overlap between the d-orbitals of iron and the porphyrin π-electrons in bis-ligated model porphyrins containing bulky substituents on axial ligands [209]. Heme distortions in both oxidized states of the cytochrome *c* tend to minimize Fe–His as well as Fe–Met bond length changes and were suggested to play an important role in fine tuning of ET between the cytochrome *c* and its biological redox partners [210,211]. Since the passage from the reactant (ferricytochrome *c*) to the reaction product (ferrocytochrome *c*) is accompanied by relatively small changes in $\Delta\theta$ and $\Delta x_j$, the $\lambda_{in}$ contribution to overall reorganization energy is also small (e.g. a few kJ $mol^{-1}$), ca. fourfold lower than is the combined contribution of protein and water molecules surrounding the heme [211]. Correspondingly, the electrochemical kinetic studies indicate that $k^{\circ}_{het}$ for the one-electron reduction of horse-heart cytochrome *c* certainly exceeds 0.1 cm $s^{-1}$ [212,213], while Bond and co-workers [25] have concluded that $k^{\circ}_{het}$ measured on carbon ultramicroelectrodes might actually exceed 1 cm $s^{-1}$. In part, the magnitude of such large value for the heterogeneous rate constant is dictated by the relatively low total reorganization energy $\lambda = 0.58$ V [117,118]. It should be noted that eventual electron tunneling (non-adiabacity of the

electrode reactions) would tend to decrease $k^{\circ}_{het}$ exponentially with increasing heme-electrode distance (cf. Section 2.3). In the next paragraph we shall point out on the effect of axial ligand replacement in ferricytochrome *c* (i.e. lysine or pyridine) on the kinetics of its redox reactions.

Preliminary cyclic voltammetric data, and their numeric simulation [205] have revealed that the addition of 0.69 M pyridine to native ferricytochrome *c* solution leads to a negative $E^{\circ\prime}$ shift of 0.236 V, while simultaneously the rate constant $k^{\circ}_{het}{}'$ [215] decreased ca. 100-fold on a 2-mercaptoethanol-modified gold electrode (1.2 mM cyt *c*, 0.1 M $NaClO_4$, 0.02 M phosphate buffer, pH 7.0). According to Ref. [215], Met-80 can be replaced by the weakly basic pyridine molecule ($pK_a = 5.22$); however, this occurs only at relatively high pyridine concentrations ( $> 0.45$ M). On the other hand, Viola et al. [216] have assigned absorbance changes, recorded for native ferricytochrome *c* in the 390–450 nm region, in the presence of pyridine ($c_{Py} < 0.316$ M, 0.1 M phosphate buffer, pH 7.5), as due to pyridine binding to the heme iron with a dissociation equilibrium constant $K = 0.31$ M. Recent two-dimensional exchange $^1$H-NMR spectroscopy (2D EXSY) experiments [204] indicate that the pyridine-bound form of cytochrome *c* shows relatively low stability at pH > 6, and it is readily displaced by Lys-73 (and other amino acid residues) to yield the alkaline form of cytochrome *c*. A mixture of native cytochrome *c* and pyridine-bound form can be obtained in the pH range from 5 to 6, while native cytochrome *c*, pyridine-bound cytochrome *c* and the lysine-form can exist simultaneously at neutral pH. Apparently, pyridine interacts with cytochrome *c* in such a way as to stabilize the alkaline form even at neutral pH.

According to voltammetric data taken from Ref. [217], the alkaline transition results in the negative $E^{\circ\prime}$ shift from $+0.08$ V to $-0.17$ V versus Ag/AgCl reference electrode (pH 5.4). As evident from the inset in Fig. 3(B), the increase in the solution pH from 5.4 to 10.2 is accompanied by an almost complete disappearance of the 695 nm-band due to Met-80 replacement by Lys-73 and Lys-79 (both of these lysine-ligated forms exist in alkaline solutions pH < 10) [218,219]. Numeric simulation of these voltammetric data [215] suggests that the apparent rate constant for the ferricytochrome *c* reduction decreases from $1.5 \times 10^{-3}$ to $9 \times 10^{-6}$ cm s$^{-1}$ ($\alpha = 0.5$, in both cases) when going from solution of pH 5.4 to 10.12 (ca. 167-fold). It should be noted that the apparent rate constant might be affected by double-layer effects PySSPy-modified gold electrode [220], and the electrode reactions can actually be even faster than determined here. The fact that conformational changes in cytochrome *c* during the alkaline transition represent the rate-limiting step in the electrode reaction, as observed in the case of yeast 1-*iso*-cytochrome *c* on carbon electrodes [221], cannot also be excluded. The observed response could be simply due to a pH-induced change in electrode reaction mechanism (an electrochemical square scheme), as described in Refs. [109,221].

As we have shown above, all the complexes presented in Table 1 are low-spin, and the electronic overlap between $d_{yz}$ and $d_{xz}$ orbitals with both axial ligands (His-18 and Met-80) is much stronger than that between $d_{xy}$ and $d_{x^2-y^2}$ orbitals located in the porphyrin plane. This leads to the charge delocalization in the direction of axial ligands rather than on the porphyrin ring. As shown above,

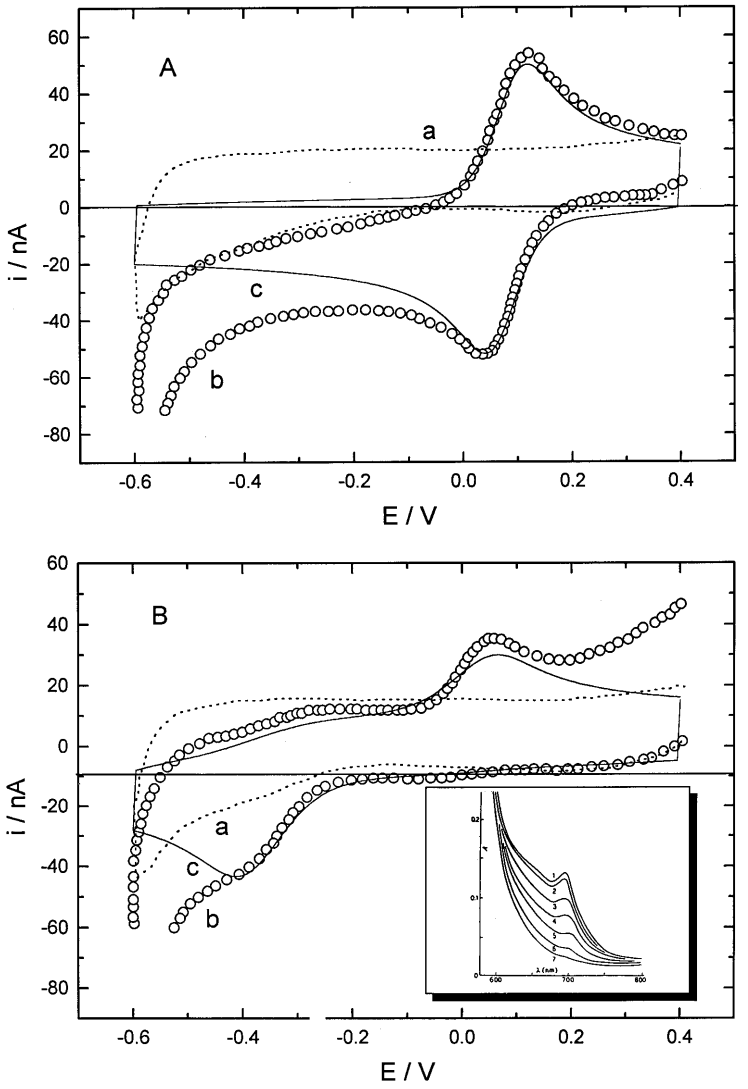


Fig. 3. (A) Cyclic voltammograms recorded for the ferricytochrome *c* on PySSPy-modified Au electrode: (a) in the solution of the supporting electrolyte of pH 5.07; (b) after addition of horse-heart cytochrome *c* (0.34 mM); (c) simulated voltammogram ($k^{\circ}_{het}{}' = 1.5 \times 10^{-3}$ cm s$^{-1}$, $\alpha = 0.5$, $E^{\circ\prime} = 0.08$ V, $R_s = 50$ Ω, $C_d = 20$ μF cm$^{-2}$). Scan rate 0.01 V s$^{-1}$. (B) Experimental (b) and simulated (c) voltammograms recorded for the alkaline form of cytochrome *c* in a solution of pH 10.12. Parameters used in the simulation: $k^{\circ}_{het}{}' = 9 \times 10^{-6}$ cm s$^{-1}$, $\alpha = 0.5$, $E^{\circ\prime} = -0.17$ V, $D_{ox} = D_{red} = 1 \times 10^{-6}$ cm$^2$ s$^{-1}$, $R_s = 50$ Ω, $C_d = 20$ μF cm$^{-2}$. Scan rate: 0.01 V s$^{-1}$. Inset illustrates the effect of the solution pH on the 695 nm band of cytochrome *c*: (1) 5.4, (2) 6.56, (c) 7.66, (4) 8.04, (5) 8.44, (6) 9.0, (7) pH 10.05 (all the experimental data taken from Ref. [217]).

Met-80 replacement by Lys73 (and/or Lys-79) leads to more than two orders of magnitude decrease in $k^{\circ}_{het}$. However, the situation in the presence of pyridine is complicated by alkaline transition which favors in neutral solution both pyridine- and lysine-ligated cytochrome *c*. It is important to realize that bulky ligands such as pyridine, histidine, or imidazole (containing delocalized system of π electrons) should provide larger effective reactant radii as compared to small in size inorganic ligands, i.e. $CN^-$, $OH^-$ or $SCN^-$. As a result, one would expect faster kinetics of ET for these large heterocyclic ligands compared to inorganic (on the basis of simple Marcus theory concepts). On the other hand, differing affinity of these ligands to heme iron in oxidized versus reduced state is likely to result in increased probability of their removal (and the replacement by another ligand) during the redox process. This in turn should contribute to the $\lambda_{in}$ term in Eq. (8) and, therefore, decrease the heterogeneous ET rate. However, one should not forget that completely new ET pathways could be established during such ligand-replacement reactions. As mentioned above, serious conformational changes on the protein occur in the process, so that the tunneling distance between the heme iron and the protein surface (as well as heme-electrode distances) might change at the same time. Importantly, the outer-shell reorganization energy $\lambda_{os}$ depends not only on the effective reactant radius of the newly formed complex but also on the polarizability of solvent molecules and amino acid dipoles surrounding the redox center. Ligand exchange, conformational changes in the protein and possible differences in the solvent accessibility to the heme in such complexes should be reflected in the experimentally measured $k^{\circ}_{het}$ and magnitude of the total reorganization energy. More detailed electrochemical experiments on the effect of pyridine, imidazole, cyanide and other complexes on the kinetics of cytochrome *c* reduction as a function of pH, are in progress in this laboratory.

### *2.3. Electron tunneling*

Theoretical estimates of $k_{et}$ for ET processes taking place in biological as well as heterogeneous systems are often complicated due to strong variation in reaction adiabaticity with increasing electron donor–acceptor distance, affecting thus the magnitude of the pre-exponential factor A in Eq. (1). The latter may vary by many orders of magnitude depending on the electron donor–acceptor separation distance, their mutual orientations and on the electronic conductivity of the medium separating the two redox centers [15,16,20–23]. In the next paragraph, we will illustrate using few examples of biological, as well as heterogeneous systems, some typical problems one can encounter when trying to assess the degree of the reaction adiabaticity.

Two redox centers in bovine cytochrome *c* oxidase, namely, hemes a and $a_3$, adopt mutual geometries where the porphyrin planes are parallel to each other (being separated by the aromatic ring of phenylalanine) at an edge-to-edge distance of only about 5 Å [3]. Providing edge-to-edge ET would be operative, electron-transfer reactions should be highly adiabatic. However, the experimentally measured rate constant ($k_{et}$) values for the intramolecular electron transfer between the

two hemes fall in the range from $10^4$ to $3 \times 10^5$ $s^{-1}$ [222,223], which indicates relatively slow ET kinetics at such a short distance. Providing that the electron would tunnel from iron to iron across the short peptide chain terminated on either side by histidine (His-376 and His-378) in a bond-to-bond fashion, the tunneling distance would be ca. 13 Å, and ET reactions would manifest a lower degree of adiabaticity than in the former case. The above mentioned example illustrates well a situation where the degree of the reaction adiabaticity is practically unknown, in spite of the crystallographic structure of the enzyme being known to 2–3 Å resolution [1]. Electron transfer between the two hemes could take place through bonds, through space between two metal centers, between the heme edges [27] or, other electron entry sites could be operative [224]. In the second example, the edge-to-edge and iron-to-iron separation distances between two hemes in cytochrome *c*/cytochrome *c* peroxidase (CcP) complex are 18 and 24 Å, respectively. Electron transfer reactions at such large distances are expected to be highly non-adiabatic [20]. Yet, experimentally measured rate constant $k_{et} = 2.7 \times 10^4$ $s^{-1}$, is of the same magnitude as that observed for cytochrome *c* oxidase. Nevertheless, a significant driving force in the ET reaction exists in the case of cytochrome *c*/CcP complex ca. 0.46 eV [16,20], while it is only ca. 0.18 eV between the hemes a and $a_3$ in cytochrome *c* oxidase [125,225–227].

Even though the metalloproteins, as discussed above, show a significant degree of structural complexity, the distances between the redox centers are more or less fixed. The same cannot be said once such metalloproteins are brought by diffusion to the electrode/solution interface. In the latter case, distances between the redox center (i.e. heme iron) and the electrode are rarely known. However, it still holds here that $k_{het}$ should decrease rapidly with increasing electrode-redox center separation distance, leading to the diminution in the pre-exponential factor A in Eq. (1). The effects of reaction adiabaticity, respectively, non-adiabaticity on kinetics of the heterogeneous ET are demonstrated on the following two examples:

1. heme octapeptide (OP), a low-spin model compound for the cytochrome *c* containing *N*-methyl-DL-methionine and histidine as axial ligands and eight amino acids of the same sequence as found in the protein (no spin changes during the redox process);
2. native form of cytochrome *c* (His-18/Met-80 ligation)

Let us consider first a simple one-electron processes represented by Eqs. (9) and (10)

$$\text{Fe(III)–OP} + e^- \rightarrow \text{Fe(II)–OP} \tag{9}$$

$$\text{Fe(II)–OP} - e^- \rightarrow \text{Fe(III)–OP} \tag{10}$$

Providing the heme octapeptide could approach the gold electrode surface to the distance $\delta r_e = 3$ Å, the probability ($P_o$) with which the so-called activated complex would be formed, and electron would cross the energy barrier, can be expressed as [228]

$$P_o = 1 - \exp[(-|H_{RP}|^2/(h\nu_n)(\pi^3/\Delta G^* RT)^{1/2}] \tag{11}$$

where the electronic coupling matrix element $|H_{RP}|^2$ expresses the effective electronic-coupling strength between the reactant and product in the transition state, $h$ is the Planck constant, $\nu_n$ and $\Delta G^*$ have the same meaning as in Eq. (2). The electronic transmission coefficient ($\kappa$) is then proportional to the probability of ET

$$\kappa = 2P_o/(1 + P_o) \tag{12}$$

Providing $P_o = 1$, it follows that the transmission coefficient will be equal to unity, and the electron transfer can be considered as perfectly *adiabatic*. According to classical Landau–Zener model [229,230], $\kappa$ depends on the effective nuclear frequency $\nu_n$, and on the electronic frequency $\nu_{el}$ at which electron crosses the saddle point [231]

$$\kappa = 2[1 - \exp(-\nu_{el}/2\nu_n)]/[2\text{-}\exp(-\nu_{el}/2\nu_n)] \tag{13}$$

Since the transmission coefficient is equal to unity, the heterogeneous rate constant takes the form of Eq. (2), where $K_p$ is determined by the work which is to be done in the system in order to bring reactant molecules to the reaction plane ($rp$), located at a distance of $\delta r_e$ from the electrode surface (and to remove product molecules from $rp$)

$$K_p = \delta r_e \exp(-\Delta G^\circ/RT) \tag{14}$$

and

$$\Delta G^\circ = nF(E - E^\circ - \varphi_{DL}) \tag{15}$$

where $E$ is the applied electrode potential, $\varphi_{DL}$ is the double layer potential, and other symbols have their usual meaning. The heterogeneous rate constant $k_{het}$ appears in cm $s^{-1}$ since it is proportional to the reaction zone thickness $\delta r_e$ [cm] and $\nu_n$ [$s^{-1}$]. Here, we assume that neither reactant nor product undergo adsorption on the electrode surface (for the theoretical treatment of kinetics associated with the surface-confined species see Refs. [232,233]). The situation dramatically changes once the heme is placed in the hydrophobic interior of cytochrome *c*, and logically, the theoretical treatment for both ET processes differs as well. This is because the electrode-redox center distance is no longer exclusively defined by the layer of water molecules in contact with the electrode surface, but also by the size of the protein itself (approximately 34 Å in diameter, spherical in shape), which prevents its heme from closer approach to the electrode surface. Moreover, the heme is asymmetrically placed within the protein envelope and the shortest bond-to-bond distance from the heme iron to the protein surface is about 13–14 Å. Electrode-surface modification by any adsorbate (i.e. thiol monolayer) will further increase the electron tunneling distance. At redox center separation distances larger than 8 Å, electrode reactions should be significantly non-adiabatic, where the transition state for the electron-transfer reaction must be formed many times before reactant molecules are successfully converted to product [15]. In the non-adiabatic limit, $\kappa \ll 1$, and is proportional to $\nu_{el}/\nu_n$, so that

$$k^\circ_{het} = \nu_{el}(\nu_n)^{-1}\delta r_e \exp(-\Delta G^*/RT) \tag{16}$$

The rate of ferricytochrome *c* reduction will gradually increase with the increasing overpotential up to the value where the reaction driving force ($-\Delta G°$) will become identical to the reorganization energy $\lambda$, the non-adiabatic ET process reaching its maximum rate

$$k_{na}(\max) = (4\pi^2/h)|H_{DA}^{eff}|^2/(4\pi\lambda k_B T)^{-1/2} \quad (17)$$

the $|H_{DA}^{eff}|^2$ term is the maximum electronic overlap between the wavefunctions of propagating electrons at the Fermi level (donor states in the metal) and the acceptor states (i.e. the hole in $d_{yz}$ orbital of heme iron in ferricytochrome *c*). In the case of ET taking place between the tuna or horse-heart cytochrome *c* and a gold electrode modified by 11-hydroxy-1-undecanethiol, such a condition is reached at ca. $-0.6$ V versus SCE [117,118] (see Fig. 4(A)). The maximum rate constant can be extracted from the $\ln k_{na}$ versus $\eta$ dependence ($\eta = E - E°$) providing data can be extrapolated to very large overpotentials. At energies exceeding $\lambda$ of cytochrome *c*, that is for $\eta > -0.6$ V, $k_{na}$ will decrease, even though the reaction driving force is still increasing (Marcus inverted region) (Fig. 4(B)).

In the case of non-adiabatic heterogeneous electron transfer, in the quantum-mechanical description of ET, the nuclear frequency factor $\nu_n$ (Eq. (16)) is replaced by a Franck–Condon overlap (FC), representing the Boltzmann-weighted sum of overlaps of vibrational wavefunctions for reactants and products, and the interactions between the electronic states in the metal and the acceptor states in the reactant should be included. The dependence of the non-adiabatic heterogeneous constant on the energy of the electron in the metal then takes the form

$$k_{na} = (4\pi^2/h)|H_{kA}^{eff}|^2\rho_f \int \mathrm{DOS}(E)\{1 + \exp[(E_F - E)/RT]\}^{-1}\,\mathrm{d}E \quad (18)$$

where $H_{kA}^{eff}$ is the effective coupling strength between the metal electrode (averaged over the *k* values on the Fermi surface) and the electron acceptor, *k* is the wave vector in the metal, $\rho_f$ is the density of states at the Fermi surface (in the case of Au equal to 0.3 $eV^{-1}$ per atom), DOS(*E*) is the potential-dependent density of acceptor states for the reactant, and $E_F$ is the energy of electron at the Fermi level in the metal [234–236]. The FC factor can be estimated from the summation over all the normal-modes obtained, for example, from a resonance Raman spectroscopy experiment. The Franck–Condon factor is then given by

$$\mathrm{FC} = [4\pi\lambda RT)]^{-1/2} \exp[-(\Delta G° + \lambda)^2/4\lambda RT] \quad (19)$$

where $\lambda$ might include a low-frequency solvent mode (50–250 $cm^{-1}$) and a high-frequency, classical vibrational mode, for example, skeletal ring vibrations [169]. Detailed analysis of 13 vibrational modes of 4-cyano-*N*-methylpyridinium cation coupled to the reduction process and their incorporation into the theory of heterogeneous electron transfer has been recently reported by Selmarten and Hupp [237]. A similar type of analysis of resonance Raman spectra measured for the cytochrome *c* at the electrode/solution interface remains to be done.

Density of states for the ferricytochrome *c*, DOS(*E*), can be obtained simply by multiplying the Franck–Condon overlap by the surface concentration of electroactive cytochrome *c* molecules, $c_{ox}^{(s)}$, at a given electrode potential.

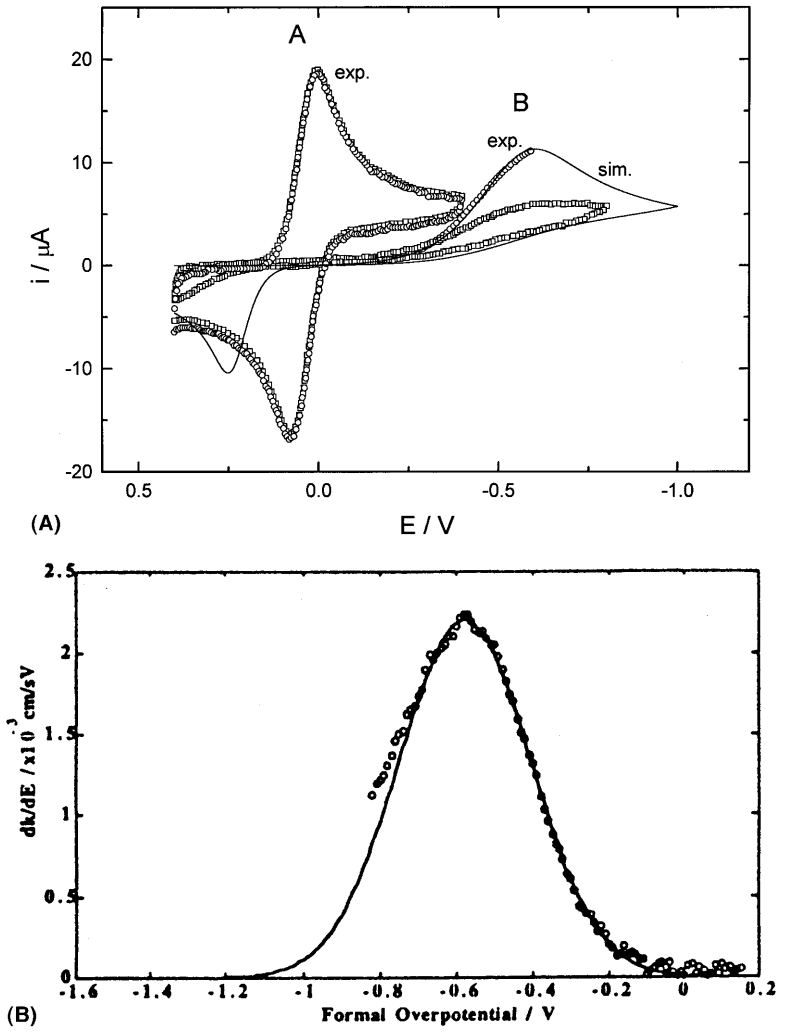


Fig. 4. (A) Cyclic voltammograms for cytochrome *c* isolated from horse heart (1.1 mM), (represented by circles), yeast (1.2 mM), shown as squares: (A) cyclic voltammograms recorded on 2-mercaptoethanol (horse-heart), 3-hydroxy-1-propanethiol (yeast); (B) recorded on a 11-hydroxy-1-undecanethiol-modified Au electrode (horse-heart, yeast). Supporting electrolyte: 1 M KCl containing 0.01 M phosphate buffer (pH 7) at 0.0°C. Scan rate: 0.5 V $s^{-1}$ (the experimental data taken from Refs. [117,118]). The voltammogram represented by the solid line comes from the numeric simulation of horse-heart cytochrome *c* reduction, oxidation on a $C_{11}$-hydroxylthiol-modified electrode at 0.0°C ($k^{\circ\prime} = 4 \times 10^{-6}$ cm $s^{-1}$, $\alpha = 0.255$, $E^{\circ\prime} = 0.023$ V, $D_{ox} = D_{red} = 4.7 \times 10^{-7}$ $cm^2$ $s^{-1}$). (B) Plot of density of states of tuna cytochrome *c* ($E^{\circ\prime} = 0.018$ V vs. SCE, $\lambda = 0.62$ eV) electroreduction on 11-hydroxy-1-undecanethiol-modified Au electrode, its Gaussian fit (solid line). The density of state distribution is the first derivative of the diffusion, double-layer-corrected rate constant, is shown as open circles.

$$\mathrm{DOS}(E) = c_{\mathrm{ox}}^{(\mathrm{s})}\mathrm{FC} \tag{20}$$

Surface concentrations of either reactant or product can be easily obtained from cyclic voltammetric data using the convolution method [83]. A simple mathematical analysis of the Gaussian-shaped $\mathrm{d}k_{\mathrm{na}}/\mathrm{d}\eta$ versus $\eta$ curve allows one to determine the total reorganization energy for a given redox couple [238], as shown for the tuna cytochrome *c* in Fig. 4(B). Some deviations from such Gaussian-shaped DOS($E$) curves were associated with ion pairing and, also due to the fact that electrons at overpotentials exceeding $\lambda$ can be also transferred from electronic states below the Fermi level [171]. The inelasticity of electron tunneling due to vibrational transitions in the thiol monolayer on gold (ca. 0.37 eV, corresponding to the carbon–hydrogen stretches at ca. 3000 $\mathrm{cm}^{-1}$) [171], has been suggested yet as another factor which might complicate reorganization energy determination.

It is important to realize that with the increase in the distance between the redox center and the electrode, the $|\mathrm{H}_{\mathrm{kA}}^{\mathrm{eff}}|^2$ term in Eq. (18) will decrease strongly. Elastic electron tunneling through the alkanethiol monolayers on Au has been frequently treated in electrochemical studies using Hopfield's model, which predicts that $|\mathrm{H}_{\mathrm{DA}}|^2$, as well as $k_{\mathrm{na}}(\mathrm{max})$ should decay exponentially with increasing donor–acceptor separation distance [15]

$$|\mathrm{H}_{\mathrm{DA}}|^2 = |\mathrm{H}_{\mathrm{DA}}^{\circ}|^2 \exp[-\beta(d - \delta r_{\mathrm{e}})] \tag{21}$$

where $d$ is the separation distance between the redox center and the electrode (Å), $\beta$ is the distance-decay constant ($\mathrm{Å}^{-1}$), describing the contribution of the bridge separating electrode and acceptor states to propagating wavefunction and $\delta r_{\mathrm{e}}$ is the minimum distance between the redox center and the electrode at which electron transfer would still be adiabatic (i.e. $\kappa = 1$). Providing all the potential drop occurs in the monolayer, the expression for the distance-decay constant can be then written as

$$\beta(\varepsilon, \eta) = (4\pi^2/h)(2m_{\mathrm{e}})^{1/2}(V_{\mathrm{B}} - \varepsilon + e\eta/2)^{1/2} \tag{22}$$

where $m_{\mathrm{e}}$ is the electron mass in vacuum, and $V_{\mathrm{E}}$ is the electrode potential-dependent height of the energy barrier, and $\varepsilon$ is the energy of the electron in the metal [83]. The latter expression is greatly simplified at the zero overpotential, where $\beta = 1.025/V_{\mathrm{B}}^{1/2}$ [239]. Experimentally, $\beta$ can be obtained from ln k versus $n$ dependence ($n$ is the number of identical bridging units (methylene groups) in the alkanethiol monolayer. In this case, Hopfield's superexchange model works relatively well, as also demonstrated in previous electron tunneling studies [83]. However, the latter model is simply not applicable to cytochrome *c* reduction and oxidation taking place on promoter-covered gold electrodes. In the following sections we will demonstrate that not only the heme-electrode separation distance, but also formation of the H-bonding contacts between the protein surface and the hydrophilic thiol monolayer on the electrode surface, affect kinetics of the heterogeneous charge-transfer process. Providing the latter cannot be established for reasons related to the molecular protein structure and of the adsorbate itself, the electron transfer rate is slowed down to such an extent that virtually no electrochemical

response of the heme protein is observed in a relatively large range of electrode potentials. This seems to hold even for electrodes covered by very thin adsorbate films $d \ll 10$ Å (cf. Fig. 8).

## 3. Effects of electrode-surface modification on the electrochemistry of cytochrome *c*

### *3.1. Hydroxyl-terminated self-assembled monolayers*

As has been discussed in previous sections, the total reorganization energy for the ferri/ferrocytochrome *c* couple can be obtained experimentally in a simple electrochemical experiment on Au electrode covered by long-chain ω-hydroxyalkanethiol [117,118]. There exist several advantages of such an approach over a solution experiment involving this heme protein and a given chemical reducing and/or oxidizing reagent:

1. electrode serves as a clean donor (or acceptor) of electrons;
2. the $\Delta G°$ term in Eq. (1) can be varied in a controlled manner well into the Marcus inverted region;
3. problems associated with the long-range electrostatic interactions between the electrode and the protein, as often experienced at unmodified electrode surfaces, are practically non-existent;
4. the experiment itself is relatively facile and, furthermore, a relatively good experimental precision in $\lambda$ determination can be achieved;
5. unusually short experimental times are required as compared to a classical activation enthalpy measurements from the Arrhenius-type of plots. For example, the kinetic data necessary for the $\lambda$ estimate for the ferri/ferrocytochrome *c* couple can be collected in 2 s in the potential range from 0 to $-1$ V at the scan rate of $v = 500$ mV $s^{-1}$ (cf. Fig. 4(A,B)).

However, one of serious problems, which might eventually complicate kinetic measurements, is the possibility that metalloproteins adsorb on such promoter-covered electrode surfaces. In fact, recent electrochemical experiments combined with in situ techniques such as SERRS [130,131], FTIR [132,133], and UV–vis electroreflectance [134–138], have established that cytochrome *c* undergoes adsorption on the majority of promoter-covered electrode surfaces. Lion-Dagan et al. [145] have also shown in their microgravimetric quartz-microbalance experiment that cytochrome *c* adsorption takes place even at bis(4-pyridyl) disulfide- and 4-mercaptopyridine-modified gold electrodes, often considered among electrochemists as non-adsorbing interfaces for this metalloprotein. It is noteworthy that the corresponding adsorption kinetics are rather sluggish, and approximately 10 min are required in order to reach plateau in the $\Delta m - t$ plot, corresponding only to ca. 20% of a cytochrome *c* monolayer. Adsorption of this protein seems to be much more important on mercaptoalkanoic acid-covered gold electrodes, reaching a maximum possible surface coverage of approximately 15 pmol $cm^{-2}$ [240]. It follows that the time scale of the electrochemical experiment (necessary to collect the kinetic data) should be carefully considered in advance.

Among common promoters of ET in horse-heart cytochrome *c*, only ω-hydroxyalkanethiol-modified gold electrodes were suggested to completely eliminate adsorption of the reactant. Also, some polymer films including poly(ethylene glycol), oligo(ethylene glycol)-terminated SAMs, or hydroxylated silica surfaces, all manifesting very low advancing contact angles for water and high wetabilities, can be very useful when trying to avoid protein adsorption at the solid/liquid interface [241–245]. In spite of large surface hydrophilicity of hydroxyl-terminated SAMs, the cytochrome adsorption might not be avoided in all cases. In fact relatively small structural changes on the protein exterior can be responsible for the increased protein adsorptivity on SAMs or, eventually, its aggregation at the electrode/solution interface. The immediate heme environment in the hydrophobic protein interior is very similar in both the yeast and the horse-heart cytochrome *c*, and corresponding $E^{\circ\prime}$ values are also very similar for both proteins. However, there exist significant differences in the distribution of charge and functional groups on their surfaces. Consequently, remarkable differences in kinetics of their electroreduction were noticed on mixed OH/COOH-terminated SAMs [246] (see also Section 3.2). Fig. 4A illustrates such differences in the electrochemical behavior of the yeast- and the horse-heart cytochrome *c* on $C_2$ or $C_3$, respectively, $C_{11}$ ω-hydroxyalkanethiol-modified electrodes. Cyclic voltammograms for both proteins, taken from Refs. [117,118], are represented here by circles and squares, and are shown together with the simulated voltammograms [215]. Note, that although there exists a relatively good agreement between the simulated and experimentally measured cathodic currents for the horse-heart cytochrome *c* ($k^\circ = 4\times10^{-6}$ cm $s^{-1}$, $D_{ox} = D_{red} = 4.7\times10^{-7}$ $cm^2$ $s^{-1}$, $\alpha = 0.255$, $T = 0.0$°C), the maximum cathodic current for the yeast cytochrome *c* at $-0.6$ V is ca. twofold lower. Surprisingly, cyclic voltammograms for both proteins are practically identical on $C_2$ and $C_3$ ω-hydroxyalkanethiol-covered Au electrodes (Fig. 4(A)). There exist at least two explanations for the observed phenomenon.

1. There is practically no adsorption of the horse-heart cytochrome *c* at $C_{11}$ SAMs, while the adsorption of the yeast cytochrome *c* is quite sizeable. In the latter case, the observed reduction in the cathodic current could be consistent with the blocking of the electrode surface by electroinactive (i.e. denaturated) protein molecules. This could also explain changes in the shape of the cyclic voltammogram (i.e. the transition from the spherical to linear diffusion at the electrode surface represented as a collection of microelectrodes). There is no adsorption of both metalloproteins at short-chain $C_2$ and $C_3$ ω-hydroxyalkanethiol films.
2. There is no adsorption of both cytochromes on the $C_{11}$ hydroxyalkanethiol SAMs. The observed effect is exclusively due to a poor electronic coupling between the yeast cytochrome *c* and the gold electrode [117]. In other words, the cathodic current measured as a function of electrode potential depends not only on the surface concentration of the electroactive species (the density of acceptor states), but also on the effective electronic coupling $|H_{kA}^{eff}|^2$ between the protein and the electrode (as evident from Eq. (18)). Such differences in the electronic coupling have been tentatively explained [118] as due to the fact that the yeast cytochrome *c* might be in direct contact with OH terminated at $C_{11}$ ω-hydroxy-

alkanethiol monolayer, with water layer excluded, while the horse-heart cytochrome *c* is electronically coupled stronger to the electrode since the water layer is being preserved on the Au–S–$C_{11}$OH surface.

Additional in situ spectroscopic or electrochemical quartz microbalance measurements will be required in order to confirm (or exclude) a strong adsorption of yeast cytochrome *c* on $C_{11}$OH-terminated SAMs.

As is evident from Fig. 4(B), once the overpotential is raised to ca. $-0.6$ V, the reaction driving force equals the reorganization energy $\lambda$, and the electron tunnels from the electronic donor states at the Fermi level of metal into the half-filled $d_{\pi}$–e($\pi$) orbital in cytochrome *c* at the maximum rate. Since the film composed of chemisorbed 11-hydroxy-1-undecanethiolate on the electrode surface contains densely packed aliphatic chains, the access of the protein to the electrode surface should be defined by the monolayer thickness (ca. 13 Å). Previous kinetic experiments on ω-hydroxyalkanethiol SAMs on gold of varying chain length [118,172,238,247,248] have revealed that in the majority of cases, the electron will tunnel across the aliphatic chain rather than through space. Even though the electron is physically transferred through the monolayer, one cannot talk about the reduction (electronation) of adsorbate molecules in the real meaning of the word, since the electron energy at $-0.6$ V is significantly lower than is the LUMO of adsorbate molecule (measured in respect to vacuum). The $C_{11}$-hydrocarbon chain is terminated by an OH group of much higher polarizability than that of methyl head group in the *n*-alkanethiol film; however, of somewhat lower polarizability than those of $NH_2$ or SH terminal groups [249]. Recent infrared reflection-absorption spectroscopy and contact angle measurements, [250] indicate that hydroxyl-terminated $C_{16}$ thiol SAMs are highly hydrated by water molecules, and hydrogen bonding interactions could be detected between the terminal groups. The advancing contact angle for $D_2O$ on OH-terminated SAM was 10°, while on methyl-terminated SAM it was as high as 112°. It appears, that such a water layer on SAM surfaces seems to be critical in order to establish favorable H-bonding interactions between the protein and monolayer, and is a prerequisite for the heterogeneous charge transfer between the electrode and protein.

Let us first assume that the cytochrome *c* molecule is brought by diffusion from the bulk of the solution to the electrode/solution interface. At this point some considerations about the electrostatics at the Au/thiol/solution interface should be made. Horse-heart cytochrome *c* is a highly charged protein at pH 7 ($q = 7+$), even though in phosphate solutions as used in Refs. [117,118], the effective charge of the protein is only $+2.4$, diminished by the phosphate and chloride binding on the protein surface [118]. The latter estimate is in a good agreement with the effective charge of the protein ($q = +3$) determined in neutral phosphate buffer solutions in Refs. [123,124]. On the other side of the interface, the potential drop across the SAM drops rapidly with increasing distance from the electrode surface; however, an excess of negative charge will certainly exist at the interface at a potential of ca. $-0.6$ V (note that potential of zero charge for the OH-terminated SAM is ca. $-0.07$ V versus SCE) [247]. It is also reasonable to assume that the positively charged cytochrome *c*, except for the translational motion, undergoes

rotational movements approximately once per 6 ns [119]. Electrostatic long-range forces at the interface might act as a torque and bring the protein into the appropriate conformation for the electron transfer to occur [115,116]. Since a projected geometric surface area of a single cytochrome *c* molecule on the electrode surface is ca. 900 $Å^2$, one would expect to find 20–25 hydroxyalkanethiol in such a circular area on the electrode surface. It is important to realize that among those adsorbate molecules covered by an adsorbed water molecule [250], several of them might establish SAM–water–protein bridges and/or direct H-bonding contacts with the amino acid residues on the cytochrome *c* surface. However, only one of those thiol chains on the metal surface is required to adopt the required geometry and conformation to allow for electron transfer to (from) cytochrome *c* to occur. The main goal in modern bioelectrochemistry is to identify how and where exactly on the protein surface such promoter/protein bridging contacts are being established and, furthermore, how the electron travels beyond the monolayer to (from) the heme iron buried in the protein interior. Some insight into the nature of interactions between SAMs (i.e. terminated by OH, COOH or $SO_3H$ groups) and hydrophilic molecules (containing COOH or $NH_3^+$ groups) can be obtained from recent grazing incidence angle FTIR experiments on Langmuir–Blodgett films [251], and surface plasmon resonance measurements [252] on self-assembled monolayers.

Let us assume that cytochrome *c* remains in the double-layer (DL) region for several hundred nanoseconds, or more, in a search for the appropriate configuration for the electron transfer to occur. The probability that the protein would undergo the electronation reaction is then expected to be proportional to the time spent by cytochrome *c* in the DL-region and the intensity and sign of the electric field. Providing the excess of the negative charge at the metal/monolayer interface is too high, the positively charged protein gets trapped at the interface and its rotation is frozen due to the strong electrostatic interactions between the electrode and the positively charged protein residues. Under the conditions of very high charge density at the electrified interface, protein/SAM interactions might become so strong that rotational movements of protein slow down to such an extent that this process becomes the limiting step of the electrode reaction. The most striking example of such a situation we shall observe on COOH-terminated SAMs (Section 3.2). The main difference between the present concept of ET and previous models [15] is only in the time spent by the redox protein in the DL region. In the latter work, the steric factor ($S$) necessarily introduces a certain degree of rigidity into the system and lowers the ET probability ($P$) taking into account the fact that the heme is asymmetrically placed in the protein, and the heme cleft occupies only 0.08% of the protein surface area. Here, we assume that $P$ is much higher due to the fact that at the negatively charged interface the protein will survive for a certain amount of time, which increases its chances to find appropriate conformation for the ET to occur. It is also claimed that electron transfer will occur with much higher probability providing an amino acid residue located on the protein surface, and being implicated directly in the electron transfer, forms H-bonding contact with the promoter of electron transfer adsorbed on the electrode surface, compared to the situation where such hydrogen bonding is not possible. Several examples supporting this view will be presented in the following sections.

In order to continue beyond the monolayer, we will have to decompose the electron's pathway into smaller segments between the protein surface and the heme iron. The electron has to cross the SAM, layer of water molecules, and finally to be transferred across the peptide backbone (eventually, H-bonding contacts in the protein interior) to get to the heme iron. The question arises at this point what is the distance between the electron donor and acceptor and, also, how should the kinetics slow down for a certain electron tunneling distance between the heme iron and electrode. Hsu and Marcus [235,236] have recently demonstrated that in the case of the ferrocene (Fc) molecule covalently attached to the electrode surface via a simple bridge composed of repeating methylene units, the electronic coupling $|H_{kA}^{eff}|^2$ decreases with increasing number of methylene units from 2 to 11 by about six orders of magnitude. In fact, the electron tunneling across Au–S–$C_{11}$Fc and Au–S–$C_{11}$OH should not differ significantly since the tunneling decay constant in both cases is close to 1.1 per $CH_2$ unit; the latter value applies to the reduction of freely-diffusing transition-metal complexes [171]. Since cytochrome *c* is a molecule of relatively large size (ca. 3.4 nm in diameter), it is not expected to penetrate into the pinholes in the SAM, so that the standard rate constant for the ferricytochrome *c* reduction should decrease at least $10^6$-fold, solely due to the electron tunneling across such distance defined by the monolayer thickness. Beyond the monolayer, the electron has to travel across a peptide chain of inferior electronic conductivity to the ω-hydroxyalkanethiol SAM [21,23,253].

Several possibilities exist here: (i) ET between the electrode and heme iron is assisted by the Met80-Lys79 chain (pathway A), directly bridging the heme iron and the protein surface (Fig. 5(A)); (ii) ET occurs via the porphyrin edge at the heme cavity entrance, for example, the propionic acid side chain and its hydrogen-bonding contact with Lys-79 residue (P in Fig. 5(A)); (iii) a direct space jump, or water-assisted electron transfer between the heme edge (i.e. labeled as S in Fig. 5(B)) and the terminal group (i.e. hydroxyl group) of the self-assembled monolayer, takes place; (iv) there exist several amino acid residues on the protein surface which participate in the electron tunneling process.

Providing the pathway for the Met80-Lys79 chain is implicated in the ET transfer, which further assumes Met80-Lys79($NH_3^+$)/$H_2O$/$HOC_{11}$–S–Au bridge formation, the total tunneling distance (bond-to-bond) would be close to 26 Å (see Fig. 5(A)) [254]. A very approximate relation for the non-adiabatic heterogeneous rate constant at the zero overpotential ($k_{na}^{\circ}$) can be written

$$k_{na}^{\circ} \sim k^{\circ} \exp[-(\beta'_1 d_{SAM} + \beta'_2 d_{HOH} + \beta'_3 d_{Prot} - \delta r_e) \quad (23)$$

where $k_o$ is the hypothetical rate constant for the cytochrome *c* reduction under perfectly adiabatic conditions ($\kappa = 1$), $\beta'_1 = 1.09$ Å$^{-1}$, is the distance-decay constant across the $C_{11}$ monolayer of the thickness $d_{SAM}$ (13 Å), $\beta'_2 = 1.4$–$2.0$ Å$^{-1}$ applies to the water bridge between the monolayer [255] of thickness $d_{HOH}$ (ranging from one to several Angstroms, depending on how many water molecules would separate the hydrated SAM and the hydrated protein surface), while $\beta'_3 = 1.4$ Å$^{-1}$ is the corresponding distance-decay constant for the Lys79-Met80 chain having bond-to-bond $d_{Prot}$ (14 Å), and $\delta r_e$ is the hypothetical distance to which the cytochrome *c*

would have to approach to the electrode surface in the highly adiabatic case (i.e. $\delta r_e = 1-3$ Å). The fact that $\beta'_3 > \beta'_1$ reflects the fact that the protein chain in the cytochrome is a worse electronic conductor than the saturated aliphatic hydrocarbon a component of the SAM. Even though the reorganization $\lambda$ for the cytochrome *c* is relatively low (ca. 0.58 eV), one would expect the experimentally measured rate to be several orders of magnitude lower than found experimentally ($k^{\circ}_{het} = 4 \times 10^{-6}$ cm $s^{-1}$) on $C_{11}$ SAM [117,118]. Can a peptide chain under some conditions become a better electronic conductor than an *n*-alkanethiol monolayer? The rate of electron tunneling is known to depend on whether the protein is composed mainly of α-helices or β-sheets, the former mediating long-range electronic coupling better than the latter [253]. According to Isied [256], peptides with organized secondary structures such as $(proline)_n$ ($n \geq 4$) have very low distance-decay constant ($\beta = 0.2-0.3$ $Å^{-1}$), due to efficient hydrogen bonding, as compared to random coil peptides and saturated hydrocarbons. However, detailed kinetic studies on Ru-modified cytochrome *c* mutants [31] show that such low values of β constants are not likely to be encountered in the case of electron tunneling in its interior (furthermore, no such proline sequence if found in this protein). Hydrogen-bonding contact can be established between the heme propionic side chain and amide group of Lys79 (Fig. 5(A), label P), providing ET would be heme-edge assisted; however, this would constitute only a slightly smaller electron tunneling distance as compared to Met80-Lys79 chain (ligand-assisted ET). Marcus and co-workers [257,258] have pointed out another very important aspect of intra-protein ET, namely, that in addition to an inhomogeneity factor (reflected in distance-decay constant), there is a stereochemical factor in biological ET reactions linked to the mutual orientation of donor and acceptor orbitals. For example, the electronic coupling between the Ru(III) complexes fixed at histidine residues located on the protein surface, varies as a function of the symmetry and the direction of iron and ligand orbitals in space [258]. Even though the relative order of non-degenerate $d_{xz}$, $d_{yz}$, and $d_{xy}$ orbitals in different Ru-modified mutants does not change, the energy level splitting depends on the through-space Fe–Ru electronic interaction. Since the energy levels are quite close to each other (30–70 meV), an electron can be removed from any of these $d^6$ $t_{2g}$ orbitals and tunnel to the hole located in the $t_{2g}$-subshell of His–Ru(III). As a result, for very similar separation Ru–Fe distances (ca. 20 Å), for Ru-complex attached to His-39 and His-62 (cytochrome *c* mutants), the total matrix element varies from 0.11 to 0.0059, which leads to a decrease in the rate constant of approximately two orders of magnitude. In the case of electron tunneling between the heme iron and the hypothetical contact point between a given surface amino acid residue and the hydroxyl groups of the SAM (or water bridge as shown in Fig. 5(A)), the total matrix element might also vary depending on the specific peptide chain involved in the electron tunneling. The intramolecular electron tunneling process has been shown to be intimately linked to the fluctuations in the square of the transfer matrix element $\langle T^2_{DA} \rangle (\sim \langle H^2_{DA} \rangle)$, which can occur on a time scale as short as 10 fs, because of the nuclear vibrational motions of the protein, i.e. C–N, C–C, C=O, and C–H

stretching vibrations [259]. The tunneling electron can be strongly coupled to such motions and absorb (or emit) vibrational energy from the medium (phonon), which can make inelastic ET almost activationless, especially, at very long electron-donor

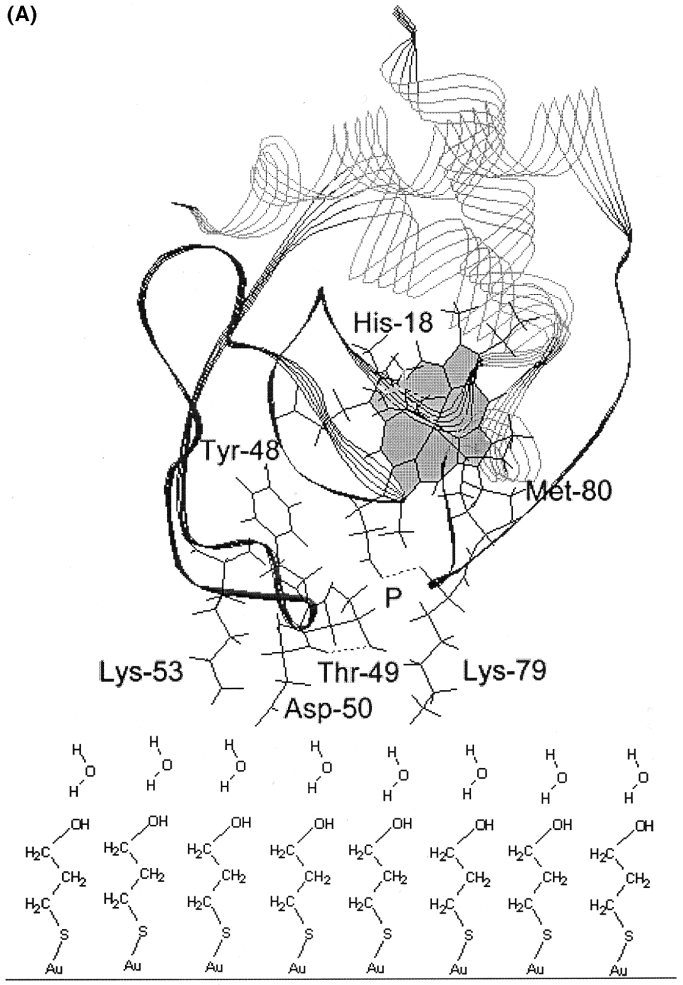


Fig. 5. (A) Illustration of the heme orientation with respect to the electrode surface assuming that two positively charged residues of Lys-53, Lys-79 (according to solution NMR data, as in Fig. 1) are directed towards the negatively charged Au–S–$C_{11}$OH/solution interface. Dotted line (P) corresponds to the hydrogen bonding contact between one of propionic groups located on the heme edge, Lys-79, constituting (together with Met80-Lys79 chain) one of the most probable electron-transfer pathways between the cytochrome *c*, the electrode. (B) A different cytochrome *c* orientation with the Lys-79, Gln-16 residues directed towards the electrode surface. Such a close to perpendicular to the electrode heme configuration would allow for very close approach of the heme edge, its Cys-17 sulfur atom (labeled as S). In the latter case, an electron jump from the heme edge could be assisted by water molecules being part of the hydration layer on the protein surface, or by a water layer on the monolayer surface.

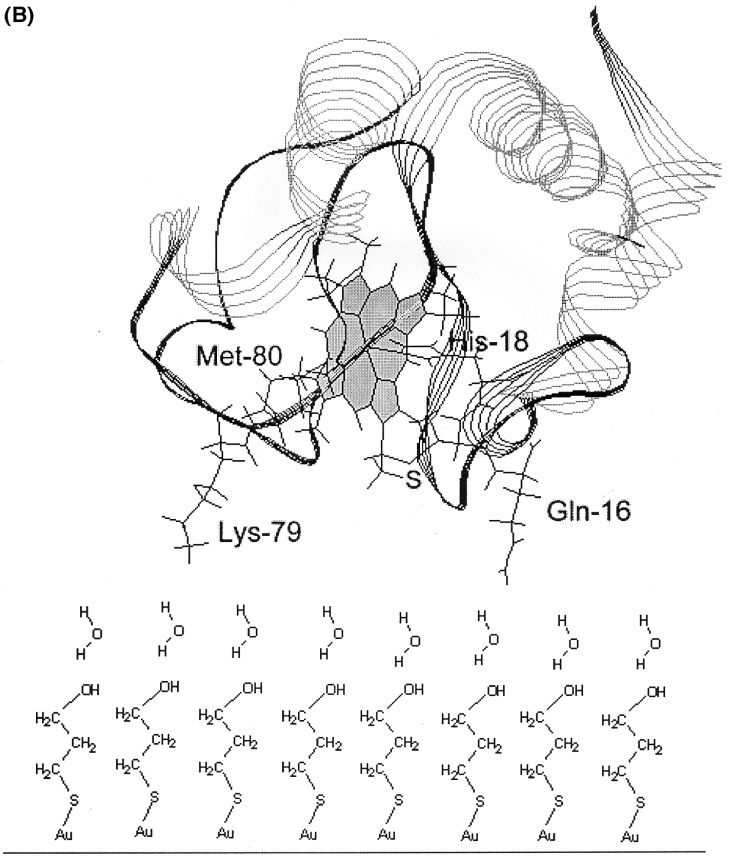


Fig. 5. (*Continued*).

separation distances (i.e. 20–30 Å). Providing electron tunneling between the protein and $C_{11}$ ω-hydroxalkanethiol modified electrode would be phonon-assisted, one should observe deviation from the classical DOS($E$) curve for cytochrome $c$ at potentials negative of $-0.6$ V. The fact that the $k^{\circ}_{het}$ for the cytochrome $c$ reduction on such modified electrode is $4 \times 10^{-6}$ cm $s^{-1}$, unusually high for donor–acceptor distance of ca. 26 Å, indicates that heme-edge assisted electron transfer (Fig. 5(B)) is more likely than pathway A (Fig. 5(A)). The latter ET pathway has been also suggested in the case of interprotein electron transfer between the cytochrome $c$ and cytochrome $c$ peroxidase and cytochrome $c$ oxidase.

One could ask at this point whether computer modeling could, eventually, identify the ET pathway between cytochrome $c$ and the gold electrode at the electrode/solution interface. Even though MD and various semiempirical calculations were conducted for the horse-heart and yeast forms of cytochrome $c$ [111,146–148,185], as well as MD studies for the thiol SAMs on gold and silver surfaces [67,68,82,260], such simulations for cytochrome $c$ at the electrochemical interface would constitute yet another challenge, and might be beyond capabilities

of today's computers. For example, MD simulations of a simple one-electron reduction of $Fe(H_2O)_6^{3+}$ at the Pt(111)/water interface (a box containing 671 water molecules), required as much as 8 months of simulation time, five dedicated HP/Apollo 735 workstations and 400 CPU h on a Cray C90 [176].

### 3.2. Carboxyl-terminated SAMs

According to Hill and co-workers [14,30], an ideal promoter of ET should provide a suitable interface between the cytochrome *c* and electrode surface and, furthermore, introduce surface hydrophilicity, which is believed either to limit, or completely eliminate its irreversible adsorption on electrode surface. Another role of the adsorbed promoter molecules is to allow cytochrome *c* to adopt an appropriate orientation with respect to the electrode, which would allow for a fast electron exchange at the electrode/solution interface. Szücs and co-workers [139] have extended the former definition. Accordingly, the role of promoter may be seen in terms of minimizing structural changes of the adsorbed cytochrome *c*, hence minimizing changes in the redox potential of adsorbed metalloprotein, and not solely in terms of its specific orientation at the electrode/solution interface. Usually, at least two functional groups are required to allow for a fast electron exchange between cytochrome *c* and the metal electrode [14]. One of them is required to be bound to metallic surface, while the other is allowed to interact with the protein. Mercaptoalkanoic acids seem to fulfill most of the criteria required from a good promoter of ET. However, interactions of cytochrome *c* with terminal carboxyl groups are so strong that the protein-modified electrode can be washed with water and transferred to a pure electrolyte solution. It is important to note in this respect that acid groups (i.e. COOH, $SO_3H$, etc) confined to electrode surfaces were shown to undergo pH- as well as electrode potential-induced ionization reactions [69,75]. Interesting is also the case of mixed $CH_3$/COOH monolayers, where the onset for their ionization occurs in the pH range from 6 to 8, which is 2–4 units above the $pK_a$ of simple carboxylic acids in solution [78]. The degree of ionization of surface-attached acid groups is then expected to affect the strength of cytochrome *c* binding to electrode surfaces, thermodynamics as well as kinetics of interfacial ET reactions associated with cytochrome *c* (vide infra). Recent studies indicate that carboxyl-terminated SAMs of varying chain length, $HS(CH_2)_nCOOH$ where $n = 2$–16, allow for reversible or quasi-reversible cyclic voltammetry of horse-heart and yeast cytochrome *c* [136–138,251,261,262]. Close-to-zero anodic-to-cathodic peak separations on short-chain SAMs ($n < 10$) clearly indicate that the protein remains adsorbed on the electrode surface during the redox process, and that corresponding kinetics of ET are fast. Even more surprising is the fact that in a majority of cases, surface coverages of electrostatically-attached cytochrome *c* molecules are unusually high (i.e. $\Gamma = 13.5$ pmol cm$^{-2}$ for $n < 11$, while $\Gamma = 17$ pmol cm$^{-2}$ on $C_{11}$ and $C_{16}$ COOH SAMs, respectively [240]. Both of these values are quite close to the calculated theoretical maximum coverage for cytochrome *c* ($\Gamma = 15$ pmol cm$^{-2}$). It should be noted that the cytochrome *c* surface coverage on PySSPy-modified electrodes varies from 2.88 to 3.74 pmol cm$^{-2}$ (ellipsometric data) [139], while

microgravimetric measurements suggest even lower coverage, $\Gamma = 2.3$ pmol cm$^{-2}$ [145]. That is to say that the surface concentration of cytochrome *c* molecules on carboxyl-containing SAM is ca. 5 times higher compared to PySSPy-covered gold surface. It seems rather surprising that all the cytochrome *c* molecules within the monolayer are electroactive, and contribute to the faradic charge-transfer reaction, especially since the heme cleft has been suggested to occupy only ca. 0.08% of the protein surface [15]. As mentioned previously, there exist as many as 18 lysine residues distributed rather homogeneously around the heme on the protein surface, and there appears no obvious reason why only those protonated lysine residues which are located close to the heme cavity entrance should be preferred in protein binding to SAM. This might speak against the idea of fixed, electrostatically frozen cytochrome *c* molecules in the monolayer.

It should be also noted that the surface coverage of cytochrome *c* molecules on COOH-terminated SAMs depends significantly on the composition of the supporting electrolyte and its ionic strength (and on the electrode washing procedure before its transfer) [240]. Electrochemical experiments are commonly conducted in solutions of a relatively low ionic strength, i.e. 0.01–20 mM phosphate buffer. Once solution ionic strength is increased, gradual desorption of cytochrome *c* molecules from the carboxylate-covered surface takes place, with 95% desorption completed in 1 M electrolyte solution. The formal redox potential for electrostatically attached cytochrome *c* is approximately 50 mV more negative than for the cytochrome *c* in neutral solution of pH 7 (which has been suggested to agree approximately with the typical $E^{\circ\prime}$ values for the protein interacting with biological membranes) [262]. Clark and Bowden [240] observed peak broadening in the cyclic voltammetric response for the surface-confined cytochrome *c*, suggesting a number of possible protein conformations all having closely spaced potential values. On the other hand, Feng et al. [137] have not observed such significant $E^{\circ\prime}$ shift on $C_{11}$COOH SAMs, and propose that the heme ligation as well as the protein envelope surrounding the heme are perfectly preserved upon cytochrome *c* adsorption. The latter conclusion seems to be supported also by recent surface-enhanced resonance Raman measurements on carboxyl-terminated SAMs on silver, confirming the existence of native form of cytochrome *c* strongly adsorbed on the monolayer surface [131].

Important information about the dynamics of cytochrome *c* electrode reactions can be obtained from kinetic experiments conducted on COOH-terminated SAMs. Distance-decay constant $\beta$ for the cytochrome *c* reduction on $C_8$–$C_{15}$ SAMs has been found to vary from 1.0 to 1.1 per $CH_2$ unit [38]. However, electrode kinetics do not seem to follow the same pattern for alkanethiol chains shorter than $C_8$. As shown in Fig. 6, logarithm of rate constant, $k^{\circ\prime}_{et}$, does not increase in a linear way with decreasing number of methylene units. Extrapolation of the kinetic data to $n = 0$ (all the methylene groups eliminated), yields $k^{\circ}_{et}$ for the electroreduction of horse-heart cytochrome *c* only slightly larger than $10^6$ s$^{-1}$. This value is still several orders of magnitude below the apparent rate constant for its reduction on carbon microelectrodes [25]. Also, the temperature-corrected rate constant $k_{et} = 8000$ s$^{-1}$ (an experiment conducted at 0°C), obtained on $C_{11}$ OH-terminated SAM [117], is ca. eight times larger than that found on $C_{11}$COOH-covered gold electrode [137].

As discussed above, apparent rate constant values obtained on short-chain carboxyl-terminated SAMs ($n = 1–6$) are virtually independent of alkanethiol chain length and, furthermore, many orders of magnitude smaller than on OH-terminated SAMs. This is quite surprising since the latter type of SAMs shows much larger degree of organization and less defects [171] compared carboxylate-terminated SAMs, which are known to be more disorganized due to electrostatic type of adsorbate–adsorbate interactions on the electrode surface (Section 3.6). What is then the cause of this rather unexpected behavior? FTIR [263], quartz crystal microbalance [264], contact angle [78] and AC-impedance measurements [265] indicate that there exists a significant degree of hydrogen bonding between neighboring mercaptoalkanoic acid chains exposed to neutral aqueous solution. Such hydrogen-bonded network is likely to be disrupted during the association of positively charged cytochrome *c* to COOH-terminated SAM. In the process, $NH_3^+$ group of protonated lysine residues might strongly interact with carboxylic head groups in the film, and replace their protons, which then results in formation of salt bridges. This kind of interactivity completely separates its electrochemical behavior from that observed on hydroxyl-terminated SAMs of comparable thickness, where such ionization reactions are simply not possible (in neutral solutions). In fact, cytochrome *c* should posses much more rotational freedom in respect to a single ω-hydroxyalkanethiol chain being the electron-transfer site, which is geometrically and conformationally more or less fixed on the electrode surface. On the other hand, once cytochrome *c* molecule gets electrostatically confined to the carboxyl-terminated SAM, it is less free to rotate and to get into a favorable geometry for the electron transfer. Remember that there exists as much as 18 lysine residues distributed rather homogeneously over the protein surface. Feng and co-workers [137] have concluded that in the case of long-chain thiols ($n > 9$), the kinetics of ET are dictated by electron tunneling with the distance-decay constant $\beta = 8.8\ nm^{-1}$,

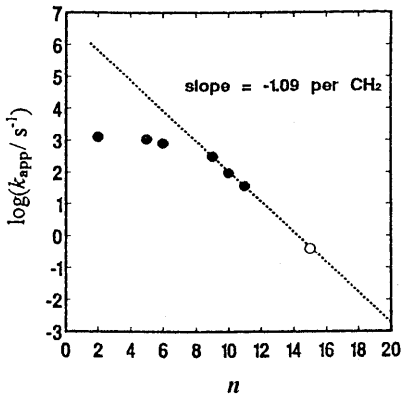


Fig. 6. Logarithmic plots of the apparent standard electron-transfer rate constant for cytochrome *c* as a function of the number of methylene groups in the alkanethiol self-assembled monolayers on gold obtained by the electroreflectance technique (●) [137]; obtained by AC impedance measurements (○) (Copyright © 1997 The Royal Society of Chemistry).

while in the case of short-chain thiols, the rate-limiting step of the electrode reaction is the reorganization equilibrium between the two different conformers of cytochrome *c*. Their transformation is characterized by the equilibrium constant $K = k_1/k_2$, where $k_1$ is the forward rate constant for the formation of cyt *c* (form II) well coupled electronically to the carboxyl-terminated SAM; while $k_2$, is the rate constant for the formation of cyt *c* (form I) not able to undergo electronation reactions (electroinactive form of the protein). For example, the latter situation could occur for the protein electrostatically attached to SAM with its heme directed away from the electrode surface (e.g. ET distances exceeding 30 Å, so that the probability of ET would become very low). Analysis of the $k_{et}^{\circ\prime}$ versus *n* (the number of $CH_2$ units in the SAM) allowed to make an estimate of the $k_1 = 3 \times 10^3$ $s^{-1}$ for the surface attached cytochrome *c*. This observation is certainly the first of its kind, and might provide evidence that the redox processes associated with the cytochrome *c* at short-chain ω-mercaptoalkanoic acid SAMs are controlled by the protein rotational dynamics, rather than by the kinetics of ET. The same seems to apply to carboxyl-terminated SAMs of aromatic thiols, i.e. 4-mercaptobenzoic acid and 4-mercaptohydrocinnamic acid on Au [266]. Formal rate constants of 1800 and 3900 $s^{-1}$, respectively, were found for electrostatically-attached cytochrome *c* molecules on corresponding SAMs using electroreflectance spectroscopy. Such relatively slow rotational movements of cytochrome *c* molecules within COOH-terminated SAMs (one revolution per 0.2–0.6 ms) should be readily observable in time-resolved SERRS experiment. Raman spectroscopy could either confirm or disapprove the existence of the protein reorientation, since the heme-electrode distance is expected to vary in the process. Therefore, monitoring of heme orientation with respect to the electrode surface as a function of time should provide definite proof whether or not cytochrome *c* rotation is the rate-limiting step in the observed electrode reactions on COOH-terminated SAMs. Note that even though SERRS spectra (413 nm excitation wavelength) were reported for cytochrome *c* films on mercaptoundecanoic acid, 4-mercaptopyridine and bis(4-pyridyl) disulfide SAMs on silver and gold [131], the time-dependence of the Raman signal was not addressed in the latter study. On the other hand, time-resolved surface-enhanced Raman experiments were conducted for the cytochrome *c* adsorption on Ag colloid stabilized by strongly adsorbed citrate [267]. In the latter case, the time-dependent reorientation of cytochrome *c* molecules adsorbed on colloidal particles was observed for protein coverages approaching the monolayer.

It should be noted that other explanations than the rate-limiting reorientation of cytochrome molecules (Fig. 6, Ref. [137]) are possible. For example, if organized structure is not maintained in a short-chain self-assembled thiol monolayer, the collapsed layer could adopt insulating properties and limit the rate of electron transfer. However, the fact that rate constant for the reduction of cytochrome *c* adsorbed on aromatic carboxyl-terminated SAMs [266] is comparable with that obtained on aliphatic SAMs of a similar film thickness would suggest that so-called 'reorientation' hypothesis [137] is more likely to be the case than the 'collapsed layer' model.

### 3.3. Ionized cysteine films

Even though it is not widely recognized, L-cysteine is undoubtedly one of the most remarkable promoters of electron transfer. Cysteine films formed by self-assembly on gold, followed by transfer of such chemically-modified electrode into freshly prepared electrolyte, allow for close-to-reversible cyclic voltammetry of cytochrome *c* in neutral [44,127,268,269], acidic [270] and alkaline solutions [130,133]. In this respect, cysteine show some advantages compared to pyridine-based promoters (cf. Section 3.4), which get protonated in acidic media (pH < 6). Under such conditions, the electrostatic repulsion between the monolayer and protein can be experienced. It is interesting that cysteine-covered gold electrodes were also used in studies on the electrochemical behavior of negatively charged cytochrome $b_5$ and fourteen of its mutants in neutral solutions [271]. Response of this bis-histidine ligated metalloprotein on such CMEs can be significantly improved in the presence of $Mg^{2+}$ ions [127]. Among other applications, a construction of a biosensor for the selective determination of cytochrome *c* using an end-column amperometric detector (cysteine-modified gold microdisk array electrode) has been reported [272].

In spite of numerous studies on cysteine adsorption reported during the last decade or so, the exact mechanism of its promoting effects on cytochrome *c* electrochemistry is not known. Earlier FTIR studies [273] conducted on cysteine films on polycrystalline gold suggest formation of bilayers, where the first layer of cysteine molecule is formed via chemisorption on the gold surface. The cysteine monolayer interacts electrostatically with the second layer of ionized zwitterionic molecules in neutral aqueous solution. However, more recent electrochemical studies on cysteine oxidation on polycrystalline gold [95,96] and gold single-crystal electrodes [97] suggest that such a bilayer-film structure is not very likely. Instead, electrostatic adsorbate–adsorbate interactions within the monolayer were suggested to be responsible for the observed electrochemical behavior of cysteine films as a function of pH and electrode potential. The latter conclusion is also in accord with kinetic studies concerning $Fe(H_2O)_6^{3+}$ reduction on cysteine-modified single crystal gold electrodes in aqueous perchloric acid solutions of pH 1–2 [274]. In fact, cysteine films do not exert any significant accelerating (or inhibiting) effects on the redox reactions of the $Fe(H_2O)_6^{3+/2+}$ redox couple, while potential-induced ionization of 2-mercaptoethanesulfonic acid (MES) and mercaptopropionic acid (MPA) SAMs on gold led to five orders of magnitude increase in the rate constant for the electroreduction of $Fe(H_2O)_6^{3+}$. Capacitance–potential (*C*–*E*) curves measured during the cysteine adsorption on polycrystalline gold from acidic solutions are rather featureless [96], in contrast to MES, the latter showing symmetric peaks on *C*–*E* curves due to the surface pH changes associated with the head group ionization [75]. Both the above mentioned capacitance measurements as well as kinetic studies on $Fe(H_2O)_6^{3+}$ reduction indicate that long-range electrostatic effects, as experienced in the case of MPA and MES monolayers on Au, are absent in the case of cysteine. This has been proposed to be due to the formation of $COO^-$:$NH_3^+$ bridges between the two neighboring cysteine molecules, which could

also explain its unusually high surface coverage on gold [96], comparable with that of simple *n*-alkanethiols. Indeed, $(\sqrt{3} \times \sqrt{3})$R30° adlayer structure for cysteine monolayer on Au(111) has been recently confirmed using in situ scanning tunneling microscopy at 0.2 V versus SCE [275]. The absence of a strong electrostatic binding of cytochrome *c* to cysteine films self-assembled on gold from neutral aqueous solutions could also be explained in a similar way. Cysteine–cysteine interactions within the film might simply compete with the interaction of positively charged lysine residues of cytochrome *c* with the cysteine monolayer. This also explains why cysteine falls into the category of promoters of ET which allow for the diffusion-controlled electrochemistry of cytochrome *c* without significant complications from its adsorption on the electrode surface (in contrast to chemisorbed ω-mercaptoalkanoic acid on gold). However, strong interaction of cytochrome *c* with cysteine-modified colloidal Ag particles were noticed in alkaline solutions of ca. pH 10 [130]. SERRS experiments showed an abrupt increase in the intensity of the Raman signal ($\nu_{13}$, in plane bending vibration) for the cytochrome *c* in solutions of pH > 9. According to the latter work, below pH 9, there is either no cytochrome *c* binding to cysteine films, or cytochrome *c* orientation on the colloid surface is such that heme is located further away from the surface and is not perceptible in the Raman spectra.

Very interesting kinetic studies on wild type cytochrome $b_5$ and its mutants (prepared by single site-directed mutagenesis) were conducted by Rodgers and Sligar [271]. While a single amino acid replacement on the protein surface did not result in significant reduction potential changes (within 20 mV compared to native cytochrome $b_5$), the corresponding rate constant, measured on gold electrodes in the presence of 2 mM cysteine, increased threefold for D66K and E44K mutants, where a positive charge was introduced near the exposed heme edge. On the other hand, the decrease in the $k^{\circ}_{het}$ upon increasing negative charge has been explained as due to electrostatic repulsion between the negatively charged protein and negatively charged cysteine film. However, it is possible that differences in the kinetics of ET for various mutants arise from other effects (related to the protein structure) rather than electrostatic repulsion from cysteine films. Note that cysteine SAMs on gold are not charged negatively in neutral solutions, as is also evident from previous spectroscopic and electrochemical studies (as discussed above).

Cysteine-modified electrodes have recently found interesting application in studies on denaturation and refolding of denaturated cytochrome *c* induced by electrolyte anions such as perchlorate (in 0.01 M HCl solutions of pH 2) [270]. The latter work clearly demonstrates that electrochemical reversibility of cytochrome *c* reactions and similar redox potential values do not necessarily mean that one is dealing with the native form of cytochrome *c*. Recent FTIR studies on pH-induced secondary-structure changes in cytochrome *c* [276] suggest, that in the pH range from 4 to 2.5, protein adopts an almost unfolded low-spin form, while the high-spin acidic form exists when pH is lowered below 2.5. Further decrease of pH gave no rise to a continued unfolding in cytochrome *c* but made it refold to the 'A state' with properties similar to those of a molten globular state. The latter conformer of cytochrome *c* gives on cysteine- or 6-mercaptopurine-modified gold electrodes [270]

close-to-reversible cyclic voltammetry differing very little from that observed at pH 7 (N-form).

A very nice example of marriage between electrochemical and in situ surface spectroscopic techniques is represented by the work of Schlereth and Mäntele [133]. These authors were looking for possible electrochemically-induced changes in the native from of cytochrome *c* on promoter-covered gold electrodes using Fourier transform infrared spectroscopy (reduced-minus-oxidized IR difference spectra). Whereas on a PySSPy-modified electrode the thermally induced transition to the alkaline form of the spectra happened in the whole pH range (6.8–10) tested, the spectra obtained with cysteine-modified electrode always show the native form. Interactions of cytochrome *c* with PySSPy modifier were found to be significantly weaker in the whole range of pH values compared to chemisorbed and ionized cysteine or DTPA carboxylate groups at pH values close to 10. The shifts in tyrosine vibrational modes obtained in neutral and slightly alkaline pH at high temperatures (40°C) suggest an intermediate state of the ferricytochrome *c* in which the heme crevice is more accessible to the solvent.

Di Gleria and co-workers [268] were first to realize that interactions between cytochrome *c* and the cysteine monolayer might change upon chemical modification of its COOH or $NH_2$ groups. The latter authors observed close-to-reversible electrochemistry of this protein on L-cysteine modified gold electrode phosphate buffer solutions of pH 7 ($\Delta E = 65$ mV at 20 mV $s^{-1}$). On L-cysteine ethyl ester (CEE)-modified electrodes (carboxyl group blocked by ester), a peak separation of $\Delta E = 70$ mV was found, quite close to that found on cysteine-modified electrodes. Corresponding rate constants for the cytochrome *c* reduction on cysteine- and CEE-modified electrodes were $4 \times 10^{-3}$ and $2 \times 10^{-3}$ cm $s^{-1}$, respectively. The rates of cytochrome *c* reduction were found to be much slower on *N*-acetyl cysteine (NAC)-modified electrodes ($\Delta E = 105$ mV). However, in contrast to that, Cooper et al. [277] have reported much more reversible behavior of cytochrome *c* on NAC-modified gold electrode in 10 mM phosphate or Tris buffers (pH 7.0) containing 10 mmol $dm^{-3}$ of KCl. For example, anodic to cathodic peak separation $\Delta E = 60$ mV (peak half width, $E_{1/2} = 25$ mV) was observed even at relatively high scan rate $v = 200$ mV $s^{-1}$. Even though the authors point at the importance of interactions of the ionized lysine groups of the cytochrome *c* with the ionized carboxylic groups in the cysteine film, their experiment conducted on CEE-modified electrodes clearly shows that such ionization might not be necessary in order to achieve fast redox chemistry of cytochrome *c*. The authors conclude: 'It is important to note that the binding between the surface-bound promoter (e.g. cysteine) and cytochrome *c* is reversible; if this were not the case the protein would adsorb on the modified electrode surface irreversibly and no diffusion-controlled faradic current would be observed after the first cycle'. On the other hand, Szücs et al. [139] suggest that irreversible binding of cytochrome *c* to the promoter does not have to result in an inhibition of the heterogeneous electron transfer since irreversibly adsorbed cytochrome *c* itself can function as a mediator of heterogeneous electron transfer.

Experimental results on redox behavior of cytochrome *c* on gold electrodes modified by the above mentioned cysteine derivatives suggest that ionization of

COOH or $NH_2$ groups in SAMs is not a necessary condition for fast ET between the electrode and the protein. Even though films of cysteine derivatives self-assembled on gold might be significantly more hydrophobic than cysteine, highly polar groups such as N–CO–R or –CO–OR– might still show some degree of hydrophilicity (contact angle measurements are to be done for these adsorbates), so that H-bonding contacts with water and/or cytochrome *c* can be established. It is likely that conformational changes of these molecules on electrode surfaces as well as the degree of orientational disorder in the SAM might be of importance during formation of such protein/promoter contacts.

### *3.4. Bis(4-pyridyl) disulfide and 4-thiopyridine SAMs*

Taniguchi and co-workers [59,60] were first to report that chemisorbed bis(4-pyridyl) disulfide or bis(4-pyridyl) sulfide on gold show promoting effects similar to those of 4,4′-bipyridine. However, reversible response of cytochrome *c* on such electrodes was much more stable than in the presence of the latter modifier. The addition of these sulfur-containing molecules (several millimolar) to a solution of cytochrome *c* showed no significant changes in the absorbance at 695 nm, indicating that neither of the molecules binds to the heme iron as an extrinsic ligand. However, even on PySSPy-modified electrodes some diminution in the reversibility of charge-transfer reactions in the presence of protein can be observed. Theoretical treatment of so-called 'time-dependent self-inhibition' of cytochrome *c* redox activity on a rotating disc gold electrode and ultramicroelectrodes (modified by PySSPy, and unmodified) has been presented by Bond et al. [278]. In the latter work, a rotating disk electrode was employed since it allows to change the mode of mass transport from diffusion to convection (i.e. by means of increase in the rotation rate). If the modifier simply provides a suitable site for the electron transfer by removing a blocked part of the electrode surface, without specific interaction with cytochrome *c*, when a time-dependent electroactive area should be created as PySSPy is adsorbed. Under these conditions, and with a sufficiently fast rotation rate so that mass transport occurs solely by convection, the theory for a reversible process predicts $E_{1/2} = E°$. Providing a specific interaction does occur at an electrode surface (e.g. the redox reaction is preceded by the formation of a surface complex which is then followed by its dissociation), then $E_{1/2}$ may or may not equal $E°$

$$E_{1/2} = E_s° + (RT/F)\ln(K_1/K_2) \tag{24}$$

where $E_s°$ is a standard potential of the surface confined redox reaction:

$$[\text{cyt } c(\text{III})\text{-PySSPy}]_{ads} + e^- \rightarrow [\text{cyt } c(\text{II})\text{-PySSPy}]_{ads} \tag{25}$$

$K_1$ and $K_2$ are stability constants of the adsorbed adducts (oxidized, respectively, reduced form of the protein); $k_f$ and $k_b$ are the forward- and back-reaction rate constants for the formation of a surface complex

$$\text{cyt } c(\text{III}) + [\text{PySSPy}]_{ads} \Leftrightarrow [\text{cyt(III)PySSPy}]_{ads} \tag{26}$$

where $K_1 = k_f/k_b$. As observed experimentally, $E_{1/2} = E^\circ_s = 0.248$ V versus NHE and therefore, both adsorbed adducts were suggested to be either equally unstable ($k_f \ll k_b$ or $K_1 \ll 1$ and $K_1 = K_2$) or equally stable. The authors conclude that while the data are consistent with specific binding between cytochrome *c* and PySSPy, it may be that adsorption of the modifier simply unblocks parts of the electrode surface by displacing an adsorbed form of cytochrome *c* and therefore providing arrays of suitable sites for electron transfer. Alternatively, both mechanisms could occur simultaneously.

Szücs et al. [139] have studied adsorption of horse-heart cytochrome *c* on gold in the presence and absence of PySSPy using ellipsometry and have concluded that the cytochrome *c* binding to unmodified gold as well as 4-pyridyl thiolate-covered electrode surface is irreversible. However, the extent of unfolding of cytochrome *c* at both surfaces is suggested to be quite different. Here, bis(4-bipyridyl) disulfide is suggested to play a key role in preventing the unfolding of adsorbed cytochrome *c* at the electrode solution interface. Cyclic voltammetric and ellipsometric measurements were performed after 120 min adsorption of cytochrome *c* from 130 μM solution saturated by PySSPy following an extensive washing of the cell in order to remove the protein from the solution. The amount of adsorbed cytochrome *c* was estimated from ellipsometric data according to Eq. (27)

$$\Gamma = d(n - n_s)/M_r \, dn/dc \tag{27}$$

where $\Gamma$ is the adsorbed amount of cytochrome *c* (mol $cm^{-2}$), *d* is the adsorbed layer thickness (cm), *n* is the refractive index of the adsorbed layer, $n_s$ is the refractive index of the buffer solution, $M_r$ is the relative molecular weight of cyt *c* ($M_r = 12\ 384$) and $dn/dc$ is the refractive index increment of the protein (taken as 0.18 $cm^3\ g^{-1}$). Cyclic voltammetry performed in cytochrome *c* free solution revealed only a partial cytochrome *c* surface coverage on the PySSPy-modified electrode surface (ca. 20% of monolayer, as discussed in the Section 3.2). Ellipsometric measurements indicate that the thickness of the cytochrome *c* film is ca. 35–40 Å (as expected for native cytochrome *c*), while protein adsorption on an unmodified gold surface gave a film thickness of only 18–22 Å. According to the authors of Ref. [139], ellipsometric data are consistent with unfolding of the protein, which leads to a decrease in the thickness of the adsorbate monolayer. However, such an unfolded protein layer is suggested to mediate reduction of the cytochrome *c* diffusing from the bulk, with the oxidation of cytochrome *c* in solution completely lacking. Accordingly, the adsorbed layer of cytochrome *c* (either in native form or accompanied by conformational changes upon adsorption) becomes an immobilized mediator for electron transfer between the underlying metal and cytochrome *c* in the solution. The latter conclusion is in apparent contradiction with the model of Bond et al. [289], as discussed above, who consider denaturated cytochrome *c* purely as inhibitor of the ET between the diffusing cytochrome *c* molecules and the electrode surface. Szücs and co-workers [139] note that the redox potential of the unfolded protein shifts by some 400 mV towards more negative potentials (in respect to that of native cytochrome *c*), however, new protein conformer is still active as mediator of ET for cytochrome *c* reduction but not for its oxidation.

It should be noted that except for other factors, i.e. electrolyte composition and the ionic strength (vide infra), an important factor in experiments involving cytochrome *c* on CME is the time of experiment itself. Note that the dipping time of Szücs and co-workers (up to 2 h) are sufficiently long to form an adsorbed protein layer on the electrode surface, eventually, to lead to its partial denaturation. Lion-Dagan et al. [145] have recently reported results of their studies on cytochrome *c* adsorption on 4-PySH-functionalized gold by means of electrochemical quartz-crystal microbalance technique. As already mentioned in the Section 3.2., the time necessary to form an equilibrium coverage of cytochrome *c* on Au–SPy surface is ca. 10 min. Experimentally determined association constant for the ferricytochrome *c*, $k_1 = 8.5 \times 10^3\ M^{-1}$, is quite close to the value for the protein and 4-mercaptopyridine measured in the solution ($k_1 = 2.1 \times 10^3\ M^{-1}$). The effect of promoter–protein association has been assigned to the favorable interactions between the positively charged lysine residues of cytochrome *c* with lone pair of electrons located on nitrogen atom of the pyridinethiolate molecules within the monolayer. The dissociation (desorption) rate constant of cytochrome *c* from 4-mercaptopyridine SAM has been estimated to be $1.2 \times 10^{-4}\ s^{-1}$. It is interesting in this respect that Sagara et al. [279] have not noticed any perceptible 4-mercaptopyridine binding to cytochrome *c* in neutral aqueous solutions, while the degree of its association to corresponding SAM on gold has been found to depend on the concentration of the supporting electrolyte. According to Xie and Dong [280], at low electrolyte concentrations (i.e. 2 mmol $l^{-1}$), irreversible binding of cytochrome *c* either to PyPy or 4-PySH-modified electrode surface takes place (long dipping times), while upon increase in the electrolyte concentration, its association had changed from irreversible to reversible. An important role of the pyridyl group in association of the protein to chemisorbed 4-PySH on gold has been also deduced from pH studies [281]. According to the latter study, cytochrome *c* can only transfer electrons providing the gold surface is covered by the unprotonated form of the pyridyl-containing modifier. When the solution pH decreased below 6, the standard heterogeneous rate constant of cytochrome *c* on the modified gold electrode dramatically decreased, and its voltammetric response changes from quasi-reversible to highly irreversible. However, the fact that pH-induced conformational changes of cytochrome *c* take place in acidic solutions were simply neglected in the latter study. It is interesting in this respect that the detailed structure of 4-mercaptopyridine on Au(111) is known on an atomic resolution from STM measurements [282] conducted in 0.05 M $HClO_4$ solution. Under such conditions, neighboring 4-pyridinethiolate molecules within the $p(5 \times \sqrt{3}R30°)$ unit cell adopts PySSPy-like configuration with pyridyl functions directed in opposite directions (as shown in Fig. 7), apparently, as to limit the electrostatic repulsion between the protonated nitrogen atoms in acidic solution. Unfortunately, no STM data exist for this adsorbate in neutral solutions of pH 7 (normally used in cytochrome *c* electrochemistry), where this molecule should exist mainly in its unprotonated form. Providing its geometry on the electrode surface would be similar to that observed in acidic media, one cytochrome *c* molecule would easily fit into the area limited by a $5 \times 5$ nm window on the right hand side of Fig. 7, and a single cytochrome *c* molecule

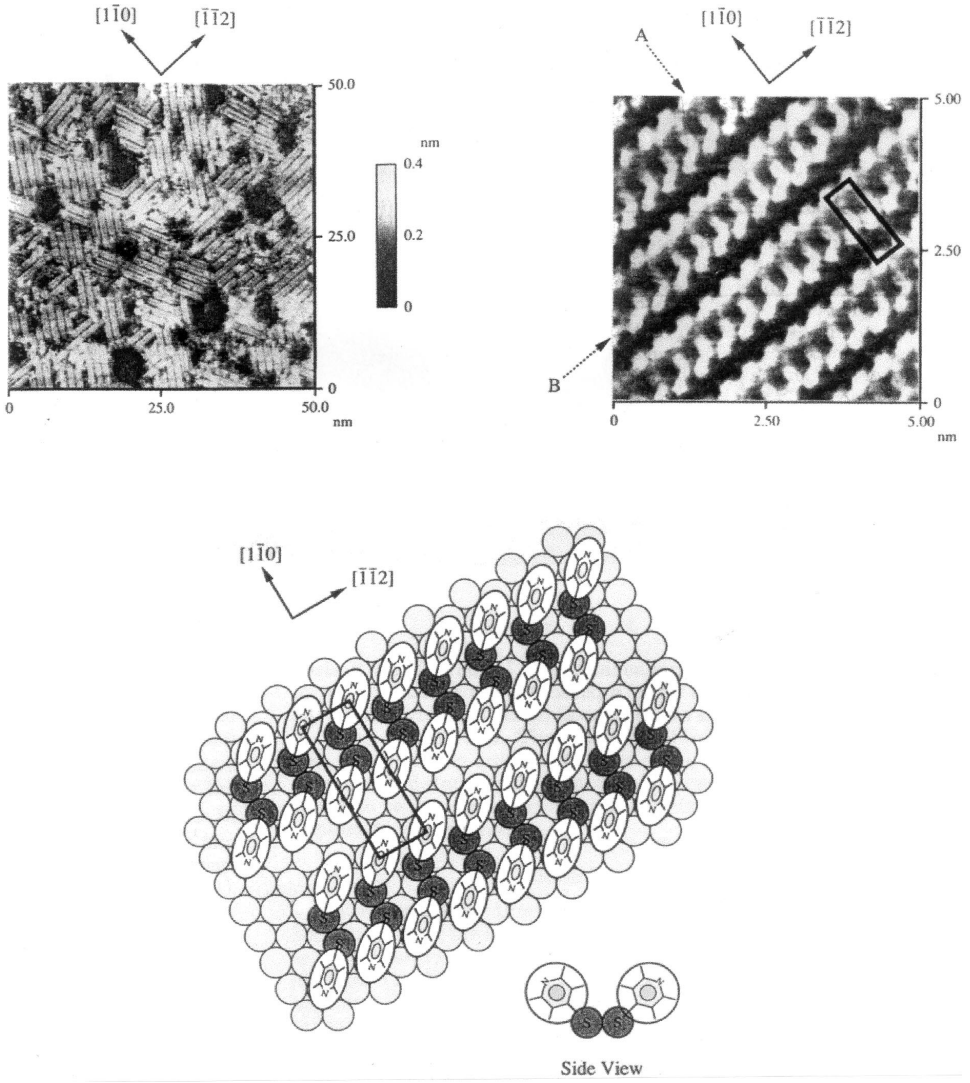


Fig. 7. In situ STM image of the 4-pyridinethiolate monolayer on Au(111) surface in 0.05 M $HClO_4$ solution (on the left), the high-resolution zoom into the 4-pyridinethiolate monolayer composed of rectangular p($5 \times \sqrt{3}$R-30°) unit cells (right image), its real space model (bottom) (taken from Ref. [282], with permission from the American Chemical Society).

should fit onto the surface area occupied by 20–25 pyridinethiolate molecules. Fig. 5 represents two of many possible orientations of cytochrome *c* in respect to the electrode surface where the redox center (heme) approaches relatively close to the electrode surface covered by hydroxyl-terminated thiolate film. In the next, we will replace ω-hydroxyalkane thiol by PySSPy and, in addition, consider the situation where cytochrome *c* would adopt the orientation with the charged Lys-53 and

Gln-16 residues towards the negatively charged SPy-covered metal (Fig. 5(B)). Under such conditions, Lys-79 would interact with one of pyridyl nitrogens, while the extremity of the Gln-16 chain would come into contact with the fourth adsorbate molecule starting from Au–SPy–Lys-79 contact (cf. Fig. 7). This is expected since the distance between the Gln-16 and Lys-79 for the cytochrome *c* conformation shown in Fig. 5(B) is ca. 15 Å. Here we consider the interaction of Lys-79 and Gln-16 with the double stripe of 4-pyridinethiolate molecules along the $\sqrt{3}$ direction. Again, because of the same reasoning as presented above in case of cytochrome *c* reduction on OH-terminated SAMs, its orientation on PySSPy-modified electrodes similar to that in Fig. 5(B) is expected to lead to faster ET kinetics as compared to the situation presented in the Fig. 5(A).

One of the very important issues in studies on interprotein as well as heterogeneous kinetics involving cytochrome *c* is the effect of protein chemical modification on the rate of such reactions. The latter is also important in order to understand promoter-assisted ET between the electrode and cytochrome *c* since electrostatic interactions of protonated lysine residues with SAMs are believed to be responsible for promoting effects of a number of adsorbates. Several studies were conducted in the past on the chemical modification of lysine groups in cytochrome *c* in order to confirm the latter hypothesis. In fact, Eddows and Hill [40] were first to propose that hydrogen bonding between lysine residues of cytochrome *c* and nitrogen of PyPy, rather than its direct coordination to the heme iron, is responsible for a rapid electron exchange between the gold electrode and this metalloprotein. Eddowes at al. [80] have shown that chemically-modified cytochrome *c* (trifluoroacetyl- or maleyl-lysyl cytochrome *c*) gave no electrochemical response on PyPy-covered gold electrodes, noting that lysine residues play an important role during the protein association at the modified electrode/solution interface. On the other hand, Tominaga et al. [283] argued that chemical treatment of lysine residues in cytochrome *c* with 4-chloro-3,5-dinitrobenzoic acid (CDNP) or 2,4-dinitrofluorobenzene (DNP) showed no significant difference from that of the native cytochrome *c* on promoter-modified electrodes. Importantly, the electron-transfer reaction between CDNP- or DNP-substituted cytochrome *c* at Lys-13 and/or Lys-72 and cytochrome *c* oxidase was not greatly affected even though one or two lysine residues of cytochrome *c* were modified. The problem of the chemical modification of lysine residues in cytochrome *c* and its effect on the ET capabilities of the protein has been addressed also in a recent work by Theodorakis and co-workers [284,285]. The latter authors prepared β-thiopropionyl derivatives of horse-heart cytochrome *c* (TP cyt *c*) having singly modified each of 18 lysine ε-amino groups. Such cytochrome *c* derivatives were grouped according to the location of modified group on the surface of the protein: (a) the top N-terminal α-helix; (b) the enzymatic interaction domain; (c) the 'lower right side' of the protein; and (d) the 'back' and 'bottom' of the molecule. The reduction potentials of the TP cytochrome *c* were determined for the TP Lys-5–8, 13, 22, 25, 27, 39, 60, 86–88 and the mixture of TP Lys-100 and 53 derivatives. The corresponding formal redox potentials for such derivatives varied from 0.262 to 0.280 V, which can be considered within experimental error the same as that for the unmodified horse-heart cytochrome *c* ($E^{\circ\prime} = 0.270$ V). This indicates

that the heme environment remains unchanged in spite of the modification at any of the above mentioned lysines, as also evident from UV–vis, EPR and NMR measurements. This is not the case of TP Lys-72, Lys-79 and Lys-73 derivatives where thiolate binding to the heme iron occurred affecting thus the redox potential as well as their ability to transfer electrons to cytochrome *c* oxidase. The reduction potentials of the TP Lys-72 and the TP Lys-79 derivatives were 0.201 and 0.196 V. Interestingly, lysine modification by CNDP yields an order of magnitude decreased activities of substituted cytochromes c similar to that provided by the TP-modified proteins, the effect being larger in the former case.

As has been discussed above, the chemical modification of a single lysine residue might lead to negligible changes in redox potential for the cytochrome *c* derivative and cause relatively unimportant effect on kinetics of ET between cytochrome *c* and cytochrome *c* oxidase. Similarly, protonated lysine residues might be important in formation of surface complexes with certain types of SAMs on electrode surfaces, but not necessarily critical for a rapid heterogeneous ET to occur. As mentioned throughout this work, several hydrogen-bonding contacts could, in principle, be established between the functional groups on the cytochrome *c* surface and polar groups on the hydrophilic monolayer. However, as an exception to the rule, there exist some modifiers of electrode surfaces which do not fulfill the general requirements of a promoter of ET (see also Section 3.5), yet such molecules allow for close-to-reversible electrochemistry of cytochrome *c*. For example, two nitrogen atoms in 2,2′-bipyridine are located on the same side of the molecule (*cis* isomer) when coordinated to the silver surface, as also evident from SERS experiments [286]. The latter promoter does not contain two functional groups at each end of the molecule required for the cytochrome *c* binding to the monolayer surface. Providing 2,2′-bipyridine indeed adsorbs as suggested on the basis of the SERS experiment, SAM should not allow for any electrostatic interactions between protonated lysine residues of cytochrome *c* and the lone pair of nitrogen atom of the modifier, since the latter is not sterically accessible for this type of association. No promoting effects of 2,2′-bipyridine and pyrazine on cytochrome *c* reduction were observed in early electrochemical studies [56], however, more recent work (Ref. [286]) suggests that differences in promoting capabilities of 2,2′-bipyridine and 4,4′-bipyridine arise exclusively from differing strengths of their adsorption on Au or Ag surfaces rather than from inability to function as promoters of ET. The former molecule has been found to adsorb very weakly on gold so that very long dipping times and relatively high bulk concentrations of the modifier are required in order to achieve a complete electrode surface coverage. One of possible roles of promoters of ET reactions associated with cytochrome *c* is to modify the potential drop at the electrode/solution interface, which is often neglected by electrochemists. One should not forget that cytochrome *c* is a highly charged molecule, and that long-range electrostatic forces might drive the protein to stronger adsorption than in the absence of molecules such as pyrazine or 2,2′-bipyridine. Relatively small variation in the charge density at the metal side of the interface might also have dramatic consequences on kinetics of the heterogeneous ET. As shown recently by Honeychurch et al. [220], kinetic data not corrected for the double-layer effects can

be subject to very large errors. According to these authors, $k°$ for the cytochrome *c* redox reactions on PySSPy-modified gold electrodes might simply not be accessible to the CV experiment at slow scan rates (i.e. $v < 1$ V $s^{-1}$), since the anodic–cathodic peak separation reflects double-layer effects rather than the electronic structure of the metalloprotein. However, a simple Frumkin correction of kinetic parameters for the cytochrome *c* reduction (or oxidation) on most of CMEs might be not be applicable to most of the voltammetric data collected during the last three decades due to the protein adsorption on promoter-covered surfaces.

### *3.5. Aliphatic or aromatic thiol monolayers?*

From the chemical point of view, *n*-alkanethiol adsorption on gold may be formally considered as an oxidative addition of the –SH bond to the gold surface, followed by a reductive elimination of the hydrogen [82]. Ab initio Hartree–Fock calculations [70] indicate that molecular orbitals located on the sulfur atom of the alkanethiolate strongly overlap with the top two layers of Au atoms on a Au(111) surface forming a strong Au–S bond through σ-, π-donation and π-back bonding. Therefore, the probability of finding the electron somewhat out of the metal increases due to such charge delocalization, and also, due to the relatively large size of the sulfur atom in the thiolate. One would tend to believe that the insertion of C=C or C≡C bonds in such an alkyl chain (or, phenyl ring), would lead to a significant improvement in electronic conductivity of resulting monolayer and, subsequently, in more rapid ET rates across the electrochemical interface. In biological systems, including cytochrome *c*, the probability of electron transfer between ferrocytochrome *c* and ferricyanide has been correlated with the number of aromatic amino acid residues within the electron transfer pathway [287]. However, results of recent electron-tunneling studies [288] do not demonstrate any significant improvement in the electronic conductivity of molecular bridges composed of amino acids, providing the aromatic amino acid residue is being separated on both sides of the chain by a sequence of saturated bonds. Cheng et al. [289] have shown that the same applies to SAMs of aliphatic thiols on gold, in cases where the multiple carbon–carbon bonds were introduced. For example, an alkyne introduction in the middle of the $C_{14}$ ω-hydroxyalkanethiol chain led to 40% decrease in electronic coupling between electrode and freely diffusing $Os(bpy)_3^{3+}$ complex, compared to the hydroxyalkyl chain before the substitution. This is because π and π* orbitals of the alkyne cannot couple osmium complex and electrode at large distances as effectively as σ and σ* orbitals along the alkane chain [289]. However, the introduction of the long alkane chains in the *para* position of aromatic thiolates on gold has been shown to dramatically increase molecular packing density [290] of the latter which, possibly, could lead to increase in the extent of through-space electronic coupling between the neighboring chains [255,289,291] due to the π-stacking of aromatic rings.

The situation is quite different, providing the double or triple carbon–carbon bonds are being introduced in a short molecular bridge and, furthermore, there is a necessary spatial orientation and coupling of metal d orbitals, and those in the

fixed metallic redox center. For example, in the case of surface-attached Co(III)-complexes on a Hg electrode, the replacement of the CH=CH bridge ($\kappa_{el} = 1$) by saturated $-CH_2-CH_2-$ led to ca. 20-fold decrease in $k_{et}$ and 100-fold decrease in the frequency factor (from ca. $2 \times 10^{12}$ to $3 \times 10^{10}$ $s^{-1}$) [292]. Note, that in the latter case, a significant change from perfectly adiabatic to non-adiabatic ET took place. A question arises at this point as to whether such a relatively small change in the promoter structure (i.e. a single saturated versus unsaturated bond) should be reflected in kinetic parameters for the charge-transfer reaction between the cytochrome *c* and gold electrode. It is interesting in this respect that Eddowes and Hill [56] reported that 1,2-bis(4-pyridyl) ethylene functions as a good promoter of ET for horse-heart cytochrome *c*, while 1,2-bis(4-pyridyl) ethane adsorbed on gold was found to be inactive. Could then SAMs composed exclusively of aromatic thiols constitute any advantage compared to aliphatic thiols? Most of the experimental evidence on cytochrome *c* redox reactions on aromatic SAMs indicates that there exist more complications than advantages when using them to modify electrode surfaces. It also appears that a large number of aromatic adsorbates do not function as promoters at all. This is the case of diphenyl disulfide or thiophenol chemisorbed on Au(100) or Au(110) electrodes (see Fig. 8) [293]. While PySSPy and 4-PySH gave well-defined and highly reversible voltammetric response on the gold

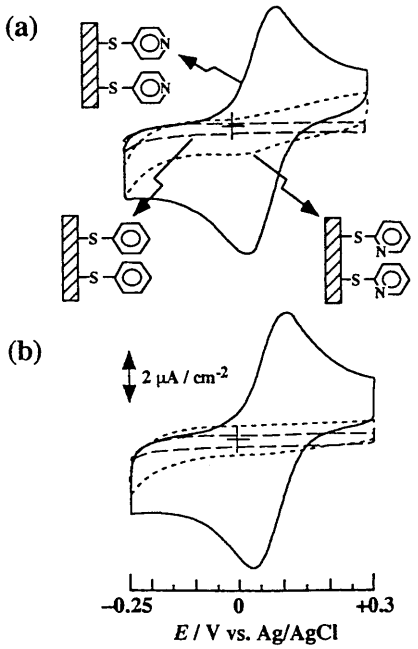


Fig. 8. Cyclic voltammograms for 100 μM horse-heart cytochrome *c* at (a) Au(100), (b) Au(110) electrodes modified with (—): 4,4′-PySSPy, (- - -): 2,2′-PySSPy, (- - -): PhSSPh recorded in a 0.1 M phosphate buffer solution containing 0.1 M $NaClO_4$ (pH 7.0) at 25°C. Scan rate: 50 mV $s^{-1}$ (Ref. [293], Copyright © 1997 The Chemical Society of Japan).

single-crystal electrodes, practically no response was seen on either 2,2′-PySSPy, 2-PySH, PhSSPh or thiophenol-modified gold single-crystal electrodes. Exposure of a gold electrode, modified with PySSPy, to thiophenol [58] produced changes in electrochemical response for cytochrome *c* from peak-shaped to sigmoidal-shaped voltammograms. The peak-shaped (linear diffusion dominant) to a sigmoidal-shaped (radial diffusion dominant) transition was accompanied by a concomitant decrease in the cathodic and anodic currents, suggested as due to so called 'self-blocking', i.e. electroinactive cytochrome *c* molecules block the electrode surface leaving only an array of microscopically small electroactive sites at which the diffusion-controlled voltammetry can be conducted [48,212,278].

As mentioned above, the sulfur atom contained in the chemisorbed aromatic thiol should extend conjugation between the phenyl ring of the adsorbed thiophenol, which adopts a perpendicular orientation with respect to the electrode surface. Since surface coverage by an aromatic thiol is in general lower than that for an aliphatic *n*-alkanethiol, solvent molecules and supporting electrolyte ions might reach the electrode surface easier than in the latter type of monolayers. However, as is evident from STM experiments [290], surface coverage by this aromatic thiol is sufficiently high as to prevent direct contact of cytochrome *c* with gold surface, due to the relatively large size of the protein. Furthermore, monolayer thickness is quite comparable to that of 4-mercaptopyridine self assembled on gold (ca. 6–7 Å) so that, seemingly, there exists no obvious reason why thiophenol should not function as an excellent promoter for this protein. However, as we have seen in a number of cases, electrochemistry of cytochrome *c* on CMEs depends strongly on the terminal head group, which seems to determine the extent of its interaction with the SAM. Does then introduction of COOH group(s) into the aromatic thiol lead to a significant improvement in the reversibility of voltammetric response for the cytochrome *c*? The answer is yes. However, the differences in kinetics associated with cytochrome *c* reduction on aliphatic and aromatic SAMs (comparable film thickness) are, in fact, very small. For example, $k^{\circ}_{et}{}'$ for cytochrome *c* reduction on ω-mercaptohexanoic acid-modified electrode are 1100 $s^{-1}$, while it increases to 1800 $s^{-1}$ on a 4-mercaptobenzoic acid-modified electrode. A sensible increase in the rate of heterogeneous ET has been observed at a SAM of another aromatic thiol, namely, 4-mercaptohydrocinnamic acid self-assembled on Au(111) ($k^{\circ}_{et}{}' = 3900 s^{-1}$) [266]. One would tend to believe that carboxyl-containing aromatic thiolates linked to gold via sulfur atoms, and forming salt bridges $COO^{-}/NH_3^{+}$ with cytochrome *c*, should provide better electronic coupling between the heme and electrode than with OH-terminated SAMs. However, it is very likely that the rate-limiting step of such electrode reactions is not the electron transfer step itself, but rather rotational movement of the cytochrome *c* at the interface (as was the case of cytochrome *c* kinetics on ω-mercaptoalkanoic acid SAMs (cf. Section 3.2).

It is interesting that one of the excellent promoters of ET that allows for the diffusion-controlled redox chemistry of cytochrome *c* (in phosphate buffer, ca. pH 7) is 4-aminothiophenol (4-ATP). According to Hill et al. [14], this molecule remains in its unprotonated aromatic form ($pK_a = 4.3$) in neutral solutions, in contrast to lysine residues of cytochrome *c* ($pK_a = 9.8$). Correspondingly, promot-

ing effects of 4-ATP were explained as due to favorable electrostatic interactions of the type Au–S–$C_6H_4$–$NH_2$:$^+H_3N$–Lys-(cyt *c*). On the other hand, Bryant and Crooks [294] have concluded on the basis of capacitance measurements for the 4-ATP SAM on Au that the surface p$K_a$ for the chemisorbed 4-ATP (measured at +0.2 V versus saturated Ag/AgCl electrode) is much higher, namely, 6.9. In addition, p$K_a$ has been suggested to shift to higher values at more negative electrode potentials. However, SERS studies on the adsorption of 4-aminothiophenol on Ag and Au electrodes [295] have shown that 4-ATP, when adsorbed on an electrode surface, undergoes pH as well as potential-dependent transitions between the aromatic and the quinonoidic forms. The quinonoidic form exists in neutral and alkaline solutions and at more positive potentials of ca. −1.5, while the aromatic form is observed mainly in acidic solutions (i.e. pH 2). It is interesting, in this respect, that 4-ATP might exist in the potential range normally used to study redox reactions of cytochrome *c* (i.e. from −0.4 to 0.4 V) as the imine rather than amine, and still exhibit very good promoting properties.

Phenyl- or benzyl-terminated thiolate SAMs (with no hydrophilic functional group) do not promote redox reactions of the cytochrome *c* on gold [14,293]. At the moment, there exists no obvious explanation for this phenomenon. The surface coverage of thiophenol, HS-$C_6H_5$, on gold is $4.4 \times 10^{-10}$ mol cm$^{-2}$, only less than twofold lower compared to $\Gamma$ found for the perfectly ordered *n*-hexadecanethiolate on Au(111) ($7.8 \times 10^{-10}$ mol cm$^{-2}$) [290]. Taking into account the fact that the surface area occupied by the cytochrome *c* molecule would be 900 Å$^2$, lower surface coverage of the former cannot explain an apparent lack of its promoting capabilities, since the aromatic SAM should prevent a direct contact of the protein with the electrode surface. Surface coverage of aromatic thiol can be further increased by introducing a long hydrophobic hexadecyl chain in the para position of the phenyl ring to yield packing densities similar to those found in the case of long-chain *n*-alkanethiol films [290]. SERS studies [296–298], as well as STM measurements [290] suggest that the orientation of the aromatic ring is almost vertical to the electrode surface in benzyl-terminated thiolate SAMs. On the other hand, thiophenol and diphenyl disulfide adopt a 'flat-lying' geometry. Carron and Hurley [297] have concluded, on basis of their SERS data, that the axial angle between the aromatic ring of thiophenol and gold is 76°. On the other hand, according to more recent SERS work by Szafranski et al. [298], and previous theoretical ab initio calculations [70], the Au–S–C angle in thiophenol monolayer on gold is 104°, characteristic of $sp^3$ hybridization of the sulfur atom (see Scheme 1). However, it is quite clear that under any geometry of this adsorbate on the electrode surface hydrogen-bonding contacts between its phenyl ring and hydrophilic groups of cytochrome *c* surface cannot be established. Apparently, the latter seems to be critical for the ET between the electrode and the protein to occur.

As discussed in the previous sections, the so-called hydrophilicity requirement, in order to show promoting effects of SAM on electrode reactions of cytochrome *c* seems to be linked directly to the degree of electronic coupling between a given monolayer (aromatic or aliphatic) and the protein. As noted above, such promoters of ET reactions can be described as bifunctional molecular bridges having one

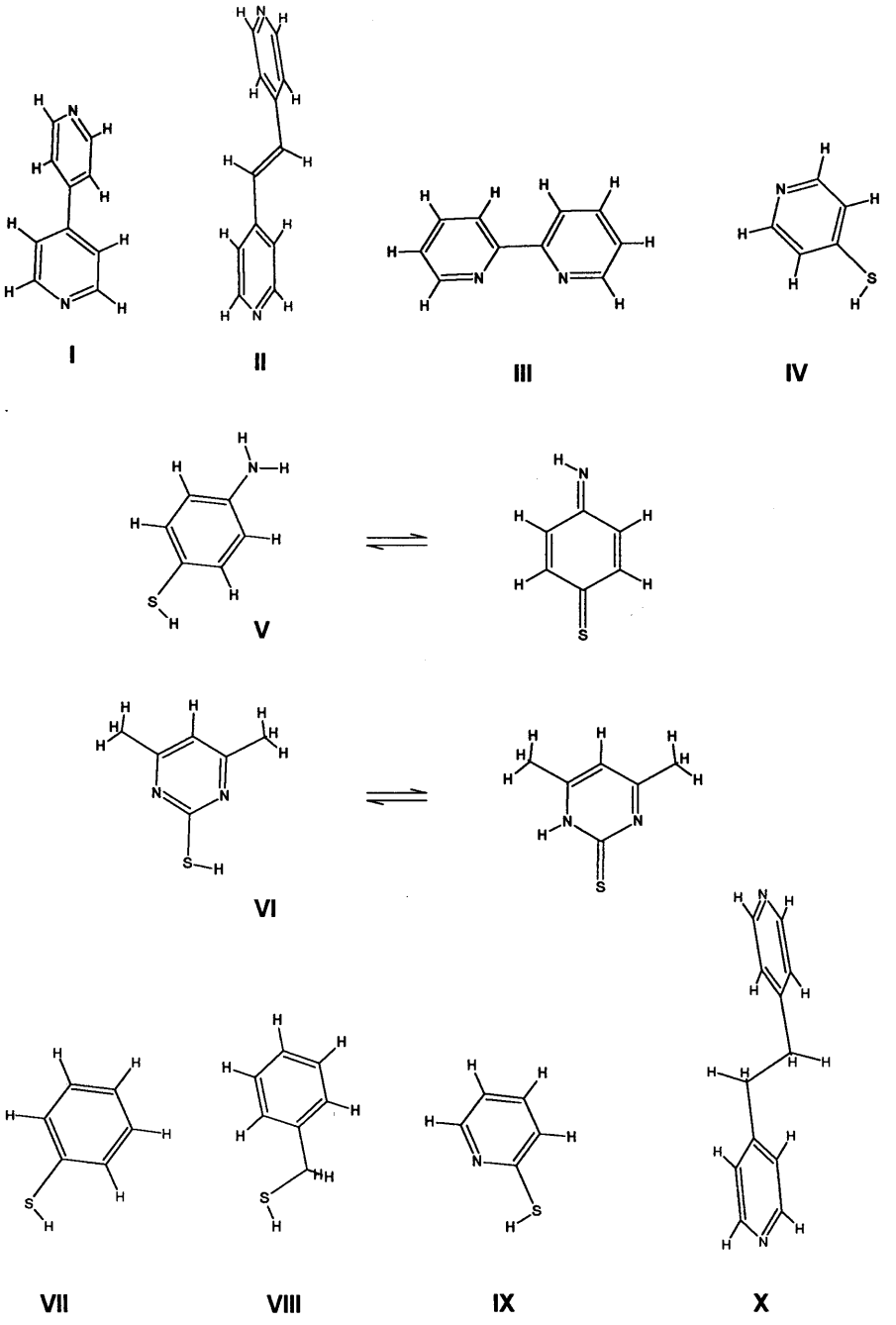


Scheme 1. Examples of organic molecules able to form self-assembled monolayers on a gold surface. Adsorbates **I**–**VI** are known to function as promoters of electron transfer for cytochrome *c*, while **VII**–**X** show no sign of such promoting effects. Note that all the chemisorbed aromatic thiols exist as corresponding thiolates on a gold surface, while molecules **V**, **VI** might undergo potential-induced isomerization reactions.

functional group (i.e. thiolate) bound to the electrode surface, while the other (head group), is available for the interaction with the metalloprotein surface (not necessarily lysine). As already mentioned in Section 3.2., there exist several exceptions to this rule, and 2,2′-bypyridine was just one such example. Even more intriguing is the case of another heterocyclic promoter, namely, 4,6-dimethyl-2-mercaptopyrimidine (DPM) [42,299], showing on gold a similar promoting capability as, for example, bis(4-pyridyl) disulfide or 4-mercaptopyridine. STM measurements [300] have shown that DPM adsorption on Au results in some kind of molecular lines having intermolecular separation of 8.5 Å, with the heterocyclic rings being perfectly perpendicular to the substrate. DPM molecules were found to be bound to gold as the tautomeric thione, C=S (Scheme 1), rather than chemisorbed thiolate. The adsorbate seems to adopt on gold surface such a geometry that both of its methyl groups prevent DPM from intermolecular hydrogen bonding (observed in the case of 2-mercaptopyrimidine). Interestingly, STM data with atomic resolution permitted also the identification of an exact position of both methyl groups within the DPM monolayer on the Au(111) surface. These seem to be directed away from the substrate surface. Providing that the adsorbate position does not change in the potential range from $-0.4$ to 0.4 V (where the cytochrome *c* undergoes ET reactions), it is difficult to envisage how any H-bonding contacts between the protein and this hydrophobic monolayer could be formed. Further in situ experiments, for example, AC admittance, contact angle measurements, quartz-crystal microbalance, SERS, ATR FTIR, etc. will be required to find out whether or not such changes in adsorbate geometry occur under controlled-potential conditions.

Finally, one could ask whether there is any apparent advantage of using aromatic rather than aliphatic promoters of electron transfer. The answer is no. However, it is clear that there exist some cases where one would like to induce cytochrome *c* adsorption, rather than to avoid it. As discussed above, SERS experiments clearly show that the surface isomerization reactions might complicate the overall picture of how cytochrome *c* interacts with such SAMs (i.e. an example of thiophenol, discussed here). On the other hand, most of the carboxyl-terminated aromatic thiolate monolayers will allow for a strong electrostatic binding of cytochrome *c*, similar to that experienced on aliphatic COOH-terminated SAMs. Providing there is no specific polarizable (i.e. hydrophilic head group) attached to the aromatic moiety, there is no electrochemical response for the redox reactions of the cytochrome *c*. It should be noted that problems might also arise from desulfurization of aromatic thiol monolayers [297,301], leaving hydrophobic aromatic residues at the electrode/aqueous solution interface. Interestingly, Lamp et al. [302] have not obtained any evidence of desulfurization of thiophenol during 4-day gold exposure to a dilute thiophenol solution (SERS experiment). On the other hand, 4-mercaptopyridine was found to undergo desulfurization reactions under similar experimental conditions (1 mM thiol solution) even at times as short as 1 hour [301]. Even though chemisorbed $S^{2-}$ or $HS^{-}$ species on gold electrodes (which could also result from such desulfurization reactions) are known to promote redox reactions of cytochrome *c* [302], as do halide anions such as $I^{-}$, $Br^{-}$ or $Cl^{-}$ [303,304].

### 3.6. Mixed hydrophilic/hydrophobic thiol SAMs

Experimental evidence collected during the last two decades shows that some promoters of electron transfer function well for one metalloprotein, but might be of no use for another. For example, reversible electrochemical response of tetraheme cytochrome $c_3$, normally observed on unmodified Au, Hg or carbon electrodes [305–310], is completely erased following electrode surface modification by PySSPy [236]. Hill and Lawarance [126] were first to realize that such 'recognition' ability of SAMs might be simply linked to electrostatic interaction between the promoter of ET and proteins differing in charge distribution on their surfaces. They have also demonstrated that so-called 'dilute' surface modification, i.e. mixed thiol SAMs, allows detecting two of metalloproteins present as a mixture in the solution. Modification of a gold working electrode with equivalent amounts of $-S(CH_2)_2COOH$ and $-S(CH_2)_2NH_2$ (suggested to exist in ionized state on the gold surface in contact with HEPES buffer, pH 7) produced an electrode which permitted direct electrochemistry of both positively-charged horse-heart cytochrome *c* and negatively charged membrane-cleaved cytochrome $b_5$.

In the next discussion, we will take a look how such dilution in the thiol monolayer affects kinetics of heterogeneous ET between the cytochrome *c* and electrode. As has been shown in Sections 3.2 and 3.5., this positively charged metalloprotein interacts strongly with most of the carboxyl-terminated SAMs, and kinetics of electrode processes seem to be often limited by the rate of its rotation at the monolayer/solution interface. Providing this conclusion is correct, the dilution of COOH SAM by ω-hydroxyalkanethiol (similar alkyl chain lengths in both cases) should result in the acceleration of such reactions. Indeed, this is what has been observed experimentally [246]. The ET rate for the yeast cytochrome *c* at the mixed $C_7OH/C_7COOH$ thiol SAMs was ca. 30 times faster than on single-component $C_7COOH$ SAM. Furthermore, a remarkable increase in $k^{\circ}_{et}$ for the reduction of yeast-cytochrome *c* was observed on mixed $C_{10}COOH/C_7OH$ films reaching 500 $s^{-1}$ compared to only $k^{\circ}_{et} = 18\ s^{-1}$ on a single-component $C_7COOH$ SAM. Naturally, a question arises here as to whether the diluting thiol should contain hydrophilic head group (i.e. hydroxyl, amine, etc), or whether it could be hydrophobic, as is the case of alkyl chains in *n*-alkanethiol SAMs. Since the pioneering work of Bain and Whitesides [63], mixed *n*-alkanethiol/mercaptoalkanoic acid monolayers were subjected to intensive research, especially regarding their wettability, phase transitions and phase separation [76,264,309]. It follows from these studies that *n*-alkanethiol SAMs on gold do not seem to promote electron-transfer reactions of cytochrome *c*. This is consistent with the fact that hydrogen bonding between the protein and such monolayers cannot be established, as was the case of phenyl-terminated SAMs. Interestingly, a *n*-alkylthiol can be used as a diluting agent in the mercaptoalkanoic acid SAM, which apparently allows for faster kinetics of cytochrome *c* reduction compared to a single-component COOH SAM. For example, $HOOC(CH_2)_{10}SH/CH_3(CH_2)_9SH$ films were prepared on Au(111) surface, and the effect of COOH: $CH_3$ ratio on the adsorptivity of cytochrome *c* and kinetics of its redox reactions (in adsorbed state) was studied using the

electroreflectance technique by Arnold et al. [138]. These authors consider methyl-terminated patches within the monolayer as the ET blocking sites, while COOH patches are suggested to serve as the electron-transfer sites, on which the protein gets immobilized electrostatically. It is interesting in this respect that $pK_a$ value for the mixed monolayer is ca. 8.2 and does not change significantly with the mole fraction of ω-mercaptoalkanoic acid ($\chi_{acid}$). The maximum rate constant $k_{et}^{\circ\prime} = 200$ $s^{-1}$ for the reduction of horse-heart ferricytochrome *c* is reached for $\chi_{acid} = 0.8$. It is noteworthy that this is a sixfold higher value as compared to a single-component COOH SAM. Lee et al. [78] concluded, on the basis of contact angle measurements, that the onset ionization of mixed $CH_3$/COOH monolayers appears to occurs in the pH range from 6 to 8, which is 2–4 units above the $pK_a$ of simple carboxylic acids in solution. Similar ionization behavior ($pK_a \sim 8$) has been deduced from AFM experiment for single-component 3-mercaptopropanoic acid monolayer on gold [311]. Also, voltammetric measurements for 11-mercaptoundecanoic acid/1-decanethiol self-assembled monolayer on Ag(111) indicate onset on set ionization at pH 6 and $pK_a = 8.4$ [312], similar to that proposed by Arnold et al. [138] for the $C_{10}COOH/C_9CH_3$ SAMs on gold. This would suggest that cytochrome *c* association to such mixed SAMs from buffered solutions of pH 7 is not a pH-driven process, but the deprotonation of COOH-terminated SAMs is simply due to replacement of protons within the monolayer by positively charged residues on the cytochrome *c* surface. The fact that the surface coverage of the cytochrome *c* was ca. 11 pmol $cm^{-2}$, and practically independent of the $CH_3$/COOH ratio suggests that other modes of protein binding to the monolayer other than purely electrostatic interactions might be of importance (i.e. van der Waals forces).

In the case of mixed $C_{11}$ mercaptoalkanoic acid/*n*-alkanethiol ($n = 9$, 10, 11, 12) SAMs, prepared by a nonreactive spreading protocol, Creager and Clarke [313] observed gradual increase in $pK_a$ values from 6.5 to 11.5 with increase in *n* from 9 to 12. The increase in the *n*-alkylthiol chain length is suggested to create a non-polar, low-dielectric constant microenvironment in such mixed SAMs, leading thus to significant $pK_a$ shifts. It would be tempting to investigate how such variation in the surface acid–base equilibria due to the variation in alkylthiol chain length would affect cytochrome *c* electrochemistry. However, electrochemical as well as electroreflectance measurements [138] revealed serious time-dependent desorption of cytochrome *c* from the mixed $COOH/CH_3$ SAM surfaces for $\chi_{acid} < 0.6$, while most of the contact-angle titrations by Creager and Clarke were conducted at $\chi_{acid} = 0.21$. Contact-angle measurements simply failed at $\chi_{acid} > 0.5$ since the monolayer surface was completely wet by droplets at high pH.

An interesting type of mixed SAMs, composed of thiols significantly differing in their chain length, i.e. 3-mercaptopropionic acid and *n*-octadecylmercaptan, $C_{18}SH$, were prepared by Sato and Mizutani [314]. Mixed short-long chain thiols were found more efficient in blocking the electron transfer to (from) cytochrome *c* than $C_{18}SH$/PySSPy monolayers forming patched domains of a certain size. The mixed 3-mercaptopropionic acid/$C_{18}SH$ monolayer completely blocked the electron transfer between $Fe(CN)_6^{4-/3-}$ when the mole fraction of $C_{18}SH$ was 0.2. On the other hand, the PySSPy/$C_{18}SH$ SAM shows much lower blocking abilities for the electron

transfer, even for the mole fraction for the latter thiol as high as 0.8. Mixing of PySSPy with *n*-alkanethiols $C_3SH$, $C_{12}SH$ and $C_{18}SH$ showed stronger blocking effects on the cytochrome *c* redox reactions [314] than those observed for the ferricyanide/ferrocyanide redox couple. Peak current for the cytochrome *c* reduction decreased significantly in the case of $C_3SH$/PySSPy SAM even though the mole fraction for the $C_3SH$ was only 0.1, while no signal for the cytochrome *c* redox reactions was detectable for $\chi > 0.3$. Interestingly, $C_3SH$ alkane thiol was found to mix better with PySSPy and showed better blocking abilities for the ET reactions than either $C_{12}SH$/PSSPy, or $C_{18}SH$/PySSPy films. In the case of SAMs consisting of these short *n*-alkanethiols, a complete inhibition of ET between the electrode and the metalloprotein was achieved at $\chi < 0.4$. The fact that the current due to the cytochrome *c* reduction or oxidation decreased in magnitude with the increasing mole fraction of the *n*-alkanethiol without affecting significantly the reversibility of the electrode process supports the idea of patched domain formation, as also confirmed by results of STM measurements [315].

## 4. Interprotein electron transfer and surface-confined heme proteins

The kinetics of interprotein ET between the two, or several, heme-containing metalloproteins are intimately linked to formation of complexes between these redox partners. Such processes are often dictated by electrostatic and/or van der Waals type of interactions between the ionized amino acid residues located in the vicinity of their heme cavities. Before the electron transfer can occur, metalloproteins have to usually approach to a certain distance and, furthermore, hemes usually adopt respective orientations characteristic for a given biological system. It is interesting in this respect that not only the charged amino acid residues, located on the protein exterior, but also the propionic acid groups attached to the heme edge of hemes a, b and c, might participate in formation of such complexes. The ionization of heme propionic groups in cytochrome *c* has also been suggested to affect directly the magnitude of its total reorganization energy [181]. Authors of the latter work have suggested that $\varepsilon$ in the protein interior could increase from 4 to 40 in the vicinity of the heme edge, providing their ionization takes place. Indeed, recent IR measurements in deuterated solvent [316] have revealed that one of the propionic acid chains indeed undergoes ionization with $pK_a < 6.5$. However, solution NMR data [8] show that propionic acid groups are directed away from the heme iron. Furthermore, protonated Lys-79 residue in cytochrome *c* (at the heme cavity entry) might under some conditions adopt conformation as to compensate negative charge of propionate side chains on the heme edge. This possibility seems even more likely following the recent hole-burning spectroscopy measurements [317], which have identified an electric field perpendicular to the porphyrin plane, suggested to be due to the ionization of one of the propionic acid chains and, another in-field component differing (ca. 13° from the former), which could be due to protonated lysine residues.

As mentioned above, the propionic acid side chains in cytochrome *c* are located at the heme cavity entry, with much larger accessibility of the external water molecules than the heme iron. Also, in cytochrome $b_5$, the propionic acid side chains are freely accessible to water, and propionate participates directly in its binding to the positively charged lysine residues of cytochrome *c* (so-called docking cyt *c*/cyt $b_5$ model [112,115,116]. The existence of such docking has been indeed confirmed recently using X-ray and solution $^{13}$C-NMR [12]. Importantly, such complexation reactions of cytochrome *c* and cytochrome $b_5$ and corresponding kinetics of homogeneous ET reactions can be observed directly at the electrode/solution interface using cyclic voltammetry on gold electrodes modified using β-mercaptopropionate [318]. Differences in the charge sign for both proteins (i.e. neutral aqueous solution) and, therefore, differing ability of both proteins to interact with the ionized films formed on electrode surfaces, are the main reason that chemically-modified electrodes (SAM or polymer) manifest a certain degree of molecular recognition. While the positively charged polylysine, strongly interacting with the surface carboxylate, excludes any direct electron transfer between cytochrome *c* and Au electrode, cytochrome $b_5$ undergoes reversible electrochemistry at the SAM/polylysine interface. In such a case, outer mitochondrial membrane cytochrome $b_5$ (rat liver) functions as a simple mediator of electron transfer since its redox potential ($E° = -0.102$ V) is much more negative than that of cytochrome *c* ($E° = 0.265$ V). Second-order homogenous rate constants between ferrocytochrome $b_5$ and ferricytochrome *c* obtained using digital simulation of cyclic voltammograms were found to be $k_f = 2.9 \times 10^8$ $M^{-1}$ $s^{-1}$ ($k_b = 1360$ $M^{-1}$ $s^{-1}$); and $k_f = 8.9 \times 10^8$ $M^{-1}$ $s^{-1}$ ($k_b = 4450$ $M^{-1}$ $s^{-1}$), for the beef liver microsomal ferrocytochrome $b_5$ ($E° = 0.003$ V) and ferricytochrome *c* [318].

Quite a different strategy, allowing one to study redox chemistry and kinetics of ET of cytochrome *c* and cytochrome $b_5$ at the same time, is based on L-cysteine-modified gold electrode, as described by Qian et al. [127]. The latter authors have noticed that the negatively charged cytochrome $b_5$ does not show any electrochemical response on gold electrode modified with L-cysteine (in contrast to cytochrome *c*). However, this situation changes once a small amount $Mg^{2+}$ (4 mM) is added into the solution containing both proteins (pH 7.0). The presence of magnesium ions has been found to improve the cyclic voltammetric behavior of horse-heart cytochrome *c* on such CME, however, it should be noted that the authors might have experienced some difficulties with maintaining cleanliness in their system. Especially, since the shape of voltammograms presented in Fig. 1(A) of Ref. [127] does not correspond to highly reversible response as found for cytochrome *c* on cysteine-modified gold electrodes by other workers [44,268,270]. Different interaction models involving protein-electrolyte-electrode were proposed. However, the shape of cyclic voltammograms for the cytochrome *c*/cytochrome $b_5$ (1:1) complex, as well as the interpretation of homogeneous ET between the two proteins, are qualitatively different from those presented in Ref. [318], as discussed above.

Even though such carboxylate/polylysine-modified electrodes show molecular recognition and allow obtaining homogeneous rate parameters, they do not provide us with information about the nature of complexation reactions between the two

proteins and their orientation at the electrode/solution interface. Polylysine binding to carboxylate-containing SAMs on gold has been studied using surface plasmon resonance technique [251]. However, this method, even though useful for the film thickness determination, does not provide deeper insight into the interprotein ET reactions. It is likely that FTIR technique and SERRS will find in the future more applications not only in studies of cytochrome *c* binding to other proteins (i.e. cytochrome $b_5$), but also to hydrophilic monolayers assembled directly on electrode surfaces. Especially, the use of reflectance FTIR [133], which is ideally suited to detecting conformational changes occurring during such processes. Resolution of SERS and resonance SERS might further increase when using the new generation of Raman microscopes which, in some cases, allow performing measurements even on atomically smooth Ag or Au single-crystal surfaces, without their electrochemical roughening, while providing very high spatial resolution.

Significant effort has been developed in last decade in order to design experimental procedures, which would allow covalent fixing of metalloproteins directly on electrode surfaces. For example, cytochrome *c* peroxidase and also cytochrome *c* were immobilized via their lysine residues to a gold surface using 3,3′-dithiobissulfosuccinimidyl propionate (DTSSP) [128]. Even though substantial changes occurred in the chemical environment of the immobilized redox center of CcP ($E°'$ for the fixed CcP was $-0.254$ V, compared to 0.848 V versus Ag/AgCl estimated in solution), its catalytic oxidation by solution phase cytochrome *c* has been achieved. It is to be noted that a value of $+0.848$ V, as stated in the above mentioned reference, seems to be unreasonably positive for the $E°'$ CcP in solution. It is not clear that the interpretation of this result in Ref. [128] is correct.

DTSSP has been also exploited to immobilize glucose oxidase (GOD) to the gold electrode surface [319], preserving its catalytic activity towards glucose but not to 2-deoxy-D-glucose and D-(+)-mannose.

It is interesting that even large enzyme complexes such as cytochrome *c* oxidase (beef-heart, mw = 204 kDa, 13 subunits) can be fixed on 3-mercaptopropionic acid-modified gold electrode using the carbodiimide method, while catalytic activity of the enzyme remains more or less preserved [125]. The quasi-reversible response of cytochrome *c* oxidase centered around 0.385 V versus NHE has been assigned as due to a one-electron redox process associated with the heme $a_3$ and the electrode surface ($k^{\circ}_{et}{}' = 1.56\ s^{-1}$). Relatively slow kinetics of heterogeneous ET has been observed for redox reactions of microperoxidase MP-11 attached to the 2,2′-diaminodiethyl disulfide-modified gold electrode [320]. Catalytic activity of MP-11 in respect to $H_2O_2$ reduction confined to the electrode has been shown to be somewhat inferior to heme covalently attached to cystamine SAM via its propionic acid groups.

Providing enzyme confinement on an electrode does not result in conformational changes or serious denaturation, analytical devices capable of biomolecular recognition can be prepared.

For example, an amperometric immunosensor based on cystamine SAM that was further coupled to a mixture of *N*-ε-2,4-dinitrophenyl lysine (the antigen) and microperoxidase (electroactive enzyme), able to detect dinitrophenyl antibody

(DNP-Ab) in the presence of persulfate acting as electrocatalyst for the latter enzyme, has been reported by Katz and Willner [321]. In spite of the fact that this method can be used qualitatively for the determination of the DNP-Ab, its use for its quantitative determination is limited due to the presence of microscopic defects within the monolayer, which do not quantitatively block persulfate diffusion to the electrode surface (causing non-monotonic decrease in the amperometric response).

Amperometric transduction of optical signals at SAMs has been recently extended from simple light-sensitive organic molecules attached to electrode surfaces to more complex systems such as proteins and/or their complexes. For example a bifunctional monolayer consisting of 4-pyridyl sulfide, cystamine and photoisomerizable spirospyran [321], has been used to attached cytochrome *c* oxidase to the electrode surface [322–325]. While irradiation of such CME with visible light ($\lambda > 475$ nm) results in the nitrospyran (SP), illumination of a SP-containing monolayer on Au in the range of wavelengths from 360 to 400 nm results in protonated nitromerocyanine, $MRH^+$, still covalently attached to the electrode surface through cystamine. Apparently, due to the electrostatic interactions between the Au-$MRH^+$ and positively charged cytochrome *c*, no electron exchange is observed between the electrode and the protein. Once the SP state of the dye is formed, such communication is allowed and, as a result, quasi-reversible cyclic voltammograms ($k^{\circ\prime}_{et} = 1 \times 10^{-3}$ cm $s^{-1}$) were recorded [323]. Favorable interactions between cytochrome *c* and chemisorbed 4-pyridyl sulfide (coexisting on Au surface with SP) allow a relatively close approach of the protein to the electrode surface. Reversible photoisomerizable properties of the monolayer allow the cyclic activation/deactivation of the electron-transfer communication between cytochrome *c* and the dye-modified electrodes. Since cytochrome *c* serves as electron-transfer mediator to cytochrome *c* oxidase, which catalyzes reduction of molecular oxygen to water, the interprotein electron transfer and subsequent biocatalyzed reduction of oxygen can be controlled by means of photoswitching between SP and $MRH^+$ states directly at the electrode surface. However, the photoisomerization of SP to $MRH^+$ required the cell to be dismounted and filled with pure buffer solution, which led to some problems in reproducibility of experimental data, apparently associated with a partial mechanical degradation of the monolayer.

## 5. Future perspectives in electrochemistry of metalloproteins

As has been illustrated throughout this paper, the electrochemical behavior of cytochrome *c* at the metal/solution interface (whether modified or not), still remains far from completely understood. As discussed above, there exist several factors that distinguish the biological ET from that taking place in artificial systems. First, heme solvation in the hydrophobic interior of the cytochrome *c* is very different from that experienced in the bulk solvent. This has been suggested to lead to lower $\lambda$ values compared to hypothetical metalloprotein having its heme completely exposed to the aqueous solution. Second, while metal-centered porphyrin reduction might be accompanied by axial ligand removal from the complex, two axial ligands in

horse-heart cytochrome *c* remain coordinated in both oxidation states with only minor metal-ligand bond length changes during the redox transition. The redox process associated with the Fe(III) reduction in cytochrome *c* is known to be accompanied by the rearrangement of the protein dipoles around the heme, changes in the hydrogen bonding in the heme cavity, and porphyrin ring deformations [210,326,327]. Apparently, these processes do not contribute significantly to the overall energy barrier for ET in cytochrome *c* and, furthermore, amino acid dipole movements in the electric field are quite rapid. Because of the complexity of interactions existing between the heme and the protein, the kinetics of its redox reactions cannot be reproduced upon the heme removal from the protein in any artificial environment, including various solvents, glass matrices, polymers, biological or artificial membranes.

Long-range electrostatic forces, acting at the polarized electrochemical interface, can bring this highly charged metalloprotein into the adsorbed state, in which protein unfolding and spin-state changes on the heme iron might occur. These phenomena were first brought to light by Hildebrandt and his colleagues in the late 1980s. In fact, most of the knowledge on structural changes of cytochrome *c* at such electrified interfaces available today comes from combined electrochemical and spectroscopic experiments (i.e. SERS, FTIR, electroreflectance, etc). However, following the short report by Eddowes and Hill in 1977, indicating that 4,4′-bipyridine promotes redox reactions of cytochrome *c*, electrochemists tried continuously to prevent its adsorption on solid electrode surfaces. Albery and co-workers [328] studied redox reactions of cytochrome *c* on a 4,4′-bipyridyl-modified rotating gold electrode and conclude that kinetics of cytochrome *c* reduction on unmodified gold electrodes should be very slow ($k^\circ \sim 10^{-9}$ m $s^{-1}$), while protein binding to PyPy films has been proposed to account for some 5 orders of magnitude increase in the electrochemical rate constant. As shown throughout this work, adsorptivity of cytochrome *c* (and other proteins) dramatically depends on the nature of the adsorbed molecules forming monolayer on the electrode surface and the degree of their ionization. However, as shown in Ref. [145], surface coverage of cytochrome *c* on pyridyl-terminated monolayers is quite low as compared to carboxyl-terminated SAMs (cf. Section 3.4.Section 3.2). On the other hand, there is virtually no measurable adsorption of cytochrome *c* on OH-terminated SAMs (Section 3.1) and yet kinetics of cytochrome *c* redox reactions are superior to any kind of other SAM (including pyrididyl-terminated SAMs). This directly contradicts the idea that a certain degree of cytochrome *c* adsorption on SAM is required in order to observe very fast ET rates (cf. 'generalized reaction scheme for ET reactions of proteins on various electrode surfaces' in Ref. [328]). The above mentioned examples clearly show that additional experimental as well as theoretical work (i.e. molecular dynamics simulations) will be required in order to understand the effect of protein adsorption on SAM surfaces on kinetics of interfacial electron transfer.

As shown in the present review, a large number of electrode surface modifiers has been described during the last 3 decades, and the successes and failures of electrode surface modification in bioelectrochemistry of proteins are well documented in the

literature. The adsorption of cytochrome *c* on chemically-modified electrode surfaces (or CMEs, as we have called it here) seems to be affected by various factors such as the solution pH, electrolyte composition, its ionic strength, experimental temperature and, importantly, chemical structure of the modifier. Systematic adsorption studies using AC admittance, quartz-crystal microbalance, and in situ spectroscopic techniques, will be required in order to establish in which cases cytochrome *c* undergoes adsorption on promoter-covered surfaces and, also, where such adsorption is completely absent. Such studies would be especially helpful in the case of phenyl or benzyl-terminated SAMs, where the lack of electrochemical signal for the cytochrome *c* could be due either to the protein adsorption on the electrode surface (and its denaturation), or to a weak electronic coupling between the metalloprotein and the electrode covered by hydrophobic film with a low degree of wettability.

A significant amount of experimental work on electrochemical behavior of cytochrome *c* has been directed in the past towards the improvement of the reversibility of its electrode reactions on CMEs. Finally, this goal has been accomplished, and today, a reasonable number of promoters exists which allow for its fast, diffusion-controlled, cyclic voltammetric response. In fact, such electrode processes became so fast that they appear to be hardly accessible to usual electrochemical techniques available for kinetic measurements today. However, in this context, little information is available on how the cytochrome *c* structure itself affects kinetics of electrode reactions. This is to say, that more attention should be directed to quasi-reversible or irreversible voltammetry of metalloproteins, which might hide precious information about conformational changes in the heme protein which, in fact, are known to occur also in biological systems (i.e. during interactions of cytochrome *c* with biological membranes, or its natural redox partners).

It is very interesting that conformational changes in cytochrome *c* can be induced in the presence of some organic molecules such as pyridine, imidazole, and others, which are known to serve at the same time as axial ligands to the heme iron. It is important that these ligands (showing very differing affinity toward ferri- and ferroheme) do not cause a complete unfolding of cytochrome *c* as would some typical denaturating agents, but rather affect the position and orientation of amino acid residues located in the heme cavity. Relatively recent experimental data have been reported (solution NMR experiments, cf. Section 3.2), which seems to support the idea that several amino acid dipoles and peptide chains on the Met-80 side of the heme undergo a complex movement in the presence of pyridine. Since substituted heterocyclic molecules were shown to introduce varying degree of disorder in the cavity, this should affect both thermodynamics of electrode reactions as well as the rate with which enzyme is able exchange electrons with the electrode (or another ET protein). Future electrochemical studies, which would address the issue of the effect of the above mentioned molecules on kinetics of the heterogeneous ET and, also, on the magnitude of reorganization energy for cyt *c* (His18-Fe(III)-L/cyt *c*(His18-Fe(II)-Met-80 (where L = pyridine, imidazole, or their alkylated analog) couple, will be required.

In addition to the pH-, temperature- and ligand-induced conformational changes in cytochrome *c*, there exist also other ways of perturbing protein structure. Following the first studies on heteropolytungstate binding to cytochrome *c* [329,330], Antalik and co-workers pursued their work on binding negatively charged polymers, such as heparin, polyglutamate, polyadenylate, polygalacturonate [331–334], Nafion [335] poly(vinylsulfate) and poly(4-styrene-sulfonate) [336], to positively-charged cytochrome *c*. Since these polymers are optically transparent from 300 to 900 nm, the corresponding changes in the cytochrome *c* structure can be followed using spectroscopic techniques such as UV–vis, fluorescence spectroscopy, Raman spectroscopy, or circular dichromism. It is interesting that there exist similarities between cytochrome *c* interactivity with such polyanions and with carboxyl-terminated self-assembled monolayers (as discussed in Section 3.2). For example, an increase in the ionic strength can completely eliminate either cytochrome *c*/polymer or cytochrome *c*/SAM interactions. However, the two systems differ in much greater ability of some polymers (e.g. Nafion) to penetrate into the protein interior (hydrophobic effect), causing more profound structural changes in the protein than normally experienced on SAM surfaces. Electrochemical studies on cytochrome *c* (and other heme-containing proteins) in Nafion films formed directly on electrode surfaces, appeared in the literature [337]. Interestingly, cytochrome *c* has been found to be electrochemically inactive, unless a Cu(II) catalyst was present in the film [338]. Electrochemical studies regarding immobilization of cytochromes on electrode surfaces modified by other polymers mentioned above (which are less hydrophobic than Nafion), are to be done in the future.

It is important that not only the intensity of electrostatic interactions between a self-assembled monolayer and a charged reactant may be varied in the presence of highly charged ions, but also the geometry of adsorbate molecules on the electrode surface. This could have interesting consequences on kinetics of electron transfer between cytochrome *c* and the CME. For example, self-assembled glutathione monolayers on gold show an interesting ion-gate response, and the conformational changes of adsorbate can be induced by $K^+$, $Ca^{2+}$ or $Ba^{2+}$ cations [339–343]. Glutathione-modified electrodes, in the presence of multiply charged cations, might be able to distinguish the cytochrome *c* from the cytochrome $b_5$ in solution (as discussed in Section 4, for a cysteine-modified electrode in the presence of $Mg^{2+}$ ions).

In recent years, bioelectrochemists have certainly succeeded in introducing some degree of molecular recognition into CMEs, a property typical to biological systems (i.e. enzymes), and we have tried in the present work to illustrate some of innovative approaches in this area. A research topic which seems to attract large interest among bioelectrochemists, is certainly the construction of biosensors and it is likely that future developments in bioelectronics will lead to practical applications of such devices (see also Ref. [344]). Biosensors capable of responding to a single (or several) analyte molecules, or allowing molecular recognition of enzymes, can be achieved by covalent attachment of metalloproteins to electrode surfaces, using chemical coupling agents. Very attractive are the ideas of stimulation of electrocatalytic reactions by light (cf. Section 4) with amperometric transduction and

amplification of optical signals. Tailored redox enzyme-linked immunosensor devices show enhanced sensitivities in the amperometric detection of antibodies or antigens, and may also serve for an indirect amperometric detection, via monitoring electroactive species such as NADH, $O_2$, $H_2O_2$ or $NH_3$, formed by the enzyme-linked antigen or antibody.

## Acknowledgements

The author is indebted to Drs M. Antalik and V. Vesela for introducing him to cytochrome *c* biochemistry, and Professor J. Augustynski for the motivation, encouragement and time necessary to complete this work. Helpful discussions with Professors M. Maroncelli, A. Warshel, S.H. Northrup, A.A. Stuchebrukhov and I. Benjamin are gratefully acknowledged. The author would like to thank to Professor F.A. Walker for numerous discussions concerning the charge delocalization in porphyrins, and for providing us with her manuscript on NMR and EPR spectroscopy of metalloproteins (Ref. [10]) before its publication. This work was supported by the National Swiss Foundation.

## References

[1] S. Yoshikawa, K. Shinzawa-Itoh, R. Nakashima, R. Yaono, E. Yamashita, N. Inoue, M. Yao, M.J. Fei, C.P. Libeu, T. Mizushima, H. Yamaguchi, T. Tomizaki, T. Tsukihara, Science 280 (1998) 1723.
[2] G.W. Bushnell, G.V. Louie, G.D. Brayer, J. Mol. Biol. 214 (1990) 585.
[3] T. Tsukihara, H. Aoyama, E. Yamashita, T. Tomizaki, H. Yamaguchi, K. Shinzawa-Itoh, R. Nakashima, R. Yaono, S. Yoshikawa, Science 269 (1995) 1069.
[4] S. Iwata, C. Ostermeier, B. Ludwig, H. Michel, Nature 376 (1995) 660.
[5] M.K. Safo, M.J.M. Nesset, F.A. Walker, P.G. Debrunner, W.R. Scheidt, J. Am. Chem. Soc. 119 (1997) 9438.
[6] P.X. Qi, R.A. Beckman, A.J. Wand, Biochemistry 38 (1996) 12275.
[7] J.-S. Park, T. Ohmura, K. Kano, T. Sagara, K. Niki, Y. Kyogoku, H. Akutsu, Biochim. Biophys. Acta 1293 (1996) 45.
[8] L. Banci, I. Bertini, H.B. Gray, C. Luchinat, T. Reddig, A. Rosato, P. Turano, Biochemistry 36 (1997) 9867.
[9] I. Bertini, C. Dalvit, J.G. Huber, C. Luchinat, M. Piccioli, FEBS Lett. 415 (1997) 45.
[10] F.A. Walker, in: K. Kadish, R. Guilard, K.M. Smith (Eds.), NMR Spectroscopy of Paramagnetic Metalloporphyrins, The Handbook of Porphyrins and Related Macrocycles, vol. 5, Academic Press, Burlington, MA, 1999, Chapter 36, pp. 81–183.
[11] T. Ohmura, T. Inobe, K. Kano, T. Horizumi, H. Akutsu, J. Electroanal. Chem. 438 (1997) 237.
[12] M.J. Rodriguez-Maranon, F. Qiu, R.E. Stark, S.P. White, X. Zhang, S.I. Foundling, V. Rodriguez, C.L. Schilling III, R.A. Bunce, M. Rivera, Biochemistry 35 (1996) 16378.
[13] L. Banci, I. Bertini, J.G. Huber, G.A. Spyroulias, P. Turano: Solution Structure of Reduced Horse Heart Cytochrome C, Brookhaven Protein Database, Code: 1GIW (in press).
[14] P.M. Allen, H.A.O. Hill, N.J. Walton, J. Electroanal. Chem. 178 (1984) 69.
[15] R.A. Marcus, N. Sutin, Biochim. Biophys. Acta 811 (1985) 265.
[16] G. McLendon, Acc. Chem. Res. 21 (1988) 160.
[17] F.A. Armstrong, H.A.O. Hill, N.J. Walton, Acc. Chem. Res. 21 (1988) 407.

[18] F.A. Armstrong, A.M. Bond, H.A.O. Hill, B.N. Oliver, I.S.M. Psalti, J. Am. Chem. Soc. 111 (1989) 9185.
[19] F.A. Armstrong, Struct. Bonding 72 (1990) 137.
[20] G. McLendon, R. Hake, Chem. Rev. 92 (1992) 481.
[21] C.C. Moser, J.M. Keske, K. Warncke, R.S. Farid, P.L. Dutton, Nature 355 (1992) 796.
[22] H.-X. Zhou, J. Am. Chem. Soc. 116 (1994) 10362.
[23] H.B. Gray, W.R. Ellis Jr., in: I. Bertini, H.B. Gray, S.J. Lippard, J.S. Valentine (Eds.), Bioinorganic Chemistry, University Science Books, Sausalito, 1994, pp. 315–364.
[24] A. Dolla, L. Blanchard, F. Guerlesquin, M. Bruschi, Biochimie 76 (1994) 471.
[25] A.M. Bond, Inorg. Chim. Acta 226 (1994) 293.
[26] F.M. Hawkridge, I. Taniguchi, Comments Inorg. Chem. 17 (1995) 163.
[27] R. Gennis, S. Ferguson-Miller, Science 269 (1995) 1063.
[28] G.R. Moore, G.W. Pettigrew, N.K. Rogers, Proc. Natl. Acad. Sci. USA 83 (1986) 4998.
[29] C. Mailer, C.P.S. Taylor, Can. J. Biochem. 50 (1972) 1048.
[30] H.A.O. Hill, L.H. Guo, G. McLendon, in: R.A. Scott, A.G. Mauk (Eds.), Cytochrome c: A Multidisciplinary Approach, University Science Books, Sausalito, 1996, pp. 317–333.
[31] H.B. Gray, J.R. Winkler, Annu. Rev. Biochem. 65 (1996) 537.
[32] J.M. Nocek, J.S. Zhou, S. De Forest, S. Priyadarshy, D.N. Beratan, J.N. Onuchic, B.M. Hoffman, Chem. Rev. 96 (1996) 2459.
[33] S.K. Chapman, S. Daff, A.W. Munro, Struct. Bonding 88 (1997) 39.
[34] A.X. Trautwein, E. Bill, E.L. Bominaar, H. Winkler, Struct. Bonding 78 (1991) 1.
[35] R. Cammack, G. Fauque, J.J.G. Moura, J. Le Gall, Biochim. Biophys. Acta 784 (1984) 68.
[36] P.M.A. Gadsby, J. Peterson, N. Foote, C. Greenwood, A.J. Thomson, Biochem. J. 246 (1987) 43.
[37] A. Warshel, A. Papazyan, I. Muegge, J. Biol. Inorg. Chem. 2 (1997) 143.
[38] E.F. Bowden, Electrochem. Soc. Interface (1997) 40.
[39] I. Taniguchi, Electrochem. Soc. Interface (1997) 34.
[40] M.J. Eddowes, H.A.O. Hill, J. Chem. Soc. Chem. Commun. (1977) 771.
[41] X. Yuan, F.M. Hawkridge, J.F. Chlebowski, J. Electroanal. Chem. 350 (1993) 29.
[42] C.-X. Cai, H.X. Ju, H.Y. Chen, Electrochim. Acta 40 (1995) 1109.
[43] G. Battistuzzi, M. Borsari, M. Sola, F. Francia, Biochemistry 36 (1997) 16247.
[44] M.T. Cruanes, K.K. Rodgers, S.G. Sligar, J. Am. Chem. Soc. 114 (1992) 9660.
[45] J. Sun, J.F. Wishart, R. van Eldik, R.D. Shalders, T.W. Swaddle, J. Am. Chem. Soc. 117 (1995) 2600.
[46] A. Szücs, M. Novak, J. Electroanal. Chem. 383 (1995) 75.
[47] A. Szücs, M. Novak, J. Electroanal. Chem. 384 (1995) 47.
[48] H.A.O. Hill, N.I. Hunt, A.M. Bond, J. Electroanal. Chem. 436 (1997) 17.
[49] G.H. Liu, W.P. Shao, S.M. Zhu, W.X. Tang, J. Inorg. Biochem. 60 (1995) 123.
[50] R. Hinnen, R. Parsons, K. Niki, J. Electroanal. Chem. 147 (1983) 329.
[51] D.E. Reed, F.M. Hawkridge, Anal. Chem. 59 (1987) 2334.
[52] S.-C. Sun, D.E. Reed, J.K. Cullison, L.H. Rickard, F.M. Hawkridge, Microchim. Acta III (1988) 97.
[53] S.R. Betso, M.H. Klapper, L.B. Anderson, J. Am. Chem. Soc. 94 (1972) 8197, and references therein.
[54] P. Hildebrandt, M. Stockburger, Biochemistry 28 (1989) 6710.
[55] G. Niaura, A.K. Gaigalas, V.L. Vilker, J. Electroanal. Chem. 416 (1996) 167.
[56] M.J. Eddowes, H.A.O. Hill, J. Am. Chem. Soc. 101 (1979) 4461.
[57] M.J. Eddowes, H.A.O. Hill, K. Uosaki, Bioelectrochem. Bioenerg. 7 (1980) 527.
[58] H.A.O. Hill, D.J. Page, N.J. Walton, D. Whitford, J. Electroanal. Chem. 187 (1985) 315.
[59] I. Taniguchi, K. Toyosawa, H. Yamaguchi, K. Yasukouchi, J. Chem. Soc. Chem. Commun. (1982) 1032.
[60] I. Taniguchi, K. Toyosawa, H. Yamaguchi, K. Yasukouchi, J. Electroanal. Chem. 140 (1982) 187.
[61] J.M. Sevilla, T. Pineda, A.J. Roman, R. Madueno, M. Blazquez, J. Electroanal. Chem. 451 (1998) 89.

[62] C.D. Bain, E.B. Troughton, Y.-T. Tao, J. Evall, G.M. Whitesides, R.G. Nuzzo, J. Am. Chem. Soc. 111 (1989) 321.
[63] C.D. Bain, G.M. Whitesides, Langmuir 5 (1989) 1370.
[64] C.D. Bain, H.A. Biebuyck, G.M. Whitesides, Langmuir 5 (1989) 723.
[65] P.E. Laibinis, G.M. Whitesides, D.L. Allara, Y.-T. Tao, A.N. Parikh, R.G. Nuzzo, J. Am. Chem. Soc. 113 (1991) 7152.
[66] M. Buck, F. Eisert, J. Fischer, M. Grunze, F. Träger, Appl. Phys. A 53 (1991) 552.
[67] A. Ulman, S.D. Evans, Y. Shnidman, R. Sharma, J.E. Eilers, J.C. Chang, J. Am. Chem. Soc. 113 (1991) 1499.
[68] A. Ulman, An Introduction to Ultrathin Organic Films from Langmuir–Blodgett to Self-Assembly, Academic Press, San Diego, 1991.
[69] C.P. Smith, H.S. White, Langmuir 9 (1993) 1.
[70] H. Sellers, A. Ulman, Y. Shnidman, J.E. Eilers, J. Am. Chem. Soc. 115 (1993) 9389.
[71] P. Fenter, A. Eberhardt, P. Eisenberger, Science 266 (1994) 1216.
[72] M. Zhang, M.R. Anderson, Langmuir 10 (1994) 2807.
[73] A. Badia, R. Back, R.B. Lennox, Angew. Chem. Int. Ed. Engl. 33 (1994) 2332.
[74] L.-H. Guo, J.S. Facci, G. McLendon, R. Mosher, Langmuir 10 (1994) 4588.
[75] W.R. Fawcett, M. Fedurco, Z. Kovacova, Langmuir 10 (1994) 2403.
[76] S.J. Stranick, A.N. Parikh, Y.-T. Tao, D.L. Allara, P.S. Weiss, J. Phys. Chem. 98 (1994) 7636.
[77] S.J. Stranick, A.N. Parikh, D.L. Allara, P.S. Weiss, J. Phys. Chem. 98 (1994) 11136.
[78] T.R. Lee, R.I. Carey, H.A. Biebuyck, G.M. Whitesides, Langmuir 10 (1994) 741.
[79] C.A. McDermott, M.T. McDermott, J.B. Green, M.D. Porter, J. Phys. Chem. 99 (1995) 13257.
[80] J.-B.D. Green, M.T. McDermott, M.D. Porter, L.M. Siperko, J. Phys. Chem. 99 (1995) 10960.
[81] M.W.J. Beulen, B.-H. Huisman, P.A. van der Heijden, F.C.J.M. Veggel, M.G. Simons, E.M.E.F Biemond, P.J. de Lange, D.N. Reinhoudt, Langmuir 12 (1996) 6170.
[82] A. Ulman, Chem. Rev. 96 (1996) 1533.
[83] H.O. Finklea, in: A.J. Bard, I. Rubinstein (Eds.), Electroanalytical Chemistry, vol. 19, Marcel Dekker, New York, 1996, pp. 109–335.
[84] N. Camillone III, T.Y.B. Leung, P. Schwartz, P. Eisenberger, G. Scoles, Langmuir 12 (1996) 2737.
[85] J. Kang, P.A. Rowntree, Langmuir 12 (1996) 2813.
[86] W. Pan, C.J. Durning, N.J. Turro, Langmuir 12 (1996) 4469.
[87] J.T. Woodward, D.K. Schwartz, J. Am. Chem. Soc. 118 (1996) 7861.
[88] R. Bhatia, J. Garrison, Langmuir 13 (1997) 765.
[89] R.P. Janek, W.R. Fawcett, A. Ulman, J. Phys. Chem. B 101 (1997) 8550.
[90] T. Ishino, H. Hieda, K. Tanaka, N. Gemma, J. Electroanal. Chem. 438 (1997) 225.
[91] H.-J. Himmel, C. Wöll, R. Gerlach, G. Polanski, H.-G. Rubahn, Langmuir 13 (1997) 602.
[92] M. Ohtani, S. Kuwabata, H. Yoneyama, Anal. Chem. 69 (1997) 1045.
[93] F.P. Zamborini, R.M. Crooks, Langmuir 14 (1998) 3279.
[94] C. Jung, O. Dannenberger, Y. Xu, M. Buck, M. Grunze, Langmuir 14 (1998) 1103.
[95] W.R. Fawcett, M. Fedurco, Z. Kovacova, Z. Borkowska, J. Electroanal. Chem. 368 (1994) 265.
[96] W.R. Fawcett, M. Fedurco, Z. Kovacova, Z. Borkowska, J. Electroanal. Chem. 368 (1994) 275.
[97] W.R. Fawcett, M. Fedurco, Z. Kovacova, Z. Borkowska, Langmuir 10 (1994) 912.
[98] D.-F. Yang, C.P. Wilde, M. Morin, Langmuir 12 (1996) 6570.
[99] G.K. Jennings, P.E. Laibinis, Langmuir 12 (1996) 6173.
[100] J.-J. Calvente, Z. Kovacova, R. Andreu, W.R. Fawcett, J. Chem. Soc. Faraday Trans. 92 (1996) 3701.
[101] D.-F. Yang, C.P. Wilde, M. Morin, Langmuir 13 (1997) 243.
[102] D.-F. Yang, H. Al-Maznai, M. Morin, J. Phys. Chem. B 101 (1997) 1158.
[103] D.-F. Yang, M. Morin, J. Electroanal. Chem. 441 (1998) 173.
[104] H. Kondoh, C. Kodama, H. Nozoye, J. Phys. Chem. B 102 (1998) 2310.
[105] D. Hobara, K. Miyake, S. Imabayashi, K. Niki, T. Kakiuchi, Langmuir 14 (1998) 3590.
[106] K. Aoki, T. Kakiuchi, J. Electroanal. Chem. 452 (1998) 187.
[107] N. Mohri, S. Matsushita, M. Inoue, K. Yoshikawa, Langmuir 14 (1998) 2343.

[108] A. Schejter, G. Taler, E. Margoliash, J. Am. Chem. Soc. 118 (1996) 477.
[109] B.A. Feinberg, X. Liu, M.D. Ryan, A. Schejter, C. Zhang, E. Margoliash, Biochemistry 37 (1998) 13091.
[110] C.M. Lett, A.M. Berghuis, H.E. Frey, J.R. Lepock, J.G. Guillemette, J. Biol. Chem. 271 (1996) 29088.
[111] T. Simonson, D. Perahia, Faraday Discuss. 103 (1996) 71.
[112] S.H. Northrup, in: R.A. Scott, A.G. Mauk (Eds.), Cytochrome c: A Multidisciplinary Approach, University Science Books, Sausalito, 1996, pp. 543–570.
[113] G. Basu, A. Kitao, A. Kuki, N. Go, J. Phys. Chem. B 102 (1998) 2076.
[114] G. Basu, A. Kitao, A. Kuki, N. Go, J. Phys. Chem. B 102 (1998) 2085.
[115] S.H. Northrup, K.A. Thomasson, C.M. Miller, P.D. Barker, L.D. Eltis, J.G. Guillemette, S.C. Inglis, C.M. Miller, Biochemistry 32 (1993) 6613.
[116] S.M. Andrew, K.A. Thomasson, S.H. Northrup, J. Am. Chem. Soc. 115 (1993) 5516.
[117] S. Terrettaz, J. Cheng, C.J. Miller, R.D. Guiles, J. Am. Chem. Soc. 118 (1996) 7857.
[118] J. Cheng, S. Terrettaz, J.I. Blankman, C.J. Miller, B. Dangi, R.D. Guiles, Isr. J. Chem. 37 (1997) 259.
[119] J. Bixler, G. Bakker, G. McLendon, J. Am. Chem. Soc. 114 (1992) 6938.
[120] T. Pascher, J.P. Chesick, J.R. Winkler, H.B. Gray, Science 271 (1996) 1558.
[121] T. Ferri, A. Poscia, F. Ascoli, R. Santucci, Biochim. Biophys. Acta 1298 (1996) 102.
[122] J.R. Winkler, P. Wittung-Stafshede, J. Leckner, B.G. Malmström, H.B. Gray, Proc. Natl. Acad. Sci. USA 94 (1997) 4246.
[123] D. Gopal, G.S. Wilson, R.A. Earl, M.A. Cusanovich, J. Biol. Chem. 263 (1988) 11652.
[124] G. Battistuzzi, M. Borsari, D. Dallari, I. Lancellotti, M. Sola, Eur. J. Biochem. 241 (1996) 208.
[125] J. Li, G. Cheng, S. Dong, J. Electroanal. Chem. 416 (1996) 97.
[126] H.A.O. Hill, G.A. Lawarance, J. Electroanal. Chem. 270 (1989) 309.
[127] W. Qian, J.-H. Zhuang, Y.-H. Wang, Z.-X. Huang, J. Electroanal. Chem. 447 (1998) 187.
[128] L. Jiang, C.J. McNeil, J.M. Cooper, Angew. Chem. Int. Ed. Engl. 34 (1995) 2409.
[129] P.D. Barker, H.A.O. Hill, N.J. Walton, J. Electroanal. Chem. 260 (1989) 303.
[130] Y. Maeda, H. Yamamoto, H. Kitano, J. Phys. Chem. 99 (1995) 4837.
[131] D. Hobara, K. Niki, C. Zhou, G. Chumanov, T.M. Cotton, Colloids Surf. A 93 (1994) 241.
[132] D. Moss, E. Nabedryk, J. Breton, W. Mäntele, Eur. J. Biochem. 187 (1990) 565.
[133] D.D. Schlereth, W. Mäntele, Biochemistry 32 (1993) 1118.
[134] C. Hinnen, K. Niki, J. Electroanal. Chem. 264 (1989) 157.
[135] T. Sagara, K. Niwa, A. Sone, C. Hinnen, K. Niki, Langmuir 36 (1990) 254.
[136] Z.Q. Feng, S. Imabayashi, T. Kakiuchi, K. Niki, J. Electroanal. Chem. 394 (1995) 149.
[137] Z.Q. Feng, S. Imabayashi, T. Kakiuchi, K. Niki, J. Chem. Soc. Faraday Trans. 93 (1997) 1367.
[138] S. Arnold, Z.Q. Feng, K. Kakiuchi, W. Knoll, K. Niki, J. Electroanal. Chem. 438 (1997) 91.
[139] A. Szücs, G.D. Hitchens, J.O'M. Bockris, Electrochim. Acta 37 (1992) 403.
[140] S. Boussaad, N.J. Tao, R. Arechabaleta, Chem. Phys. Lett. 280 (1997) 397.
[141] J.E.T. Andersen, P. Moller, M.V. Pedersen, J. Ulstrup, Surf. Sci. 325 (1995) 193.
[142] B. Zhang, E. Wang, J. Chem. Soc. Faraday Trans. 93 (1997) 327.
[143] J.E.T. Andersen, A.A. Kornyshev, A.M. Kuznetsov, L.L. Madsen, P. Moller, J. Ulstrup, Electrochim. Acta 42 (1997) 819.
[144] E.P. Friis, J.E.T. Andersen, L.L. Madesn, P. Moller, R.J. Nichols, K.G. Olesen, J. Ulstrup, Electrochim. Acta 43 (1998) 2889.
[145] M. Lion-Dagan, I. Ben-Dov, I. Willner, Colloids Surf. B: Biointerfaces 8 (1997) 251.
[146] X.H. Mu, F.A. Schultz, J. Electroanal. Chem. 353 (1993) 349.
[147] W.R. Fawcett, M. Fedurco, K.M. Smith, H. Xie, J. Electroanal. Chem. 354 (1993) 281.
[148] I. Benjamin, Chem. Rev. 96 (1996) 1449.
[149] L.D. Zusman, Chem. Phys. 49 (1980) 295.
[150] G. van der Zwan, J.T. Hynes, J. Phys. Chem. 89 (1985) 4181.
[151] A. Kapturkiewicz, B. Behr, J. Electroanal. Chem. 179 (1984) 187.
[152] W.R. Fawcett, M. Fedurco, J. Phys. Chem. 97 (1993) 7075.
[153] X.H. Mu, F.A. Schultz, Inorg. Chem. 34 (1995) 3835.

[154] M. Maroncelli, J. Chem. Phys. 94 (1991) 2084.
[155] W.R. Fawcett, C.A. Foss Jr., J. Electroanal. Chem. 306 (1991) 71.
[156] M.J. Weaver, Chem. Rev. 92 (1992) 463.
[157] M. Maroncelli, V.P. Kumar, A. Papazyan, J. Phys. Chem. 97 (1993) 13.
[158] X. Song, R.A. Marcus, J. Chem. Phys. 99 (1993) 7768.
[159] I. Ohmine, H. Tanaka, Chem. Rev. 93 (1993) 2545.
[160] W.R. Fawcett, M. Opallo, Angew. Chem. Int. Ed. Engl. 33 (1994) 2131.
[161] R. Jimenez, G.R. Fleming, P.V. Kumar, M. Maroncelli, Nature 369 (1994) 471.
[162] P.L. Muino, P.R. Callis, J. Chem. Phys. 100 (1994) 4093.
[163] P.J. Reid, C. Silva, P.F. Barbara, L. Karki, J.T. Hupp, J. Phys. Chem. 99 (1995) 2609.
[164] P.F. Barbara, T.J. Meyer, M.A. Ratner, J. Phys. Chem. 100 (1996) 13148.
[165] L. Reynolds, J.A. Gardecki, S.J.V. Frankland, M.L. Horng, M. Maroncelli, J. Phys. Chem. 100 (1996) 10337.
[166] R.A. Marcus, J. Electroanal. Chem. 438 (1997) 251.
[167] M.L. Horng, J. Gardecki, M. Maroncelli, J. Phys. Chem. 101 (1997) 1030.
[168] A. Calhoun, G.A. Voth, J. Electroanal. Chem. 450 (1998) 253.
[169] B. Bagchi, N. Gayathri, in: J. Jortner, M. Bixon (Eds), Electron Transfer: From Isolated Molecules to Biomolecules, Part II. Advances in Chemical Physics Series, vol. 107, Wiley, New York, 1999, pp. 1–80.
[170] J.T. Kindt, C.A. Schumettenmaer, J. Phys. Chem. 100 (1996) 10373.
[171] A.M. Becka, C.J. Miller, J. Phys. Chem. 96 (1992) 2657.
[172] S. Terrettaz, A.M. Becka, M.J. Traub, J.C. Fettinger, C.J. Miller, J. Phys. Chem. 99 (1995) 11216.
[173] R.A. Kuharski, J.S. Bader, D. Chandler, M. Sprik, M.L. Klein, J. Chem. Phys. 89 (1988) 3248.
[174] D.A. Rose, I. Benjamin, J. Chem. Phys. 100 (1994) 3545.
[175] D.A. Rose, I. Benjamin, Chem. Phys. Lett. 234 (1995) 209.
[176] J.B. Straus, A. Calhoun, G.A. Voth, J. Chem. Phys. 102 (1995) 529.
[177] A. Calhoun, G.A. Voth, J. Phys. Chem. 100 (1996) 10746.
[178] J. Li, C.L. Fisher, J.L. Chen, D. Bashford, L. Noodleman, Inorg. Chem. 35 (1996) 4694.
[179] J.M. Martinez, R.R. Pappalardo, E.S. Marcos, J. Chem. Phys. 109 (1998) 1445.
[180] A.K. Churg, R.M. Weiss, A. Warshel, J. Phys. Chem. 87 (1983) 1683.
[181] I. Muegge, P.X. Qi, J. Wand, Z.T. Chu, A. Warshel, J. Phys. Chem. B 101 (1997) 825.
[182] K.A. Sharp, Biophys. J. 73 (1998) 1241.
[183] S. Jeon, T. Bruice, Inorg. Chem. 31 (1992) 4843.
[184] K.M. Kadish, J. Jordan, J. Electrochem. Soc. 125 (1978) 1250.
[185] R.S. Tieman, L.A. Coury Jr., J.R. Kirhoff, W.R. Heineman, J. Electroanal. Chem. 281 (1990) 133.
[186] H.A. Harbury, P.A. Loach, J. Biol. Chem. 235 (1960) 3640.
[187] H.A. Harbury, P.A. Loach, J. Biol. Chem. 241 (1966) 4299.
[188] A.D. Carraway, M.G. McCollum, J. Peterson, Inorg. Chem. 35 (1996) 6885.
[189] E. Fraga, M.A. Webb, G.R. Loppnow, J. Phys. Chem. 100 (1996) 3278.
[190] J. Wu, D.G. Gorenstein, J. Am. Chem. Soc. 115 (1993) 6843.
[191] G. Battistuzzi, M. Borsari, G. Rossi, M. Sola, Inorg. Chim. Acta 272 (1998) 168.
[192] G. De Sanctis, A. Maranesi, T. Ferro, A. Poscia, F. Ascoli, R. Santucci, J. Protein Chem. 15 (1996) 599.
[193] T. Simonson, D. Perahia, Proc. Natl. Acad. Sci. USA 92 (1995) 1082.
[194] T. Simonson, C.L. Brooks III, J. Am. Chem. Soc. 118 (1996) 8452.
[195] T. Simonson, J. Am. Chem. Soc. 120 (1998) 4875.
[196] K.S. Reddy, P.J. Angiolillo, W.W. Wright, M. Laberge, J.M. Vanderkooi, Biochemistry 35 (1996) 12820.
[197] P.M.A. Gadsby, A.J. Thomson, J. Am. Chem. Soc. 112 (1990) 5003.
[198] J. McKnight, M.R. Cheesman, C.A. Reed, R.D. Orosz, A.J. Thomson, J. Chem. Soc. Dalton Trans. (1991) 1887.
[199] I. Salmeen, G. Palmer, J. Chem. Phys. 48 (1968) 2049.
[200] M.R. Cheesman, F.A. Walker, J. Am. Chem. Soc. 118 (1996) 7373.

[201] N.V. Shokhirev, F.A. Walker, J. Am. Chem. Soc. 120 (1998) 981.
[202] F.A. Walker, B.H. Huynh, W.R. Scheidt, S.R. Osvath, J. Am. Chem. Soc. 108 (1986) 5288, and references therein.
[203] W.E. Blumberg, J. Peisach, Adv. Chem. Ser. 100 (1971) 271.
[204] G. Liu, Y. Chen, W. Tang, J. Chem. Soc. Dalton Trans. (1997) 795.
[205] M. Fedurco, J. Augustynski, in preparation
[206] P. George, A. Schejter, J. Biol. Chem. 239 (1964) 1504.
[207] G. Liu, W. Shao, X. Huang, H. Wu, W. Tang, Biochim. Biophys. Acta 1277 (1996) 61.
[208] J. Lu, D. Ma, J. Hu, W. Tang, D. Zhu, J. Chem. Soc. Dalton Trans. (1998) 2267.
[209] M. Grodzicki, H. Flint, H. Winkler, F.A. Walker, A.X. Trautwein, J. Phys. Chem. A 101 (1997) 4202.
[210] J.D. Hobbs, J.A. Shelnutt, J. Protein. Chem. 14 (1995) 19.
[211] M.C. Simpson, F. Millett, L.P. Pan, R.W. Larsen, J.D. Hobbs, B. Fan, M.R. Ondrias, Biochemistry 35 (1996) 10019, and references therein.
[212] F.N. Büchi, A.M. Bond, J. Electroanal. Chem. 314 (1991) 191.
[213] H.A.O. Hill, Y. Nakagawa, F. Marken, R.G. Compton, J. Phys. Chem. 100 (1996) 17395.
[214] M. Smith, G. McLendon, J. Am. Chem. Soc. 103 (1981) 4912.
[215] Antigona CV simulation software package was kindly provided to us by L. Mottier, University of Bologna, Italy.
[216] F. Viola, S. Aime, M. Coletta, A. Desideri, M. Fasano, S. Paoletti, C. Tarricone, P. Ascenzi, J. Inorg. Biochem. 62 (1996) 213.
[217] J. Haladjian, R. Pilard, P. Bianco, P.-A. Serre, Bioelectrochem. Bioenerg. 9 (1982) 91.
[218] S. Döpner, P. Hildebrandt, G.E. Heibel, F. Vanhecke, A.G. Mauk, J. Mol. Struct. 349 (1995) 125.
[219] S. Döpner, P. Hildebrandt, F.I. Rosell, A.G. Mauk, in: P. Carmona, R. Navarro, A. Hernanz (Eds.), Spectroscopy of Biological Molecules: Modern Trends, Kluwer, Dordrecht, 1997, pp. 87–88.
[220] M.J. Honeychurch, G.A. Rechnitz, J. Phys. Chem. B 101 (1997) 7472.
[221] P.D. Barker, A.G. Mauk, J. Am. Chem. Soc. 114 (1992) 3619.
[222] M. Brunori, A. Giuffrè, E. D'Itri, P. Sarti, J. Biol. Chem. 272 (1997) 19870.
[223] M.I. Verkhovsky, J.E. Morgan, M. Wikström, Biochemistry 34 (1995) 7483.
[224] F. Malatesta, F. Nicoletti, V. Zickermann, B. Ludwig, M. Brunori, FEBS Lett. 434 (1998) 322.
[225] N. Kojima, G. Palmer, J. Biol. Chem. 258 (1983) 14908.
[226] D.F. Wilson, J.G. Lindsay, E.S. Brocklehurst, Arch. Biochem. Biophys. 156 (1972) 277.
[227] D.F. Wilson, E.S. Brocklehurst, Arch. Biochem. Biophys. 158 (1973) 200.
[228] M.D. Newton, N. Sutin, Annu. Rev. Phys. Chem. 35 (1984) 437.
[229] C. Zener, Proc. R. Soc. London A 137 (1932) 696.
[230] L. Landau, Phys. Z. Sowjetunion 1 (1932) 88.
[231] N. Sutin, Prog. Inorg. Chem. 30 (1983) 441.
[232] T.M. Nahir, R.E. Clark, E.F. Bowden, Anal. Chem. 66 (1994) 2595.
[233] T.M. Nahir, E.F. Bowden, J. Electroanal. Chem. 410 (1996) 9.
[234] R.A. Marcus, J. Chem. Soc. Faraday Trans. 92 (1996) 3905.
[235] C.-P. Hsu, J. Electroanal. Chem. 438 (1997) 27.
[236] C.-P. Hsu, R.A. Marcus, J. Chem. Phys. 106 (1997) 584.
[237] D.C. Selmarten, J.T. Hupp, J. Chem. Soc. Faraday Trans. 92 (1996) 3909.
[238] C.J. Miller, P. Cuendet, M. Grätzel, J. Phys. Chem. 95 (1991) 877.
[239] H.O. Finklea, D.D. Hanshew, J. Am. Chem. Soc. 114 (1992) 3173.
[240] R.A. Clark, E.F. Bowden, Langmuir 13 (1997) 559.
[241] P. Harder, M. Grunze, R. Dahint, G.M. Whitesides, P.E. Laibinis, J. Phys. Chem. B 102 (1998) 426.
[242] G.B. Sigal, M. Mrksich, G.M. Whitesides, J. Am. Chem. Soc. 120 (1998) 3464.
[243] L. Deng, M. Mrksich, G.M. Whitesides, J. Am. Chem. Soc. 118 (1996) 5136.
[244] G.B. Sigal, M. Mrksich, G.M. Whitesides, Langmuir 13 (1997) 2749.
[245] C.D. Tidwell, S.I. Ertel, B.D. Ratner, B.J. Tarasevich, S. Atre, D.L. Allara, Langmuir 13 (1997) 3404.

[246] A. El Kasmi, J.M. Wallace, E.F. Bowden, S.M. Binet, R.J. Linderman, J. Am. Chem. Soc. 120 (1998) 225.
[247] C.J. Miller, M. Grätzel, J. Phys. Chem. 91 (1991) 5225.
[248] A.M. Becka, C.J. Miller, J. Phys. Chem. 97 (1993) 6233.
[249] D.M. Cyr, B. Venkataraman, G.W. Flynn, A. Black, G.M. Whitesides, J. Phys. Chem. 100 (1996) 13747.
[250] D.J. Olbris, A. Ulman, Y. Shnidman, J. Chem. Phys. 102 (1995) 6865.
[251] Z.F. Liu, C.X. Zhao, J. Zhang, M. Tang, T. Zhu, S.M. Cai, Ber. Bunsen. Ges. Phys. Chem. 101 (1997) 1113.
[252] D.G. Hanken, C.E. Jordan, B.L. Frey, R.M. Corn, in: A.J. Bard, I. Rubinstein (Eds.), Electroanalytical Chemistry, vol. 20, Marcel Dekker, New York, 1998, pp. 141–225.
[253] R. Langen, I.-J. Chang, J.P. Germanas, J.H. Richards, J.R. Winkler, H.B. Gray, Science 268 (1995) 1733.
[254] Image created by Swiss-PdbViewer v3.0, Geneva Biomedical Research Institution, Glaxo Wellcome S.A., http://www.expasy.ch/spdbv/mainpage.html
[255] J. Cheng, C.J. Miller, J. Phys. Chem. 101 (1997) 1058.
[256] S.S. Isied, in: S.S. Isied (Ed.), Long-Range Intramolecular Electron-Transfer Reactions across Simple Organic Bridges, Peptides, Proteins, vol. 253, American Chemical Society, Washington, DC, 1997, p. 331.
[257] R.J. Cave, P. Siders, R.A. Marcus, J. Phys. Chem. 90 (1986) 1436.
[258] A.A. Stuchebrukhov, R.A. Marcus, J. Phys. Chem. 99 (1995) 7581.
[259] I. Daizadeh, E.S. Medvedev, A.A. Stuchebrukhov, Proc. Natl. Acad. Sci. USA 94 (1997) 3703.
[260] W. Mar, M.L. Klein, Langmuir 10 (1994) 188.
[261] M.J. Tarlov, E.F. Bowden, J. Am. Chem. Soc. 113 (1991) 1847.
[262] S. Song, R.A. Clark, E.F. Bowden, M.J. Tarlov, J. Phys. Chem. 97 (1993) 6564.
[263] H. Tokuhisa, R.M. Crooks, Langmuir 13 (1997) 5608.
[264] J. Wang, L.M. Frostman, M.D. Ward, J. Phys. Chem. 96 (1992) 5224.
[265] T.M. Nahir, E.F. Bowden, Electrochim. Acta 39 (1994) 2347.
[266] S. Imabayashi, T. Mita, Z.Q. Feng, M. Ida, K. Niki, T. Kakiuchi, Denki Kagaku 65 (1997) 467.
[267] I.D.G. Macdonald, W.E. Smith, Langmuir 12 (1996) 706.
[268] K. Di Gleria, H.A.O. Hill, V.J. Lowe, D.J. Page, J. Electroanal. Chem. 213 (1986) 333.
[269] Z.-X. Huang, M. Feng, Y.-H. Wang, J. Cui, D.-S. Zou, J. Electroanal. Chem. 416 (1996) 31.
[270] T. Pineda, J.M. Sevilla, A.J. Roman, M. Blazquez, Biochim. Biophys. Acta 1434 (1997) 227.
[271] K.K. Rodgers, S.G. Sligar, J. Am. Chem. Soc. 113 (1991) 9419.
[272] W. Jin, Q. Weng, J. Wu, Anal. Lett. 30 (1997) 753.
[273] K. Uvdal, P. Bodö, B. Liedberg, J. Colloid Interface Sci. 149 (1992) 162.
[274] M. Fedurco, Ph.D. Thesis, J. Heyrovsky Institute of Physical Chemistry, Prague, 1995.
[275] A.S. Dakkouri, D.M. Kolb, R. Edelstein-Shima, D. Mandler, Langmuir 12 (1996) 2849.
[276] J. Lu, J.L. Fang, D.X. Zhu, W.X. Tang, Spectrosc. Lett. 30 (1997) 1369.
[277] J.M. Cooper, K.R. Greenough, C.J. McNeil, J. Electroanal. Chem. 347 (1993) 267.
[278] A.M. Bond, H.A.O. Hill, S. Komorsky-Lovric, M. Lovric, M.E. McCarthy, I.S.M. Psalti, N.J. Walton, J. Phys. Chem. 96 (1992) 8100.
[279] T. Sagara, I. Satake, H. Murakami, H. Akutsu, K. Niki, J. Electroanal. Chem. 301 (1991) 285.
[280] Y. Xie, S. Dong, Electroanalysis 6 (1994) 567.
[281] Y. Xie, S. Dong, Bioelectrochem. Bioenerg. 29 (1992) 71.
[282] T. Sawaguchi, F. Mizutani, I. Taniguchi, Langmuir 14 (1998) 3565.
[283] M. Tominaga, K. Hayashi, I. Taniguchi, Anal. Sci. 8 (1992) 829.
[284] J.L. Theodorakis, E.A.E. Garber, J. Mccracken, J. Peisach, A. Schejter, E. Margoliash, Biochim. Biophys. Acta 1252 (1995) 103.
[285] J.L. Theodorakis, L.G. Armes, E. Margoliash, Biochim. Biophys. Acta 1252 (1995) 114.
[286] C. Zhou, S. Ye, J.-H. Kim, T.M. Cotton, X. Yu, T. Lu, S. Dong, J. Electroanal. Chem. 319 (1991) 71.
[287] K.C. Cho, W.F. Chu, C.L. Choy, C.M. Che, Biochim. Biophys. Acta 934 (1988) 161.
[288] T.-C. Tsai, I.-J. Chang, J. Am. Chem. Soc. 120 (1998) 227.

[289] J. Cheng, G.-S. Szabó, J.A. Tossell, C.J. Miller, J. Am. Chem. Soc. 118 (1996) 680.
[290] Y.-T. Tao, C.-C. Wu, J.-Y. Eu, W.-L. Lin, Langmuir 13 (1997) 4018.
[291] K. Slowinski, R.V. Chamberlain, C.J. Miller, M. Majda, J. Am. Chem. Soc. 119 (1997) 11910.
[292] T.T.-T. Tomi, H.Y. Li, L. Kendall, K.L. Guyer, S.W. Barr, M.J. Weaver, J. Electroanal. Chem. 164 (1984) 27.
[293] I. Taniguchi, S. Yoshimoto, K. Nishiyama, Chem. Lett. (1997) 353.
[294] M.A. Bryant, R.M. Crooks, Langmuir 9 (1993) 385.
[295] W. Hill, B. Wehling, J. Phys. Chem. 97 (1993) 9451.
[296] C.J. Sandroff, D.R. Herschbach, J. Phys. Chem. 86 (1982) 3277.
[297] K.T. Carron, L.G. Hurley, J. Phys. Chem. 95 (1991) 9979.
[298] C.A. Szafranski, W. Tanner, P.E. Laibinis, R.L. Garrell, Langmuir 14 (1998) 3570.
[299] C.-X. Cai, J. Electroanal. Chem. 393 (1995) 119.
[300] J.J. Davis, H.A.O. Hill, R. Yamada, H. Naohara, K. Uosaki, J. Chem. Soc. Faraday Trans. 94 (1998) 1315.
[301] B.D. Lamp, D. Hobara, M.D. Porter, K. Niki, T.M. Cotton, Langmuir 13 (1997) 736.
[302] M. Shibata, N.J. Furuya, J. Electroanal. Chem. 250 (1988) 201.
[303] T. Lu, X. Yu, S. Dong, C. Zhou, S. Ye, T.M. Cotton, J. Electroanal. Chem. 369 (1994) 79.
[304] Q. Qu, J. Chou, T. Lu, S. Dong, C. Zhou, T.M. Cotton, J. Electroanal. Chem. 381 (1995) 81.
[305] V. Brabec, P. Bianco, J. Haladjian, Gen. Physiol. Biophys. 1 (1982) 269.
[306] S. Sagara, H. Nakajima, K. Akutsu, K. Niki, G.S. Wilson, J. Electroanal. Chem. 297 (1991) 271.
[307] D. Zhang, G.S. Wilson, K. Niki, Anal. Chem. 66 (1994) 3873.
[308] K.L. Egodage, B.S. de Silva, G.S. Wilson, J. Am. Chem. Soc. 119 (1997) 5295.
[309] P. Bianco, J. Haladjian, Electrochim. Acta 42 (1997) 587.
[310] D. Hobara, K. Niki, T.M. Cotton, Biospectroscopy 4 (1998) 161.
[311] S. Imabayashi, N. Gon, T. Sasaki, D. Hobara, T. Kakiuchi, Langmuir 14 (1998) 2348.
[312] Q. Cui, K.J. Stevenson, H.S. White, Electrochemical Society Proceedings, vol. 97–17, The Electrochemical Society, Inc., Montreal, 1997, p. 158.
[313] S.E. Creager, J. Clarke, Langmuir 10 (1994) 3675.
[314] Y. Sato, F. Mizutani, Denki Kagaku 63 (1995) 1173.
[315] Y. Sato, R. Yamada, F. Mizutani, K. Uosaki, Chem. Lett. (1997) 987.
[316] W.W. Wright, M. Laberge, J.M. Vanderkooi, Biochemistry 36 (1997) 14724.
[317] P. Geissinger, B.E. Kohler, J.C. Woehl, Synth. Met. 84 (1997) 937.
[318] R. Seetharaman, S.P. White, M. Rivera, Biochemistry 35 (1996) 12455.
[319] L. Jiang, C.J. McNeil, J.M. Cooper, J. Chem. Soc. Chem. Commun. (1995) 1293.
[320] T. Lötzbeyer, W. Schuhman, E. Katz, J. Falter, H.-L. Schmidt, J. Electroanal. Chem. 367 (1994) 59.
[321] E. Katz, I. Willner, J. Electroanal. Chem. 418 (1996) 67.
[322] I. Willner, S. Rubin, Y. Cohen, J. Am. Chem. Soc. 115 (1993) 4937.
[323] M. Lion-Dagan, E. Katz, I. Willner, J. Chem. Soc. Chem. Commun. (1994) 2741.
[324] I. Willner, M. Lion-Dagan, S. Marx-Tibbon, E. Katz, J. Am. Chem. Soc. 117 (1995) 6581.
[325] I. Willner, E. Katz, B. Willner, R. Blonder, V. Heleg-Shabtai, A.F. Bückmann, Biosens. Bioelectron. 12 (1997) 337.
[326] W. Jentzen, X.-Z. Song, J.A. Shelnutt, J. Phys. Chem. B 101 (1997) 1684.
[327] W. Jentzen, J.-G. Ma, J.A. Shelnutt, Biophys. J. 74 (1998) 753.
[328] G. Chottard, M. Michelon, M. Hervé, G. Hervé, Biochim. Biophys. Acta 916 (1987) 402.
[329] W.J. Albery, M.J. Eddowes, H.A.O. Hill, A.R. Hillman, J. Am. Chem. Soc. 103 (1981) 3904.
[330] P. Hildebrandt, Biochim. Biophys. Acta 1040 (1990) 175.
[331] M. Antalik, M. Bona, J. Bagelova, Biochemistry 28 (1992) 675.
[332] M. Antalik, M. Bona, Z. Gazova, A. Kuchar, Biochim. Biophys. Acta 1110 (1992) 155.
[333] J. Bagelova, M. Antalik, M. Bona, Biochem. J. 297 (1994) 99.
[334] J. Bagelova, M. Antalik, Z. Tomori, Biochem. Mol. Biol. Int. 43 (1997) 891.
[335] E. Sedlak, M. Antalik, J. Bagelova, M. Fedurco, Biochim. Biophys. Acta 1319 (1997) 258.
[336] E. Sedlak, M. Antalik, Biopolymers 46 (1998) 145.
[337] C.E.V. Hahn, H.A.O. Hill, M.D. Ritchie, J.W. Sear, J. Chem. Soc. Chem. Commun. (1990) 125.

[338] J.W. Furbee Jr., R. Thomas, R.S. Kelly, M.R. Malachowski, Anal. Chem. 65 (1993) 1654.
[339] K. Takehara, Y. Ide, M. Aihara, E. Obuchi, Bioelectrochem. Bioenerg. 29 (1992) 103.
[340] K. Takehara, Y. Ide, M. Aihara, Bioelectrochem. Bioenerg. 29 (1992) 113.
[341] K. Takehara, S. Yamada, Y. Ide, J. Electroanal. Chem. 333 (1992) 339.
[342] K. Takehara, Y. Ide, Bioelectrochem. Bioenerg. 27 (1992) 207.
[343] K. Takehara, Y. Ide, Bioelectrochem. Bioenerg. 27 (1992) 501.
[344] T. Wink, S.J. van Zuilen, A. Bult, W.P. van Bennekom, Analyst 122 (1997) 43R.